NORTHWESTERN UNIVERSITY

Molecular organization of EphA2 cell-cell communication complexes in human keratinocytes

A DISSERTATION

SUBMITTED TO THE GRADUATE SCHOOL

IN PARTIAL FULFILLMENT OF THE REQUIREMENTS

for the degree

DOCTOR OF PHILOSOPHY

Driskill Graduate Training Program in Life Sciences

Field of Dermatology

By

Rosa Ventrella

EVANSTON, IL

June 2018

Table of Contents

ABSTRACT

Erythropoietin-producing human hepatocellular (Eph) receptors and their corresponding ephrin ligands are asymmetrically expressed at cell-cell contacts allowing for bidirectional signaling with forward signaling through the receptor expressing cell and reverse signaling through the ligand expressing cell. Eph receptors are the largest family of receptor tyrosine kinases (RTKs) in mammals, which allows for a vast array of signaling responses depending on which receptor and ligand are interacting and the cell type involved. In addition, when ephrin ligands are expressed on the same cell, Eph signaling is inhibited adding an additional mechanism of signal regulation. Most notably, Eph/ephrins have been shown to play important roles in cell sorting, boundary formation, and tissue morphogenesis. Misregulation of Eph/ephrins often lead to aberrant signaling pathways, leading to a variety of diseases. Specifically, in the epidermis, ephrin-A1 promotes keratinocyte differentiation and inhibits keratinocyte migration through EphA2. Alterations in this signaling axis is associated with inflammatory skin diseases such as psoriasis and non-melanoma skin cancer.

Ephrin-A1 contains a glycosylphosphatidylinositol (GPI)-linked tail, which targets this ligand to specific membrane microdomains known as lipid rafts. Lipid raft domains are important for regulating the distribution of membrane proteins and are enriched in sterols, most notably cholesterol, making them thicker and less fluid than the surrounding membrane. Due to the importance of ephrin localization relative to its receptor, one would hypothesize that lipid rafts play an important role in the downstream signaling elicited by EphA2 and ephrin-A1; however, the ability of this receptor and ligand to localize to lipid raft domains and the mechanisms governing their localization patterns in keratinocytes is unknown. Additionally, due

to the importance of EphA2 and ephrin-A1 in keratinocyte biology, it is likely that ephrin-A1 and EphA2 cellular distribution is important in controlling keratinocyte behaviors like differentiation and migration.

In order to address these hypotheses, we used a combination of biochemical and imaging approaches to study the molecular organization of ephrin-A1 and EphA2 signaling complexes in a primary human keratinocyte culture model. We provide evidence that ephrin-A1-induced forward signaling promoted keratinocyte differentiation as assessed by tight junction proteins that are expressed during the final stages of epidermal differentiation. We also provide evidence that EphA2 is present in lipid raft domains along with ephrin-A1. The recruitment of EphA2 to lipid raft domains at cell-cell junctions was dependent on the unique properties of its transmembrane domain (TMD). Swapping the EphA2 TMD with a shorter and molecularly distinct TMD of the highly homologous EphA1 caused failure of this transmembrane mutant chimera to localize to cell-cell contacts, likely affecting its interaction with ephrin-A1. Correspondingly, this chimera increased ephrin-A1 expression levels and impaired the ability of keratinocytes to efficiently seal linear scratch wounds in an ephrin-A1-dependent manner. However, this chimera had minimal impact on calcium-induced keratinocyte differentiation. These findings suggest that cell-cell contact stabilization of EphA2 is not required to promote keratinocyte differentiation. Moreover, ephrin-A1 protein levels negatively regulate keratinocyte migration, but do not necessarily enhance keratinocyte migration.

Collectively, these studies highlight a key role for the EphA2 TMD and its association with lipid rafts in modulating downstream signaling. Our data highlight the importance of EphA2 localization to lipid raft domains at cell-cell contacts in controlling ligand expression level.

Specifically, these findings suggest the importance of the EphA2 TMD in regulating keratinocyte migration, which has relevance to cutaneous wound healing. These findings likely have broader implications for the understanding of Eph/ephrin and transmembrane receptor biology. It is likely that lipid rafts play important roles in organizing Eph/ephrin signaling networks at boundaries to control Eph/ephrin and other membrane receptor interactions that govern cell segregation and tissue patterning. In addition to modulating Eph/ephrin interactions, lipid rafts likely organize receptor crosstalk in different membrane regions. These discoveries will be important in understanding how lipid raft disruption or Eph/ephrin misregulation leads to abnormal signaling, resulting in loss of tissue homeostasis. Lastly, these outcomes show the significance of the TMD of RTKs in regulating downstream signaling pathways.

ACKNOWLEDGEMENTS

First, I would like to acknowledge my thesis advisor, Dr. Spiro Getsios. Without his mentorship and guidance, this accomplishment would not have been possible. I am so grateful to have had the opportunity to have him as my advisor. He has not only made me a better, more independent scientist, but he has also made me a stronger person. He taught me how to stay motivated when things get difficult and how to celebrate life's successes. I am thankful that I had the opportunity to be a small part of his distinguished scientific career.

I would also like to thank my thesis committee for their additional support throughout graduate school. Specifically, a special thank you to Dr. Robert Lavker, who provided me with his advice and leadership, especially as I was in the final stages of this process. I am lucky to have had the chance to work beside him. His passion and work ethic are truly inspirational to all of those around him. Additionally, I would like to acknowledge Dr. Kathy Green, Dr. Cara Gottardi, and Dr. James Bartles who have been extremely encouraging throughout my graduate career. Their motivation and constructive criticism has continually pushed me to become a better scientist.

Throughout the last five years I have been very fortunate to not just work in a lab beside great scientists, but also very good friends. Dr. Nihal Kaplan, Dr. Bethany Perez White, and Paul Hoover have been by my side since day one in the Getsios lab. On a daily basis, they inspired me when experiments seemed to never be working out and celebrated with me when things began to fall into place. I could not have asked for better scientists to work with throughout this journey and I truly could not have done it without them. Also, a special thank you to Dr. Nihal Kaplan who was instrumental in helping me complete the massive sucrose gradient experiments. I would

additionally like to thank the other Getsios and Lavker lab members, Dr. Jessica Wahi, Dr. Han Peng, Dr. Jong Kook Park, Dr. Wending Yang, Dr. Ariel Finkielsztein, Calvin Cable, Heath McDonald, and Andrea Brown for their continual advice and commitment to my success. Furthermore, I would like to acknowledge the Northwestern University Skin Disease Research Center, Dermatology Department, and Driskill Graduate Program (DGP) for their continued enthusiasm throughout my graduate career. I have been very fortunate to be surrounded by fantastic company during my graduate tenure.

During my time at graduate school I had the opportunity to live with two of my best friends whom I now consider family. Kyle, I am so grateful to have experienced graduate school with you. Looking back to those first few days, I would have never imagined that you would not only become one of my best friends, but also the brother that I never had. Thank you so much for always providing me with the advice, laughs, and deep conversations that I needed. I know we have developed a friendship that will last a lifetime. Amy, I am so thankful for that first day you sat down next to me in our Introduction to Bioengineering class. I can't imagine completing this journey without you. You have never failed to support me whether it was helping to clear my mind when things got stressful or making sure I didn't forget to eat dinner. Your friendship to me is truly irreplaceable. And finally, I would be remiss if I did not thank my unofficial roommate, Stephanie Woods. You have never ceased to put a smile on my face when things got difficult. I am so grateful for your friendship over the years. I could not have completed this crazy journey without all of your continued encouragement and camaraderie.

When I came to visit Northwestern University for interview weekend I was immediately attracted to the friendliness of the potential students. Many of the interviewees that I met that

weekend also chose to come to here and allowed me the chance to form some truly amazing friendships. Specifically, that night I met two people who have become best friends over these past several years. Daniela, you have been by my side since interview weekend and I am so appreciative for this wonderful friendship. You have not only been there to help brainstorm new hypotheses and troubleshoot failed experiments, but more importantly you were there when I needed a shoulder to lean on or someone to have a good laugh with. Erin, I could not have completed this journey without your continued positivity. Our regular last-minute coffee dates and dinners always gave me something to look forward to during the week. Also, I am so thankful for all the mentorship you have given me in my passion for teaching. Thank you to all the other DGP students that were by my side through the challenging moments and lent me the support I needed as my graduate career continued to develop. I could not have completed these past several years without the encouragement of my fellow DGPers, nor would I be able to look back with such fond memories.

Marcos, you came into my life at the most demanding point of my graduate school career. It was a time when I felt like every week was more stressful than the prior, but this did not scare you away. Thank you so much for not just dealing with my passion for science, but for embracing it and joining me every weekend when I had to run to lab and for waking up to spend time with me while I had to write. Most importantly, thank you for proving me with your unconditional love and constant inspiration.

Finally, I would like to thank my family for never giving up on me since the day I said I wanted to become a scientist. You have all been there in my moments of weakness to lift me up and remind me of my goals. Thank you Mom, for being my role model in life. You have been a

constant reminder of the person that I aspire to be and instilled a love of science in me. Words cannot express how appreciative I am that you learned how to help me quantify my data and I am thrilled you were able to make a contribution to my dissertation. Dad, thanks for always giving me the strength and encouragement that I could accomplish anything that I set my mind to. You have always been there to provide me with words of wisdom to believe in my potential. A very special thank you to my twin and best friend, Rina, for always being my partner-in-crime and other half. Throughout my lifetime you have always been by my side to challenge and motivate me to reach my highest potential. I am so lucky that I have been able to have you as my best friend to share in all of life's adventures with. Moreover, I appreciate all the time that you spent editing my dissertation. I know it was not a small feat. Gianna, thanks for being such a supportive little sister. I am so thankful that throughout this journey you were only a short drive away so we had had the opportunity to share so many memories together. It is so nice to know that I always have someone that I can count on to lift my spirits and motivate me to keep following my passions. Nonna Rosa, thank you for providing me with so much positivity during my graduate school career. I am so proud to have you, such a strong and caring person, as my namesake. Nonno, the opportunity to go to graduate school near you was one of my main factors in choosing Northwestern. I am so thankful for the memories we have made together and I will be forever grateful for the special relationship that we share. Lastly, a special thanks to the rest of my family, including my compassionate aunts, uncles, and cousins, for providing me with the support and guidance throughout all of my life's endeavors. I have no doubt that completion of my dissertation could not have been down without the encouragement of my family, friends, and mentors.

LIST OF ABBREVIATIONS

ABE	Acyl-biotin exchange
ADAM	Disintegrin and metalloproteinase domain-
AJ	Adherens Junction
AKT	Protein kinase B
ALI	Air-liquid interface
APE	Acyl-PEG exchange
Arf	ADP-ribosylation factor
BM	Basement membrane
BP230	Bullous pemphigoid antigen 1e
Ca^{2+}	Calcium
CD	Cytoplasmic domain
Cdc42	Cell division cycle 42
CDE	Clathrin-dependent endocytosis
CIE	Clathrin-independent endocytosis
CRD	Cysteine-rich domain
Dock180	Dedicator of cytokinesis 180
Dpc	Days post coitum
DRM	Detergent resistant membrane
Dsc	Desmocollin
Dsg	Desmoglein
E-Cadherin	Epithelial calcium-dependent adhesion protein
ECD	Extracellular domain
ECM	Extracellular matrix
EDC	Epidermal differentiation complex
EDTA	Ethylenediaminetetraacetic acid
EGF	Epidermal growth factor
EGFR	Epidermal growth factor receptor

EHD1	EH-Domain Containing Protein 1
Eph	Erythropoietin-producing human hepatocellular
ErbB	Avian erythroblastic leukemia viral oncogene
ERC	Endosome recycling complex
ERK	Extracellular signal-related kinase
ESCRT-1	Endosomal sorting complex required for
FAK	Focal adhesion kinase
FGF	Fibroblast growth factor
FGFR	Fibroblast growth factor receptor
FNIII	Fibronectin-type-3
FPKM	Fragments per kilobase of exon per million
GEF	Guanine exchange factor
Git1	GPCR kinase-interacting protein 1
GPCR	G-protein-coupled receptor
GPI	Glycosylphosphatidylinositol
Grb	Growth Factor Receptor-Bound Protein
H&E	Hematoxylin and eosin
HA	Hydroxylamine
HB-EGF	Heparin-binding EGF
HRAS	Harvey rat sarcoma proto-oncogene
HUVEC	Human umbilical vein endothelial cell
IFE	Interfollicular epidermis
IL	Interleukin
JAK2	Janus kinase 2
JMD	Juxtamembrane domain
JNK	c-Jun N-terminal kinase
K10	Keratin-10
LAT	Linker for activation of T-cells

LBD	Ligand-binding domain
MAPK	Mitogen-activated protein kinase
MDCK	Madin-Darby canine kidney
MMC	Mitomycin C
MMP	Matrix metallopeptidase
mPEG-Mal	Methoxy-Polyethylene glycol-Maleimide
MVBs	Multivesicular bodies
NEM	*N*-Ethylmaleimide
NHEK	Normal human epidermal keratinocyte
NMSC	Non-melanoma skin cancer
NRAS	Neuroblastoma RAS viral oncogene homolog
PAK	P21Activated Kinase
Par6	Partitioning defective-6
PAT	Palmitoyl acyl transferase
PDGFR	Platelet-derived growth factor receptor
PDZ	PSD95/Dlg/ZO1
PFO	Perfringolysin O
PI3K	Phosphoinositide 3-kinase
PIC	Protease inhibitor cocktail
PIP3	Phosphatidylinositol (3,4,5)-trisphosphate
PKC	Protein kinase C
PMSF	Phenylmethanesulfonyl fluoride
PPT	Palmitoyl protein thioesterases
pS	Phosphoserine
PTP1B	Protein tyrosine phosphatase 1B
pY	Phosphotyrosine
RAB	Ras-related protein
Rac	Ras-related C3 botulinum toxin substrate

RBD	Receptor binding domain
RHE	Reconstituted human epidermis
RhoA	Ras homolog gene family member A
ROCK	Rho-associated protein kinase
RPTP	Receptor protein tyrosine phosphatase
RTK	Receptor tyrosine kinase
SA	Streptavidin
SAM	Sterile-α motif
SFK	Src family kinase
SG	Stratum granulosum
SDS	Sodium dodecyl sulfate
SH2/SH3	Src homology 2/Src homology 3
SHIP2	SH2 domain-containing inositol 5-phosphatase
SIM	Structured illumination microscopy
SNAP	Synaptosomal-associated proteins
SNARE	Snap receptor
STAT3	Signal transducer and activator of transcription
TAC	Transit amplifying cell
TGF	Transforming growth factor
TGN	Trans-golgi network
Tiam1	T-Cell Lymphoma Invasion and Metastasis 1
TJ	Tight junction
TMD	Transmembrane domain
TNF	Tumor necrosis factor
VE-cadherin	Vascular endothelial cadherin
VEGFR	Vascular endothelial growth factor receptor
WT	Wild type
ZO	Zona occluden

DEDICATION

To my Papa.

This journey began for me the moment I lost you, much too soon, over fifteen years ago. You taught me how important it is to live every day like it's a celebration and to dream as vast and endless as the view of the ocean from your deck. My hope is that one day my work will make a contribution that can help someone else's Papa get one more "Chicken Dance" in with their grandchildren. Your love, strength, courage, and positivity is what inspires me every day. Although you may be gone, your spirit forever lives on.

To my Nonna Rina.

Thank you for showing me what it means to take on life's greatest challenges with a youthful spirit. I will never forget all those times you took us hiking through the Italian mountains telling us the stories of your childhood. No matter how difficult things were, you managed to live everyday full of love, joy, and faith. I dream that one day I will make an impact in helping someone else's Nonna, so they can have many more sette gusti cones of gelato with their grandchildren. I know that you have been with me at every step of this journey. Remembering how excited you were to be at my high school graduation makes me really wish you could be here to see me graduate one more time. You would be so proud.

LIST OF FIGURES

LIST OF TABLES

CHAPTERS

I. INTRODUCTION

1. Overview

Skin is one of the largest organs in humans and it is vital to protecting the body [1]. Skin creates a barrier that is important for preventing water loss, while impeding the entry of external pathogens. The outer layer of skin is a stratified epithelium that continuously regenerates throughout one's lifetime. Keratinocytes in the epidermal basal layer either proliferate to expand the basal cell population or commit to a program of differentiation. As keratinocytes stratify and undergo differentiation, they reorganize their membrane signaling complexes and adhesive receptors. These adhesive receptors not only anchor cells together, but also attach to different cytoskeletal networks in order to provide keratinocytes with structural support. Throughout the epidermis there are differential expression patterns of signaling receptors, adhesive complexes, and cytoskeletal networks. Alterations in these proteins can cause abnormalities in epidermal differentiation and lead to defects in barrier function [2].

Although membrane receptors span the cell membrane, they can be very dynamic and move into different membrane regions. Lipid rafts are a specific type of membrane microdomain enriched in cholesterol, and other sterols, that are highly organized and important to organizing protein complexes for proper downstream signaling to occur. Misregulation of these complexes or disruption of lipid raft microdomains can lead to aberrations in epidermal differentiation leading to a variety of skin diseases including psoriasis and non-melanoma skin cancers [3-7].

The erythropoietin-producing hepatocellular (Eph) receptors and their ephrin ligands are important for maintaining epidermal homeostasis. Eph receptors are a highly conserved receptor

tyrosine kinase (RTK) family that has evolved to regulate cell-cell communication. Eph receptors are activated by ephrin ligands at cell-cell contact resulting in bidirectional signaling with forward signaling through the receptor expressing cell and reverse signaling through the ligand expressing cell. Activation of Eph/ephrin signaling complexes has been shown to play important roles in cell repulsion during embryogenesis and neurogenesis [8]. Additionally, alterations in Eph/ephrin signaling can often lead to tumorigenesis [9].

Specifically, the EphA2/ephrin-A1 signaling axis plays a key role in many keratinocyte functions [10, 11]. For example, ephrin-A1 induced forward signaling promotes keratinocyte differentiation by inhibition of pro-proliferative signaling pathways [12]. Additionally, ephrin-A1 can inhibit keratinocyte migration [13, 14]. These ephrin-A1 responses are largely mediated by its high affinity receptor, EphA2. In psoriasis and non-melanoma skin cancers, where the epidermal differentiation process is perturbed, there is often upregulation of EphA2 and loss of ephrin-A1 resulting in ligand-independent pro-proliferative and pro-migratory EphA2 signaling [10, 15].

In the following sections, background information relevant to Chapters III and IV are provided. First, an introduction of Eph/ephrin complex structure and downstream signaling are explained. Then, a review of skin and its adhesive and cell-cell signaling complexes that help to maintain epidermal homeostasis are described. Lastly, details about the roles of Eph/ephrins, most notably EphA2 and ephrin-A1, in keratinocyte biology and membrane trafficking are highlighted. Collectively, these sections highlight the significance of EphA2 and ephrin-A1 lipid raft localization and its significance to epidermal biology.

2. Background of Eph/ephrins

2.1 Discovery and evolution of Eph/ephrins

The Eph family of RTKs was first identified and characterized in 1987 by molecular cloning in an erythropoietin-producing human hepatocellular carcinoma cell line (ETL-1). Overexpression of the *eph* gene was observed in colon carcinoma, lung adenocarcinoma, mammary carcinoma, and hepatocellular carcinoma suggesting the potential for the *eph* gene to act as an oncogene [16]. Since Eph receptors did not have a known ligand they were considered "orphan" receptors. Then their first ligand, ephrin-A1, was cloned from human umbilical vein endothelial cells (HUVECs) and identified as a ligand for these RTKs in 1990 and 1994, respectively [17, 18]. It was then determined that ephrin ligands contain a glycosylphosphatidylinositol (GPI)-linkage or a transmembrane domain (TMD) causing them to be anchored to the cell membrane [19-21]. The ability of both receptor and ligand to be attached to the cell membrane suggested that this receptor/ligand combination could play important roles at cell-cell contacts during tissue ontogenesis [20].

Eph receptors represent the largest family of RTKs in mammals. Of the sixteen Eph receptors in vertebrates, humans express fourteen Eph receptor genes along with nine ephrin ligands. Eph receptors are subdivided into two subclasses; the EphA receptors (EphA 1-8, 10), which have a high affinity for GPI-linked ephrin-A ligands (ephrin-A 1-5), and the EphB receptors (EphB 1-4, 6), which have a high affinity for transmembrane containing ephrin-B ligands (ephrin-B 1-3) [22-24]. However, some promiscuity can occur between different subclasses of Eph/ephrins [24-26].

Eph receptors are highly conserved and have been found in chordates, arthropods, nematodes, and sponges [27-29]. Although Eph/ephrins have many functions in neuronal signaling, lack of neurons in sponges suggest that they play additional roles in signaling in addition to axon guidance. Due to the expression of Eph/ephrins during gastrulation, it has been suggested that the ancestral function of Eph receptors might have been the regulation of cell movement [28, 30]. Interestingly, Eph receptors and ephrin ligands followed different evolutionary paths in which there was a single receptor for the two different classes of ephrin ligands. Functional similarities between EphA and B subclasses suggest that duplication and diversification of ancestral receptors and ligands likely occurred to allow for subtle variations of the same function in different cell and tissue types [30].

2.2 Bidirectional signaling of Eph/ephrins

Ephrin interaction with an Eph receptor on a neighboring cell can activate both forward and reverse signaling through the receptor and ligand, respectively (Figure 1). Although there is some promiscuity in Eph receptors binding to the alternative ephrin subclass, each receptor-ligand combination has a distinct binding affinity for one another and, depending on the tissue, there can be a variety of receptor-ligand combinations expressed at boundaries [25, 26, 31]. This asymmetric expression pattern of receptor and ligand helps initiate and maintain differential signaling outputs in distinct cell populations.

Ephrin-B ligands contain a cytoplasmic domain that can be phosphorylated upon activation by Eph receptors, thereby having its own signaling properties [32-37]. Effector binding can be increased or decreased depending on ephrin-B phosphorylation status. Reverse signaling through ephrin-Bs often results in alterations in cytoskeletal dynamics. For example,

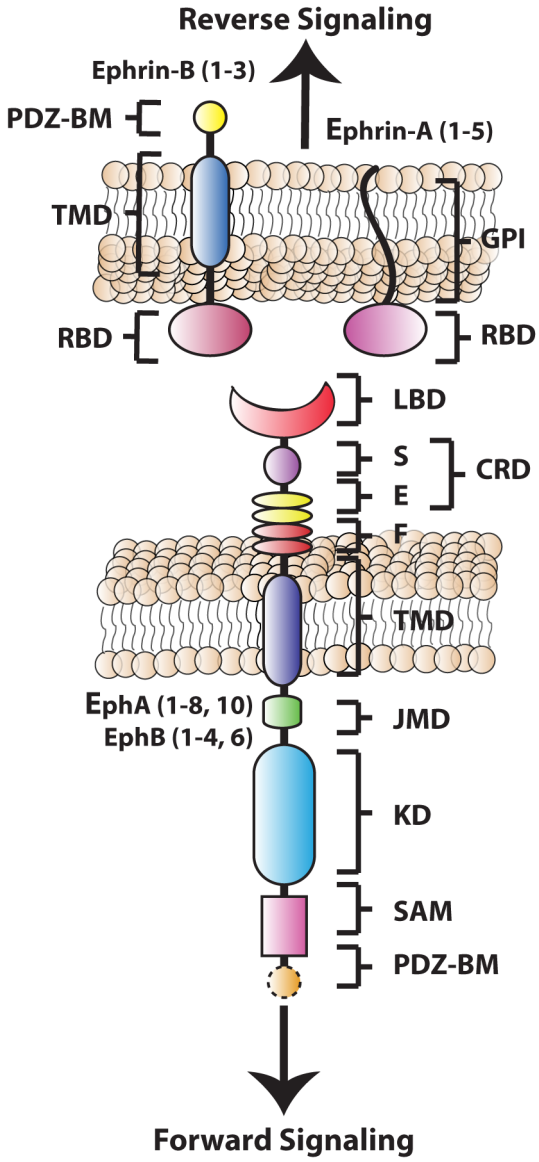

Figure 1: Eph receptors are activated by ephrin ligands at cell-cell contacts.
Eph receptors are activated by ephrin ligands on adjacent cells. Eph receptors contain a ligand binding domain (LBD), cysteine-rich region (CRD) that is composed of a Sushi domain (S) and an epidermal growth factor-like motif (E), fibronectin type-III repeats (F), transmembrane domain (TMD), juxtamembrane domain (JMD), kinase domain (KD), sterile-α-motif domain (SAM), and a PSD95/Dlg/ZO1 (PDZ)-binding motif. Ephrins contain a receptor binding domain (RBD) and either have a GPI-linkage or a TMD followed by a PDZ-binding motif. Eph receptors are subdivided into A and B subfamilies; EphA receptors have a higher affinity for GPI-linked ephrin-A ligands and EphB receptors preferentially bind transmembrane ephrin-B ligands. Eph receptor activation can result in bidirectional signaling, where there is forward signaling through the receptor expressing cell and reverse signaling through the ligand expressing cell.

ephrin-B1 and ephrin-B3 phosphorylation results in the binding of Src homology 2/Src homology 3 (SH2/SH3) adaptor protein, Growth Factor Receptor-Bound Protein 4 (Grb4). When Grb4 binds to ephrin-B1, it can act as a linker to a variety of cytoskeletal regulating proteins causing an increase focal adhesion kinase (FAK) activity and disassembly of F-actin stress fibers [33]. Also, Grb4 recruitment to ephrin-B3 can lead to Ras-related C3 botulinum toxin substrate (Rac)/Cycle division cycle 42 (Cdc42) and effector P21 Activated Kinase (PAK) activation by interacting with dedicator of cytokinesis 180 (Dock180) guanine exchange factor (GEF) [35]. Alternatively, ephrin-B1 phosphorylation can disrupt its interaction with partitioning defective-6 (Par6) resulting in increased Par-6 binding to Cdc42 and subsequent TJ formation [38]. The activity of ephrin-Bs can be initiated by phosphorylation through Src family kinase (SFKs) and terminated by PSD95/Dlg/ZO1 (PDZ) domain-containing phosphatases [37].

Ephrin-A ligands lack a cytoplasmic domain, which requires their reverse signaling to be exclusively PDZ-independent. As such, the mechanisms governing ephrin-A reverse signaling remain relatively unclear [9, 39]. Most notably, ephrin-A5 can be compartmentalized in caveolae-like membrane domains where its activation causes Src-family kinase phosphorylation and initiation of mitogen-activated protein kinase (MAPK) signaling through integrin β1 [40, 41]. Additionally, ephrin-A5 can negatively regulate epidermal growth factor receptor (EGFR) signaling by enhancing E3 ubiquitin-protein ligase c-Cbl binding to EGFR thereby promoting EGFR ubiquitination and degradation [42]. Similarly, ephrin-A4 can also induce Src kinase activation [43]. It is likely that these responses are facilitated by interaction with transmembrane domain receptors or membrane reorganization; however, these elements remain unknown.

2.3 Formation of Eph/ephrin signaling clusters

Ligand binding causes the formation of Eph signaling clusters that exceed the size of their interacting ephrin surface. Therefore ligand binding elicits receptor oligomerization of unbound receptors [44]. This is initiated by dimerization of two liganded Eph/ephrins to form a tetramer [45]. The Eph extracellular domain (ECD) acts as a dimerization interface and promotes the assembly of continuous oligomers. The speed of Eph receptor clustering can alter downstream signaling pathways. Following initial activation and nucleation of Eph/ephrin polymers, large-scale Eph/ephrin complexes can be formed by condensation of several Eph/ephrin polymers rather than the recruitment of additional Eph receptor monomers [46]. When Eph receptors are expressed at high enough concentrations, oligomerization can also occur independently of ligand biding [47]. The size of higher-order clustering is a mechanism utilized by Eph receptors to regulate the strength of downstream signaling [48, 49].

2.4 Cis-inhibition by ephrin ligands

Opposed to canonical trans-induced activation of Eph receptors, ephrin ligands can inhibit Eph forward signaling when ligand and receptor are expressed in the same cell [50]. This cis-inhibition can occur when ephrin ligands directly interact with the Eph ligand binding domain (LBD) or indirectly by preventing formation of Eph signaling clusters within the plasma membrane [51, 52]. Cis-inhibition is a mechanism employed by cells for repulsion and boundary formation [8]. Conversely, when cis-inhibition is misregulated it can lead to tumor development [9].

2.5 Eph/ephrins in cell repulsion and boundary formation

Eph/ephrin signaling is important for initiating cell repulsion cues in a variety of cell types. For example, axon repulsion for retinotectal patterning is dependent on Eph RTK activity [53]. This mapping is partially controlled by the balance of cis and trans interactions between Eph receptors and their ligands [51, 52, 54]. The relative degree of trans and cis interactions leads to either repulsion or attraction, respectively, therefore controlling cell connectivity and neuronal responses. Ephrin-A1-induced forward signaling through EphA4 targets the Ras homolog gene family member A (RhoA) GEF ephexin, ultimately leading to growth cone collapse [55]. This suggests that the complementary expression profile of Eph/ephrins can lead to guidance cues for the trajectory of neurons and the formation of topographic maps in the visual system.

Counter gradients of Eph receptors and ephrin ligands in adult tissues helps set functional boundaries within an organ system [11]. Many tissues including skin, intestine, and bone marrow contain a stem cell niche where the progenitor cell population is separated from their differentiated progeny [56-58]. EphA2 expressing cardiac stem cells are separated from ephrin-A1 expressing cardiomyocytes creating a segregated niche for the receptor bearing stem cell population. Cardiac infarction causes an increase in cardiomyocyte ephrin-A1 expression, which drives the migration of EphA2 expressing progenitor cells into the infarcted area [59]. There is a similar countergradient of EphA2 and ephrin-A1 seen in the limbus and cornea, although the expression pattern is reversed. Ephrin-A1 is abundantly expressed in the stem-cell enriched cornea, whereas EphA2 is increased in the differentiated corneal epithelium. In corneal wounds there is an enrichment of ephrin-A1 expression, possibly driving repulsion of EphA2 expressing

cells into the wounded area to promote closure [60]. These differential Eph/ephrin expression patterns can be altered or perturbed under stress or in diseased states resulting in disruption of cell-cell communication and tissue homeostasis [9, 61, 62].

Similar gradients of Eph/ephrins play important roles during the early stages of tissue morphogenesis where ephrin stability at the membrane can modulate adhesive and transcriptional pathways. During gastrulation, increased expression of XLerk, the Xenopus laevis ortholog of human ephrin-B1, is important in mesoderm formation [63]. Ephrin-B1 reverse signaling can activate RhoA and Janus kinase 2 (JAK2)-induced signal transducer and activator of transcription 3 (STAT3) transcriptional activity, thereby modulating c-Jun N-terminal kinase (JNK)-induced cell survival cues and the expression of genes involved in tissue separation [64-66] (Figure 2). Similarly, activation of STAT3 is required for cell movement during gastrulation in zebrafish embryos [67]. These coordinated events initiated by ephrin-B1 effect early tissue separation events that lay the path for precise morphogenetic outcomes later in development.

As embryonic development progresses, there is differential expression of Eph/ephrins at the ectoderm-mesoderm boundary [68]. The ectoderm expresses high levels of EphB3, EphB4, and ephrin-B3, whereas the mesoderm expresses EphA4 and ephrin-B2. The asymmetry of these receptor-ligand pairs in their distinctive compartments is required to maintain the boundary between ectoderm and mesoderm [69]. This interface contains a continuous cycle of cell repulsion, detachment, and reattachment between receptor and ligand bearing cells. For example, forward signaling through EphB4 in the ectoderm activates RhoA and Rac, resulting in

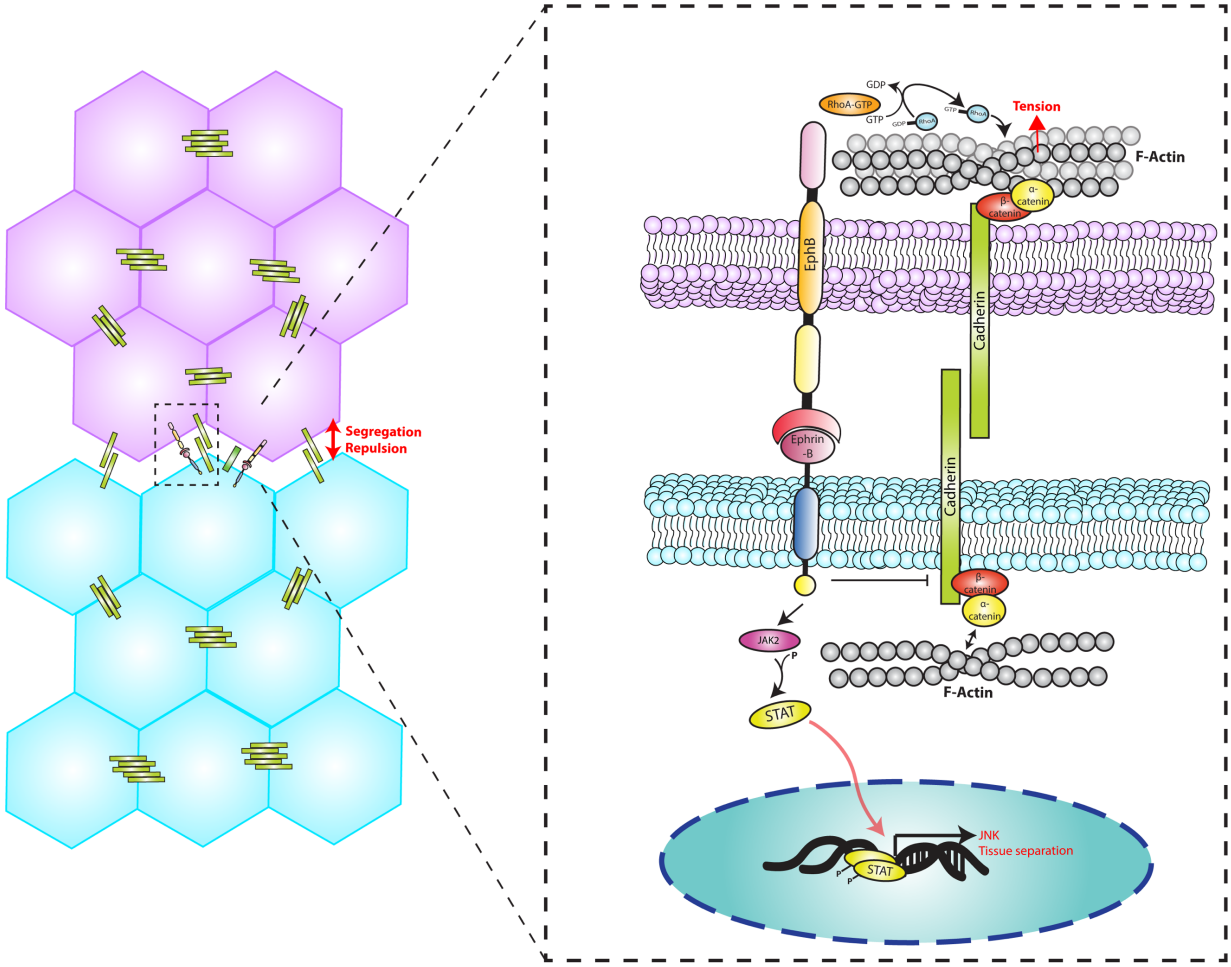

Figure 2: Eph/ephrin signaling promotes cell repulsion and boundary formation.
Eph receptors are asymmetrically distributed from their ligands at cell-cell contacts. Eph forward signaling promotes actin reorganization through RhoA-GTP signaling generating the tension needed to form discrete regions. Reverse signaling through ephrin-Bs activate a JAK2/STAT pathway that promotes JNK-induced cell survival pathways and tissue separation. Reverse signaling also inhibits cadherin-dependent adhesion strength resulting in tissue separation. This figure is modified from [8].

cell repulsion, but once this receptor signal decays at the membrane, the boundary stabilizes again allowing for the juxtamembrane presentation of receptor-ligand pairs that then set off another round of repulsive events [70]. This complementary expression of Eph/ephrins is a common theme that drives tissue patterning and organization in the blastula, formation of stripes in the presumptive hindbrain of zebrafish embryos, and patterning of the developing nervous system [8].

2.6 Eph/ephrins in carcinogenesis

There are many similarities between the cellular mechanisms that govern developmental processes and tumorigenesis [71]. Since Eph/ephrin signaling regulates embryogenesis and organogenesis it is not surprising that they have also been shown to be involved in cancer development. Forward signaling initiated by ephrin ligand can inhibit oncogenic pathways such as the proliferative, Harvey rat sarcoma proto-oncogene (HRAS)-Extracellular signal-regulated kinase (ERK), and the migratory, Phosphoinositide 3-kinase (PI3K)-Protein kinase B (Akt), pathways [9]. Also, activation of Eph receptors enhances formation of cadherin-based cell-cell contacts, promotes cell compaction, and induces apico-basal cellular polarity [72-74]. Cis-inhibition can promote tumor formation by mitigating these tumor suppressive effects of Eph receptor activation. For example, when endogenous ephrin-A ligands are removed from the cell surface in breast cancer cell lines that express both EphA2 and ephrin-A ligands, it results in enhanced EphA2 activation by ephrin-A1-Fc in trans [54]. Thus, the subcellular distribution of ephrin ligands relative to their receptors plays an important role in the balance between forward and reverse Eph signaling [75, 76].

Misregulated expression of Eph/ephrins is seen in many different types of cancers due to chromosomal abnormalities, altered epigenetics, and abnormal transcriptional regulation due to aberrant upstream signaling pathways [9]. In many cases, there is an upregulation of Eph receptors that are poorly activated due to lack of ligand [77-80]. Moreover, activation of Akt promotes phosphorylation of S897 of EphA2, which leads to EphA2-dependent cell migration and invasion. This signaling can be mitigated by ephrin-A1-induced activation of EphA2 and decreased pS897 EphA2, implying that forward signaling initiated by ephrin ligands can prevent hyperproliferation [9, 12, 80-82].

3. Structural features of Eph/ephrins

3.1 Contrasting ephrin ligands

Although both ephrin-A and –B ligands activate Eph receptors, they have many structural differences (Figure 1). The main difference between ephrin-A and ephrin-B ligands is the mechanism of attachment to the cell membrane; Ephrin-A ligands contain a GPI-anchor which can target it to lipid raft membrane microdomains, whereas ephrin-Bs contain a single-pass TMD. For ephrin-Bs, the TMD is followed by a highly conserved PDZ binding motif. This motif can mediate interactions with proteins that contain a PDZ domain, therefore acting as a scaffold for downstream signaling mediators [32, 83-85]. Also, upon Eph binding, ephrin-B ligands can be phosphorylated on cytoplasmic tyrosine residues causing it to have both ligand- and receptor-like properties [36]. Both ephrin-A and –B ligands contain a receptor-binding domain (RBD) at its N-terminus that undergoes significant rearrangement when binding to a receptor. The RBD is followed by a flexible membrane-proximal linker containing approximately 40 amino acids [84,

86]. Ligand binding then causes activation of their corresponding subclass of receptors, although some promiscuity between subclasses does occur [24, 25].

3.2 Molecular domains of Eph receptors

Eph RTKs are single-pass transmembrane receptors and therefore have an ECD, TMD, and cytoplasmic domain (CD) (Figure 1) [87]. The LBD of Eph receptors is located at the most N-terminal region and is composed of β-sheet segments interspersed with loops [88]. When an Eph receptor binds to an ephrin ligand they form heterodimers that can then tetramerize to form high-ordered oligomers [87]. Neighboring the LBD is a cysteine-rich domain (CRD) that contains a sushi domain followed by an EGF-like motif [87]. The CRD plays a role in ligand-binding affinity and the polymerization of Eph receptor oligomers by interacting with the LBD of adjacent receptors [88, 89]. Finally, most proximal to the membrane are two fibronectin-type-3 (FNIII) domains [87]. The FNIII domains contain a membrane-binding site that stabilizes the flat unliganded and upright liganded configurations [90]. These ECD domains are not only important for ligand binding, but also for forming an interface for receptor oligomerization [87].

Similar to many other RTKs, Eph receptors are embedded into the cell membrane by their single-pass TMD [91]. Ligand binding induces a TMD conformational change that is stabilized through a dimerization motif and promotes reorganization of neighboring unliganded receptors [92]. Inactive dimers are arranged with a TMD crossing angle of 15 degrees; upon activation, the TMD crossing angle transitions to 45 degrees. This causes the TMD helix to shorten by about three Angstroms and transitions the CD into a proactive confirmation [92, 93]. Interestingly, it has been shown that lipid bilayer thickness can affect the receptor tilt angle of platelet-derived growth factor receptor (PDGFR); as the lipid bilayer gets thicker, the tilt angle

of PDGFR decreases [94]. Therefore, one would predict that when EphA2 has a larger crossing angle it would favor a thinner lipid bilayer compared to when EphA2 has a smaller crossing angle.

Following ligand binding, autophosphorylation of two conserved tyrosine residues in the juxtamembrane domain (JMD) causes the Eph CD to have a conformational change, which moves the kinase domain away from the plasma membrane thereby removing its steric hindrance. Opening of the CD allows for phosphorylation of the activation loop within the kinase domain, which can then activate downstream effectors or act as a scaffold for signaling molecules [84, 95-98]. Adjacent to the kinase domain is a sterile-α motif (SAM) domain that acts as a protein binding module to SH2-domain containing and SAM-domain containing proteins, including other Eph receptors aiding in receptor dimerization [99, 100]. Lastly, Eph receptors contain a PDZ-binding motif at their cytoplasmic tail that can interact with PDZ domain-containing proteins [84, 101]. These structural features allow for the formation of signaling complexes at sites of cell-cell contacts resulting in activation of a vast array of downstream signaling pathways [9, 102].

3.3 Differences between EphA1 and EphA2 protein structure

Although EphA1 and EphA2 have a high amino acid sequence homology, approximately 65 percent, they contain a few key structural domain differences that may lead to differences in their downstream signaling. The in vitro binding affinity of EphA1 and EphA2 to ephrin-Fc recombinant proteins varies greatly; EphA2 has higher affinity for all ephrin-A ligands except for ephrin-A4, which has a similar binding affinity to EphA1 and EphA2 [24, 31]. It is unknown

whether the LBD or another region of the ECD is the underlying reason for the differences observed in binding affinities.

The TMD plays an important role in membrane microdomain localization; small differences in the amino acid sequence and length of the TMD can alter a protein's membrane localization due to minimization of the hydrophobic effect [103]. EphA1 and EphA2 exhibit low sequence homology in their TMD, approximately 36 percent, which is much lower than the entirety of the receptor. Also, the TMD of EphA2 is predicted to be comprised of 24 amino acids, whereas EphA1's TMD is predicted to be 21 amino acids [92]. On the contrary, it was experimentally determined that the TMDs of EphA1 and EphA2 both likely contain 25 amino acids. However, due to EphA2 having a smaller TMD crossing angle compared to EphA1, the TMD length of EphA2 is approximately 3 Angstroms longer than EphA1. Therefore, even though there are some discrepancies between predicted and experimentally identified TMD regions it is likely that the TMD length of EphA2 is greater than that of EphA1 [93].

The CDs between EphA1 and EphA2 are highly conserved. EphA2 is known to have four tyrosine phosphorylation sites (Y589, Y594, Y735, Y772) and a serine phosphorylation site (S897) in its cytoplasmic tail, all of which are conserved with EphA1 [97]. However, one major structural divergence between the CD of EphA1 and EphA2 is that EphA1 lacks a PDZ-binding motif at its cytoplasmic tail [104]. The consequence of this difference is unknown, but it may lead to differences in binding partners that likely alter downstream signaling outputs.

4. Background of skin

4.1 Anatomy of skin

Although it is debated whether skin is the largest organ in the body, it is the outer layer of the body that provides protection from external insults [1]. Skin is composed of two main layers including the outer epithelium called the epidermis and the lower layers of connective tissue called the dermis. The dermis is separated from the epidermis by a basement membrane (BM) extracellular matrix that is rich in type IV collagen and laminin [105].

The epidermis is a multilayered squamous epithelium that contains the interfollicular epidermis (IFE) and its associated appendages including hair follicles, sebaceous glands, and sweat glands. Keratinocytes, melanocytes, immune cells, and mechanosensory cells compose the epidermis. Terminally differentiated keratinocytes are shed from the uppermost layers of the skin and are replenished from keratinocyte stem cell populations [105, 106].

The dermis is organized into two layers. The layer closest to the epidermis is the papillary layer and the layer beneath, is the reticular layer. Fibroblasts are the main cell type of the dermis and their density is higher in the papillary layer compared to the reticular layer. Additionally, the reticular layer of the dermis has a high abundance of fibrillar collagen [105, 106]. The deepest layer of skin is the subcutaneous fat layer that is primarily comprised of adipocytes. Adipocytes play an important role in regulating the growth factor niche during the hair follicle cycle and promoting fibroblast function during wound healing [107, 108].

4.2 Epidermal morphogenesis

The epidermis must balance proliferation and differentiation in order to develop a functional barrier to protect from dehydration, microbial insults, and mechanical trauma. The

epidermal differentiation process occurs as proliferating basal cells divide asymmetrically, perpendicular to the BM, to form both a suprabasal differentiated cell and another basal cell. Alternatively, basal cells can delaminate from the BM resulting in stratification. In order to increase progenitor cell number, basal keratinocytes can divide symmetrically and parallel to the BM, thus generating two basal daughter cells [109]. Once fully developed, the epidermis is composed of the stratum basale attached to the BM and the suprabasal layers composed of the stratum spinosum, stratum granulosum, and the outer barrier known as the stratum corneum [2].

The epidermis is established during embryogenesis, where development is tightly regulated with specific transcriptional programs. In mice, epidermal development is completed in about ten days between E8.5, when the ectoderm commits to an epidermal fate, until E18.5, when the epidermal barrier is sufficiently formed [110-112]. Interestingly, ephrin-A1 begins to be expressed at 8 days post coitum (dpc) in the primitive streak and lateral mesoderm, similar in time as epidermal commitment. Then, EphA receptors begin to be expressed at 9 to 9.5 dpc [113]. Throughout mouse and *Xenopus laevis* embryogenesis, ephrin-A ligands and their corresponding EphA receptors are often expressed in complementary domains [68, 69, 114]. These expression patterns suggest that Eph/ephrin borders play an important role in determining boundaries during gastrulation, thus promoting ectoderm and mesoderm maturation.

Adult epidermis contains an integrated network of cellular junctions, signaling complexes, and cytoskeletal components. During stratification and differentiation, keratinocytes undergo a dynamic process in which these networks have to be reorganized. Additionally, the organization of many adhesion complexes are polarized throughout the tissue in a similar manner to polarized simple epithelium [2, 115]. Keratinocytes in the basal layer are attached to

extracellular matrix (ECM) components through heterodimerization of alpha and beta integrin subunits to form focal adhesions. These adhesions then associate with the actin cytoskeleton through various adaptor proteins like paxillin, talin, and kindlin. However, specific dimerization of α6 and β4 integrins form a hemidesmosome, which is tethered to intermediate filaments by cytolinker proteins plectin and bullous pemphigoid antigen 1e (BP230) [2, 116]. Epidermal stem cells contain a high expression of integrin β4 [117]. These integrin-based complexes can crosstalk with EGFR to induce proliferation through MAPK signaling therefore maintaining proliferation of progenitor cells [118]. Expansion of integrins into suprabasal cells are seen during wound healing or diseased states like psoriasis leading to hyperproliferation [116]. Alternatively, loss of focal adhesions is seen in tumors and likely play a role in tumor progression eventually leading to tumor invasion into the BM [119, 120].

In addition to focal adhesions, adherens junctions (AJs) are also anchored to the actin cytoskeleton, but attach cells to each other rather than to the basement membrane. Epithelial calcium-dependent adhesion protein (E-cadherin) is a transmembrane adhesion molecule that forms AJs. E-cadherin contains extracellular cadherin-binding domains that undergo calcium-dependent conformational changes allowing for it to homodimerize at the membrane. Dimer stabilization is also dependent on the intracellular domain that binds to β-catenin which can then link to α-catenin. Subsequently, α-catenin can recruit actin nucleating proteins and actin binding protein like vinculin, Ajuba, myosin VIIA, and α-actinin. Also, p120 catenin binds to the E-cadherin juxtamembrane domain and regulates E-cadherin turnover and trafficking [121]. During calcium-induced cell-cell contact stabilization, AJs form at the apical region of contacting cells and generate RhoA and Rho-associated protein kinase (ROCK)-dependent actin tension. AJs

continue to assemble top-down resulting in an “adhesion zipper” of actin cables that extend through the epidermal sheet. Adhesion zipper formation allows for neighboring cells to displace each other in order to generate a stratified tissue [122]. Although loss of E-cadherin in the IFE can be compensated by other cadherins, its loss leads to hyperproliferation and decreased differentiation having features of precancerous lesions [123, 124]. These defects show the importance of AJs in anchoring cells to the actin cytoskeleton network to maintain epidermal homeostasis.

Desmosomes are another type of cell-cell adhesion complex in keratinocytes and are composed of transmembrane desmosomal cadherins, armadillo family proteins, and the plakin family of cytolinker proteins. Opposed to AJs, desmosomes provide a link to the intermediate filament keratin network, which is the major structural cytoskeletal component in keratinocytes. Desmoglein (Dsg) and desmocollin (Dsc) are the two types of desmosomal cadherins that mediate cellular adhesion in the intercellular space. The armadillo family proteins, plakoglobin and plakophilin, bind to the cytoplasmic tail of Dsg and Dsc. These armadillo family proteins recruit the cytolinker protein, desmoplakin, which bind keratin intermediate filaments. Epidermal keratins are a family of closely related, but distinct proteins that are differentially expressed during the course of differentiation [2, 125-127]. Upon keratinocyte differentiation, keratin-5 and keratin-14 are downregulated and keratin-1 and keratin-10 (K10) are induced in the suprabasal layers [128]. Similarly, desmosomes display a differentiation-dependent expression profile; during differentiation Dsg2/3 and Dsc2/3 are decreased, whereas Dsg1 and Dsc1 are increased [2, 129]. Specifically, expression of Dsg1 is required to suppress EGFR activity, promoting keratinocytes to commit to a program of terminal differentiation [130]. Due to the specific

localization in the epidermis, keratins and desmosomal cadherins are often used as markers to assess keratinocyte differentiation.

The most apically localized adhesive complexes are tight junctions (TJs). TJs contribute to the skin's barrier function by forming a network in the second stratum granulosum (SG) layer, SG2, of the epidermis [131]. TJs create both an "outside-in" barrier that protects the skin from environmental insults like toxins, allergens, and pathogens and an "inside-out" barrier that prevents the body from water loss [2, 132, 133]. SG2 cells have a flattened Kelvin's tetrakaidecahedron shape that contains 14-sides, of which six are rectangular and the other eight are hexagonal with TJs formed along the edges. This unique cell shape allows for TJ replacement during cell turnover while maintaining the TJ barrier [134]. TJs are composed of the quadruple transmembrane spanning proteins, claudin and occludin, and the scaffolding proteins, zona occludens (ZOs), which connect the TJ transmembrane proteins to the actin cytoskeleton [135-137]. The importance of a functional TJ barrier in skin is seen in mice lacking claudin-1, which causes mice to die shortly after birth due to excessive dehydration [138]. In humans, a TJ barrier defect has been associated with skin diseases like psoriasis and atopic dermatitis [132].

4.3 Epidermal RTK signaling

In addition to adhesion transmembrane receptors, keratinocytes also contain a variety of transmembrane signaling receptors that send and receive autocrine, juxtacrine, paracrine, and endocrine signals. Although there is an extensive list of these proteins, a majority of these complexes can be categorized as either ion channels, G-protein coupled receptors (GPCRs), or enzyme-linked receptors, including RTKs and receptor protein tyrosine phosphatases (RPTPs)

[139]. Specifically, RTKs, RPTPs, and GPCRs are known to crosstalk with Eph receptors thus modulating each other's downstream signaling [96, 140-143].

In addition to Eph RTKs, there are many other RTK families that play important roles in regulating epidermal homeostasis, one of which is the transmembrane avian erythroblastic leukemia viral oncogene (ErbB) tyrosine kinase receptor family. They are activated by ligands that include epidermal growth factor (EGF), heparin-binding EGF (HB-EGF), transforming growth factor (TGF), amphiregulin, epiregulin, epigen, betacellulin and more distantly neuregulins. These ligands are often proteolytically processed by cleavage of the extracellular fragment containing the EGF module resulting in autocrine, endocrine, and paracrine signaling [144]. Ligand binding causes homo- or heterodimerization of EGFR (EGFR/ErbB1), HER2 (ErbB2), HER3 (ErbB3), and HER4 (ErbB4) and can lead to activation of downstream signaling pathways including STAT, Akt, ERK, and protein kinase C (PKC) affecting survival, proliferation, cell-cycle, migration, and differentiation [145, 146].

The EGFR signaling pathway plays an important role in keratinocyte migration beginning at ligand shedding. When ligand cleavage is inhibited, keratinocyte migration is suppressed resulting in delayed reepithelization [147]. As exhibited in HB-EGF knockout mice, wound healing is delayed due to decreased keratinocyte migration [148]. Also, wound repair is delayed in EGFR knockout mice from impaired reepithelization and wound contraction due to aberrations in migration, proliferation, inflammation, and angiogenesis. A large contributing factor to the EGFR migration response is because its downstream signaling pathways enhance proliferation. However, EGFR can also phosphorylate β4 integrin, promoting hemidesmosome disassembly, thus enhancing migration [149].

Another essential RTK in keratinocytes is the fibroblast growth factor receptor (FGFR) [145]. There are 22 types of fibroblast growth factors (FGFs) that can bind and activate the four FGFR family members (FGFR1-4) [150]. Specifically, FGF7, FGF10, and FGF22 can target FGFR1 and FGFR2 on keratinocytes [151]. Individual knockout of FGF7, FGF22, or FGFR1 does not affect wound healing. But, expression of a dominant negative FGFR2 in keratinocytes decreases keratinocyte migration. This mutant inhibits signaling through all FGFRs in response to common ligands suggesting that FGFR1 and FBFR2 collaborate to stimulate reepithelization [152].

4.4 Eph crosstalk with other RTKs

Eph/ephrins can interact with a variety of RTKs resulting in receptor crosstalk [141]. The juxtamembrane domain of FGFR can bind to the kinase domain of EphA4 to form a complex. FGFR and EphA4 can promote phosphorylation of the alternative receptor resulting in activation of downstream signaling pathways [153]. Moreover, there is crosstalk between FGFR and ephrin-B1 ligand. Ectopic expression of ephrin-B1 results in cell dissociation, which can be rescued with FGF treatment. Following FGF-induced activation of FGFR, FGFR can interact with ephrin-B1 inducing tyrosine phosphorylation of its cytoplasmic tail increasing cell adhesion [154, 155].

EphA2 can also bind to EGFR in cis orientation. EGFR can interact with and stabilize EphA2 in an EGFR tyrosine-kinase independent manner [156]. Whereas ephrin-A binding to EphA2 inhibits MAPK activity, when the growth factor progranulin binds and activates EphA2, as well as EphA4 and EphB2, it leads to EGFR phosphorylation and subsequent activation of MAPK and Akt signaling pathways [157, 158]. The ability of EphA2 to crosstalk with EGFR is further

corroborated by the EphA2 interactome in keratinocytes. EGFR is one of the most abundant interactors identified in keratinocyte cultures [159]. The ability of EphA2 to crosstalk with other RTKs is dependent on being in close proximity to each other. However, the relative membrane microdomain localization between EphA2 and other RTKs and how this affects their downstream signaling is relatively unknown.

4.5 Models utilized for studying epidermal biology

In order to better understand epidermal differentiation in vitro, 2-D submerged and 3-D reconstituted human epidermis (RHE) models can be used (Figure 3 A). When keratinocytes are plated at low density and in low calcium (Ca^{2+}) (<0.1 mM) they continue to proliferate and remain in an undifferentiated state. However, when normal keratinocytes are confluent they undergo contact-dependent inhibition of growth and cease to proliferate. Confluent keratinocytes can then be induced to differentiate with the addition of high Ca^{2+} (> 1mM) [160]. Lastly, when keratinocytes are cultured with an intermediate Ca^{2+} concentration (~0.1 mM), they can form loose colonies with AJs, but lack desmosomes. This results in stabilized cell-cell contacts with minimal differentiation [161]. Although a variety of keratinocyte cell lines exist, we utilized primary normal human epidermal keratinocytes (NHEKs) allowing for us to better study physiological mechanisms governing keratinocyte behaviors [162].

Epidermal differentiation can be further studied in 3-D RHE cultures, in which keratinocytes are plated onto a fibroblast-containing collagen plug. After lifting the collagen plug to an air-liquid interface (ALI), the keratinocytes begin to stratify and differentiate to form all the layers of the epidermis over a period of nine days (Figure 3 B). Utilizing these different strategies allows for a better understanding of the epidermal differentiation process [163-165].

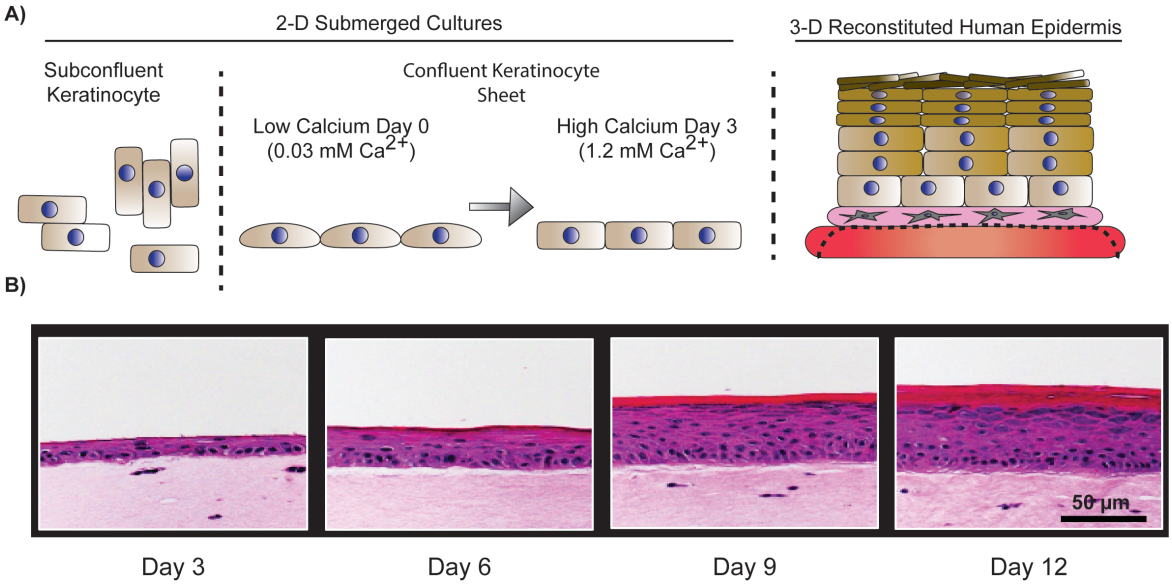

Figure 3: Epidermal models of keratinocyte differentiation.
(A) Subconfluent keratinocytes can be used to study keratinocytes in an undifferentiated, proliferative state. In order to understand mechanisms governing epidermal differentiation, confluent keratinocyte sheets can be switched from low (0.03 mM) to high (1.2 mM) calcium concentrations. Reconstituted epidermis models can be used to mimic the 3-D architecture of the human epidermis. In this model, keratinocytes are plated onto a fibroblast-containing collagen plug and then lifted to an air-liquid interface. After lifting, keratinocytes stratify to form all the epidermal layers. **(B)** H&E staining of RHE at different days after airlifting. (Scale bar=50 µm).

Similarly, wound healing can be studied in vitro in both 2-D and 3-D keratinocyte models. To mimic wound healing in 2-D cultures a scratch can be made in confluent keratinocytes. The keratinocytes then form a leading edge and migrate into the wounded area until the wound is fully closed [166]. This process can also be studied in 3-D RHE models. After RHE cultures have differentiated, a punch biopsy can be made to mimic a wound. This allows for keratinocytes to generate an extending epidermal tongue and migrate into the wounded area. After wound closure, keratinocytes can stratify and form a fully differentiated epidermis [167]. Combining these differentiation and migration models helps give insight into the mechanisms underlying disease development.

5. Eph/ephrins mediate epidermal functions

5.1 Opposing roles of ephrin-A1 in keratinocyte differentiation and migration

Eph/ephrin signaling has been shown to play an important role in balancing proliferation of the basal epidermal layers with differentiation of the suprabasal layers [10, 11]. EphA2 is the predominant Eph receptor transcript in subconfluent keratinocytes. But, its mRNA and protein level decrease during calcium-induced differentiation. EphA1 and EphA4 are the other prevalent Eph receptors expressed in keratinocytes. EphA1 protein expression remains relatively stable during calcium-induced differentiation, whereas EphA4 increases. As calcium-induced differentiation continues there is also an upregulation of ephrin-A1 transcript levels, but its protein level remains unchanged [15]. Induction of forward signaling by ephrin-A1-Fc treatment, activates EphA2, dampens extracellular signal-related kinase (ERK) signaling, and promotes keratinocyte differentiation. Similar patterns are seen with calcium-induced keratinocyte

differentiation suggesting that ephrin-A1 is a positive regulator of keratinocyte differentiation [12].

Although the protein expression level of ephrin-A1 does not change during keratinocyte differentiation, the ephrin-A1 gene is located, along with ephrin-A3 and ephrin-A4, on Ch1q21-22 within the epidermal differentiation complex (EDC) that contains a series of genes associated with keratinization [10, 15, 22]. Ephrin-A1 is concentrated in the basal layer of the epidermis, which is where EphA2 has a cytoplasmic localization pattern. In the suprabasal layers where there is less ephrin-A1, EphA2 then localizes to cell junctions [15, 168]. The distribution pattern likely allows for Eph/ephrin interactions between adjacent cells in the proliferative basal layer and at the basal/suprabasal interface, where keratinocytes commit to a program of terminal differentiation [10].

As opposed to keratinocyte differentiation, keratinocyte migration is negatively regulated by ephrin-A1. Ephrin-A1 inhibits keratinocyte migration in part by acting through EphA2 [13, 14, 80]. In absence of ligand, EphA2 is a substrate of Akt, which phosphorylates EphA2 at its serine 897 residue. Ligand-independent activation of EphA2 promotes EphA2 polarization to the leading edge of a migrating cell resulting in cell migration. However, ephrin-A1-induced activation of EphA2 inhibits keratinocyte migration through dampening of Akt signaling [14, 80]. Therefore, EphA2 ligand-independent signaling is downstream of Akt signaling, whereas ligand-dependent EphA2 activation acts upstream of Akt inhibition making EphA2 an integral regulator of Akt signaling pathways.

5.2 Role of EphA2 in cellular adhesion

One reason Eph/ephrins play a predominant role in boundary formation is due to their ability to regulate adhesive strength [141, 169]. The importance of EphA2 in adhesion is seen in the EphA2 keratinocyte interactome in which cell junction and cell adhesion molecules are abundant [159]. Also, EphA2 can act both upstream and downstream of AJs. E-cadherin expression causes cell-cell contact localization of EphA2 resulting in enhanced EphA2 tyrosine phosphorylation. This causes decreased ECM adhesion, cell growth, and proliferation [12, 72]. Conversely, activation of EphA2 can suppress the activity of ADP-ribosylation factor (Arf)-6 through the GPCR kinase-interacting protein 1, Git1. This results in enhanced E-cadherin adhesion and epithelial cell polarization causing a positive feedback loop with EphA2 [73]. Furthermore, EphA2 forward signaling strengthens Dsg1-dependent adhesion in keratinocytes [12].

5.3 Ephrin-A1 in barrier formation

Since ephrin-A1 can promote early differentiation it may seem logical to predict that ephrin-A1 would enhance the formation of the tight junction barrier. However, in both epithelial and endothelial cell types, ephrin-A1 has been shown to negatively regulate the functionality of tight junctions [15]. In Madin-Darby Canine Kidney (MDCK) cells, activation of EphA2 by ephrin-A1-Fc protein delays Claudin-4 recruitment to tight junctions causing an increase in the permeability of the barrier [170]. Additionally, ephrin-A1-induced activation of EphA2 in pulmonary artery endothelial cells decreased the endothelial monolayer barrier [171]. Furthermore, in brain microvascular endothelial cells, ephrin-A1-induced phosphorylation of EphA2 resulted in misdistribution of ZO-1 and occludin, and increased the permeability of the tight junction barrier [172]. However, in keratinocytes EphA2 has been shown to interact with

the actin-binding protein, Afadin, in order to promote the functionality of the TJ barrier [159]. This suggests that in keratinocytes EphA2 may have a positive role in TJ formation as opposed to its inhibitory role in other cell types.

5.4 Alterations of EphA2/ephrin-A1 signaling in epidermal disease

5.4.1 Wound healing

Wound healing is a dynamic process and keratinocytes are required to coordinate proliferation and junctional rearrangement to allow for complete re-epithelization to occur. When an injury transpires, cells at the wound edge begin to migrate. Proliferation then occurs behind the leading edge causing migratory cells to be lifted and transported upwards to become a suprabasal cell [167, 173]. Aberrations in the wound healing process can lead to chronic ulcers like those developed from ischemia or diabetes [174]. For example, diabetic corneal wounds, which are also a stratified epithelium like that of the epidermis, display a significant delay in wound healing [175]. In diabetic cornea, ephrin-A1 is upregulated, which suggests that reverse signaling through ephrin-A1 can restrict epithelial cell migration [14].

5.4.2 Psoriasis

Due to the ability of ephrin-A1-induced activation of EphA2 to promote keratinocyte differentiation, it is not surprising that alterations in Eph/ephrin signaling are seen in epidermal diseases that have abnormal differentiation programs [12]. In 3-D RHE cultures exposed to the pro-inflammatory cytokines, EGF and interleukin (IL)-1α or tumor necrosis factor (TNF)-α and IL-17A, there is a loss of epidermal differentiation. This correlated with increased EphA2 and decreased ephrin-A1 mRNA and protein expression levels. These differentiation defects can be normalized by treatment with recombinant ephrin-A1-Fc ligand that targets EphA2 to promote

its forward signaling, followed by EphA2 downregulation. Analogous to cytokine-induced RHE studies, microarray analysis revealed that EphA2 transcripts are upregulated and ephrin-A1 transcripts are downregulated in psoriatic plaques [15]. These aberrations are suggestive of a role for EphA2-induced forward signaling in maintaining epidermal homeostasis.

5.4.3 Non-Melanoma Skin Cancer (NMSC)

Similar to psoriasis, EphA2 and ephrin-A1 signaling are often misregulated in NMSCs. In mouse skin carcinogenesis models, loss of EphA2 resulted in accelerated rate of growth and progression to malignancy. This was, in part, due to lack of inhibition of ERK signaling, suggesting that EphA2 acts as a tumor suppressor [168]. EphA2 is also involved in a negative feedback loop through Ras; EphA2 is a direct transcriptional target of the Ras/MAPK pathway and ephrin-A1 stimulation inhibits activation of Ras [176]. This regulatory loop likely maintains increased EphA2 expression resulting in enhanced ERK and MAPK pro-proliferative signaling.

5.4.4 Melanoma

Melanoma develops from the malignant transformation of neural-derived pigment-producing melanocyte cells that normally reside in the basal layer of the epidermis [177]. EphA2 is often upregulated and plays an oncogenic role in melanoma cell lines [178]. This may be in part because neuroblastoma RAS viral oncogene homolog (NRAS) is a common gene mutation that is hyperactive in malignant melanoma. Also, suppression of NRAS results in a downregulation of EphA2, which suggests that hyperactive NRAS would increase the expression of EphA2 [179]. Furthermore, knockdown of EphA2 in EphA2 overexpressing melanoma cell lines reduces cellular viability, colony formation, and in vivo migration and tumorigenic potential [178, 180]. The migratory potential induced by EphA2 is dependent on RhoA signaling [181]. Therefore,

better understanding of EphA2 trafficking and signaling will give insight into how to therapeutically target the EphA2 signaling axis in melanomas where NRAS is mutated.

6. Cell membrane trafficking and signaling complexes

6.1 Membrane trafficking pathways

Endocytosis is required for trafficking of nutrients, pathogens, antigens, growth factors, and receptors into the cell. This can occur by either clathrin-dependent or –independent mechanisms. Three heavy and three light chain clathrin molecules form triskelia and then assemble into a polygonal lattice at the plasma membrane to form clathrin-coated pits. During clathrin-dependent endocytosis (CDE), plasma membrane proteins are recognized by adaptor proteins and packaged into clathrin-coated vesicles and then brought into the cell. However, clathrin-independent endocytosis (CIE) can occur in membrane regions lacking clathrin. Examples of CIE include micropinocytosis and phagocytosis. Independent of entry route, endocytic cargo is delivered to early endosomes were protein sorting occurs. Endosomes can act as signaling platforms by sustaining signals that originate from the plasma membrane or generating unique signaling that was originally prohibited by the plasma membrane due to enrichment of certain lipids and proteins. Endosomes have an acidic pH, which can cause conformational changes that disengage a ligand from its receptor. Endosomal sorting is dependent on PI3K signaling and Ras-related protein Rab (RAB)-5. From early endosomes, cargo can be delivered to either late endosomes and lysosomes for degradation, the trans-golgi network (TGN) for additional sorting, or recycling endosomes that bring the cargo back to the membrane [182-184].

Cargo can be recycled back to the membrane by slow or fast recycling pathways. During fast recycling, proteins are recycled directly back to the membrane from the early endosome. These recycling endosomes are dependent on RAB35 and RAB4. However, most proteins undergo a slow recycling process in which they are transported to an endosome recycling complex (ERC) and then back to the plasma membrane. The ERC contains RAB11 and/or EH-Domain Containing Protein 1 (EHD1) [183].

Polyubiquitination is a signal that is recognized in the early endosome by the endosomal sorting complex required for transport-1 (ESCRT-I) complexes and directs cargo into multivesicular bodies (MVBs). MVBS are transported along microtubules where they eventually fuse with late endosomes. Protein sorting again takes place in late endosomes and proteins can be transported back to the TGN network or towards lysosomes [185]. Lysosomes contain hydrolytic enzymes that function optimally at an acidic pH to degrade internalized proteins [186]. Lysosomes also play an important role during autophagy in which the lysosome fuses with an autophagosome that contains cytosolic proteins and organelles. This generates an autolysosome that leads to degradation of sequestered cargo [187].

6.2 Membrane trafficking pathways of EphA2

Eph/ephrin endocytosis is an important cellular process that regulates the extent of Eph/ephrin signaling [83]. When EphA2 exists as an unliganded monomer it is continuously internalized and recycled back to the membrane via Rab11-positive recycling endosomes. Once recycled back to the membrane it continues to be available for ephrin binding and activation [188].

Following ligand binding and EphA2 activation, EphA2 can recruit PI3K and upregulate phosphatidylinositol (3,4,5)-trisphosphate (PIP3) levels. This causes Rac1 GTPase activation, which promotes cytoskeletal changes resulting in EphA2 endocytosis. During this process, EphA2 also has a negative feedback loop where it binds to SH2 domain-containing inositol 5-phosphatase 2 (SHIP2) and causes a reduction in PIP3 levels therefore attenuating endocytosis mediated by PIP3 and Rac1 [189].

Ephrin-A1-induced activation and oligomerization of EphA2 causes E3 ubiquitin-protein ligase c-Cbl to bind the tyrosine 813 residue of EphA2, where it induces EphA2 ubiquitination. This causes internalization of the EphA2 complex into early endosomes where it can be dephosphorylated by protein phosphatase 1B (PTP1B) and degraded in the lysosome [188, 190]. Instead, EphA2 can be recycled back to the membrane through early endosomes. In these vesicles EphA2 interacts with and activates the Rho GEF T-Cell lymphoma invasion and metastasis 1 (Tiam1). Tiam1 increases Rac1 activity and further promotes Eph/ephrin endocytosis [191]. Overall about 35 percent of internalized receptors are recycled back to the membrane, whereas the remainder goes through a degradation pathway therefore terminating downstream signaling [191]. Although there is some knowledge of the general trafficking pathways of EphA2 from work in cancer cell lines, the trafficking pathways utilized by unliganded EphA2 and following ephrin-A1-induced activation of EphA2 in normal epithelia, like keratinocytes, remain relatively unknown. These pathways likely play important roles in keratinocytes in which ephrin-A1 induces differentiation and inhibits of migration.

6.3 Lipid raft membrane microdomains

Lipid rafts are highly ordered membrane microdomains located in the plasma membrane and rich with a variety of sterols, most notably cholesterol [3]. In mammalian cells, there are two main types of lipid rafts: planar lipid rafts are continuous with the plane of the membrane whereas caveolae-positive lipid rafts form invaginations in the plasma membrane and contain caveolin proteins. Both types of lipid rafts undergo CIE. Lipid raft membrane area can vary greatly ranging from small isolated domains to continuous lipid rafts that cover over 75 percent of the membrane [7, 192]. Lipid rafts are thought to organize protein complexes at the membrane to allow for efficient signal transduction or, alternatively, separate membrane-associated molecules thereby limiting downstream signaling [183, 193].

Highly organized lipid rafts are surrounded by a more dynamic and liquid-disordered cell membrane [194]. Due to their increased order and decreased fluidity, lipid raft microdomains are thicker than non-lipid raft domains [195-197]. Therefore, proteins containing longer TMDs are preferentially targeted to lipid rafts [103]. For example, TMD length has been shown to be important for lipid raft localization in a variety of proteins including linker for activation of T-cells (LAT) and perfringolysin O (PFO) [103, 198]. Also, there is an indirect relationship between TMD amino acid side chain surface area and a protein's affinity for lipid raft domains. Interestingly, the sequence of amino acids in the TMD is less important than the actual amino acids that are present [199]. Furthermore, saturated fatty acids, such as GPI-anchors and palmitate, can target proteins to lipid rafts [200]. Palmitoylation occurs when a saturated 16-carbon palmitic acid is added to specific cysteine residues through the formation of a thioester bond. This process is mediated by palmitoyl acyl transferases (PATs) and depalmitoylated by

palmitoyl protein thioesterases (PPTs) [201]. This reversible process can occur within minutes [202]. However, these lipid modifications are not absolutely required for lipid raft association [7, 203].

6.4 Lipid rafts in the epidermis

In keratinocytes, lipid rafts impact proliferation, migration, apoptosis, and differentiation through mechanisms that remain somewhat unclear, but likely include modulation of signaling proteins, proteases, and adhesion molecules [204-210]. The basal layer of the epidermis is composed of relatively quiescent stem cells and pluripotent transit amplifying cells (TACs), which are derived from these epidermal stem cells and can divide to become differentiated keratinocytes. In the epidermis, lipid rafts are enriched in TACs where they are purported to contribute to the regulation of processes governing tissue homeostasis [204, 211].

6.5 Perturbations of lipid rafts in epidermal disease

Mice lacking caveolin-1 in the epidermis are more susceptible to carcinogen-induced skin tumorigenesis [4]. Additionally, psoriatic lesions exhibit an inverse correlation between severity of disease phenotype and caveolin-1 expression levels [5]. Lipid raft disruption by cholesterol in 3-D RHE results in a transcriptional response that shares features with genomic patterns observed in the inflammatory skin disease, atopic dermatitis [6]. These studies indicate that lipid raft disruption may contribute to skin disease development possibly through impaired epidermal differentiation. However, the mechanisms that are altered in response to epidermal lipid raft disruption still remain unclear.

6.6 RTKs in lipid raft domains

Most proteins that bind to caveolin have a caveolin-binding motif which contains an abundance of aromatic amino acid residues in a short stretch, along with a characteristic spacing of these residues. This caveolin-binding site has been identified in many RTKs including EGFR, insulin receptor, ErbB2, FGFR, and Eph receptors [212, 213]. EGFR is found in both caveolae and non-caveolar planar lipid rafts [214, 215]. Lack of caveolin-1 or lipid raft disruption by cholesterol depletion leads to EGFR hyperactivation [206, 216, 217]. However, depending on EGFR expression level, flotillin-1 knockdown can lead to decreased EGFR activation and signaling [218]. Conversely, increased caveolin-1 suppresses EGFR and its downstream MAPK pathway [219]. Also, ligand-induced phosphorylation of EGFR results in EGFR dissociation from caveolae, implying that caveolin-positive lipid rafts likely negatively regulate EGFR signaling, however planar lipid rafts may have different effects on EGFR signaling [214].

Both EphA2 and EphB1 contain a caveolin-binding motif in their cytoplasmic tail and can interact with caveolin-1 in response to ephrin-A1 and ephrin-B2 treatment, respectively. The aromatic residues in the caveolin-binding motif of EphB1 are not only required for caveolin-binding, but also for cell membrane localization and ephrin-B2-induced activation of ERK [220]. Other than the potential to interact with caveolin-1, the ability of EphA2 to localize to lipid raft domains and its effect on downstream signaling is unknown.

6.7 Ephrins in lipid raft domains

Compartmentalization of ephrins into lipid raft and non-lipid raft domains likely plays an important role in regulating ephrin reverse signaling. Ephrin-As contain a GPI-anchor, which aids in targeting to lipid rafts. Even though ephrin-Bs lack this moiety, they can also localize to

these membrane domains [221]. In murine fibroblasts both ephrin-A5 and ephrin-B1 can localize to lipid rafts; ephrin-A5 is constitutively localized in lipid rafts whereas ephrin-B5 increases its concentration in these domains once activated with EphB2. Reverse signaling through these ligands can cause cytoskeletal reorganization; activation of ephrin-A5 promotes formation of an actin cortical ring and lamellipodia, whereas activation of ephrin-B1 generates actin fibers and filopodia [222]. Additionally, activation of ephrin-A5 recruits Fyn tyrosine kinase to lipid raft domains and causes an increase in cellular adhesion [41]. Moreover, evidence suggests that ephrin-B1 and ephrin-B2 can localize to lipid rafts in leukemia (Jurkat) and melanoma (B16) cells lines, respectively. Lipid raft localization of ephrin-Bs plays an important role in promoting the formation of signaling complexes that induce cell repulsion and migration [223-225].

7. Relevance and research focus

Skin diseases comprise one of the largest burdens of disease worldwide and can include fungal, inflammatory, and proliferative diseases; making it the fourth leading cause of nonfatal burden worldwide [226]. Additionally, in the past 20 years, the United States had one of the largest increases in Disability-Adjusted Life Years worldwide due to skin conditions [227]. Aberrations in RTK signaling pathways can lead to disruption of epidermal homeostasis contributing to the formation of skin disease. One specific RTK pathway that is often altered in skin disease is the EphA2/ephrin-A1 signaling axis [10]. Misregulation of EphA2 and ephrin-A1 is seen in inflammatory skin diseases, NMSCs, and in delayed epidermal wound healing [10]. Better understanding the roles of this signaling pathway in skin disease progression will allow for development of targeted therapeutics that will greatly improve treatment of these diseases.

During keratinocyte cell-cell contact stabilization, EphA2 is abundantly recruited to cell borders where it can be activated by ephrin ligand [12]. Upon Eph/ephrin binding, bidirectional signaling can occur, which can alter many cellular behaviors including proliferation, survival, migration, differentiation, and boundary formation [8, 10, 22]. In keratinocytes, forward signaling induced by ephrin-A1 through EphA2 results in enhanced differentiation and reduced migration [12, 14]. In addition to trans-activation of Eph receptors by ephrin ligands, ephrin ligands can also modify Eph signaling responses through cis-inhibition [76]. Therefore, membrane localization of Eph receptors and ephrin ligands likely play an important role in regulating Eph/ephrin bidirectional signaling in keratinocytes; yet it is unknown how EphA2 and ephrin-A1 localize to specific membrane domains and how this can affect keratinocyte biology.

In the epidermis, ephrin-A ligands are concentrated in basal cells, whereas EphA receptors are localized throughout all epidermal layers. This allows for the formation of Eph/ephrin interactions in basal cells and asymmetrically divided Eph/ephrin boundaries at the basal/suprabasal interface. Ephrin-A ligands contain a GPI-anchor enabling specific targeting to lipid raft membrane microdomains, but the ability of EphA receptors to localize to these membrane domains remains unknown [221]. Interestingly, lipid rafts are also abundant in the basal cell layer of the epidermis leading to the hypothesis that lipid rafts play an important role in organizing Eph/ephrin complexes at cell-cell contacts in keratinocytes [204, 211].

In combination with protein palmitoylation ability and TMD amino acid side chain surface area, a protein's TMD length and amino acid composition can affect lipid raft affinity [199]. Therefore, we aimed to identify the ability of EphA receptors to localize to lipid raft domains and understand how the TMD of EphA2 affects lipid raft and cell-cell contact

localization [199]. The localization of EphA2 is postulated to affect the ability of this RTK to engage with ephrin-A1 ligand to affect keratinocyte differentiation and migration. Appreciation of these mechanisms will give insight into ways to modulate ephrin-A1 and EphA2 localization in order to control downstream signaling and subsequent keratinocyte behavior.

Lipid raft disruption is correlated with inflammatory skin disease development and increased tumorigenesis [5, 6]. This suggests that these membrane microdomains are important for organizing signaling complexes at the membrane in order to maintain epidermal homeostasis. Since Eph/ephrin activation is dependent on cell-cell contacts and ephrin-A ligands contain a GPI-anchor, we anticipated that lipid raft disruption would likely perturb the EphA2/ephrin-A1 signaling axis thus contributing to disease progression. Therefore, elucidating mechanisms governing EphA2 and ephrin-A1 localization, activation, and subsequent downstream signaling under homeostatic conditions will give us insight into how we can normalize these alterations in epidermal disease.

II. MATERIALS AND METHODS

1. Antibodies

Information for antibodies used for Western Blot analysis is in Table 1 and antibodies used for immunofluorescent staining is in Table 2.

2. Primary human keratinocyte cultures

Primary NHEKs were isolated from neonatal foreskins obtained from the Skin Disease Research Center, Skin-Tissue Engineering Core (Northwestern University, Chicago, IL) and isolated as previously described [164]. Foreskins were washed in phosphate buffered saline (PBS), cut into small pieces, and placed in dispase (Roche, Indianapolis, IN; 2.4 U/mL in 50 mM HEPES pH=7.4, 150 mM NaCl) overnight at 4°C. The following day epidermis was peeled away from dermis and incubated in 0.25% trypsin/1 mM ethylenediaminetetraacetic acid (EDTA) for 10-15 minutes at 37°C. Trypsin was inactivated with Fetal Bovine Serum (ThermoFisher Scientific, Walthan, MA) and then epidermal sheets were scraped against the bottom of the plate to extract keratinocytes from the tissue. The suspension was filtered through a 40 μm sieve and the flow through was centrifuged to pellet the cells. NHEKs were resuspended and plated in M154 Complete media (M154; ThermoFisher Scientific) supplemented with human keratinocyte growth supplement (HKGS; ThermoFisher Scientific), 0.25 μg/ml amphotericin B (Mediatech, Manassas, VA), 10 μg/ml gentamicin (Millipore Sigma, St. Louis, MO) and 0.07 mM $CaCl_2$ (ThermoFisher Scientific). Experimental replicates used clones isolated from at least three different donors and pooled in order to account for possible clonal variation. Media was changed every other day.

Table 1: Antibodies used for Western blot.

Protein	Species	Clone/Catalog Number	Dilution	Company	Location
Primary antibodies for Western Blot					
Caveolin-1	mouse	2297	1:500	BD Biosciences	San Jose, TX
Claudin-1	rabbit	51-9000	1:500	ThermoFisher Scientific	Walthan, MA
Claudin-4	mouse	3E2C1	1:250	ThermoFisher Scientific	Walthan, MA
Desmocollin-1	mouse	U100	1:50 (supernatent)	PROGEN Biotechnik GmbH	Heidelberg, Germany
Desmoglein-1	mouse	27B2	1:1000	ThermoFisher Scientific	Walthan, MA
EphA1	goat	AF638	1:500	R&D Systems	Minneapolis, MN
EphA2	mouse	D7	1:500	Millipore Sigma	Billerica, MA
Ephrin-A1	rabbit	V18	1:500	Santa Cruz Biotechnology	Dallas, TX
Flotillin-1	rabbit	3253	1:1000	Cell Signaling Technology	Danvers, MA
GAPDH	rabbit	FL-335	1:2000	Santa Cruz Biotechnology	Dallas, TX
Cytokeratin 10	mouse	RKSE60	1:1000	Santa Cruz Biotechnology	Dallas, TX
Occludin	mouse	OC-3F10	1:500	ThermoFisher Scientific	Walthan, MA
Phosphotyrosine (pY)	mouse	4G10	1:500	Millipore Sigma	Billerica, MA
pS897 EphA2	rabbit	D9A1	1:1000	Cell Signaling Technology	Danvers, MA
pY772 EphA2	rabbit	8244	1:1000	Cell Signaling Technology	Danvers, MA
Ras	mouse	8832	1:1000	Cell Signaling Technology	Danvers, MA
ZO-1	rabbit	61-7300	1:500	ThermoFisher Scientific	Walthan, MA
Secondary antibodies for Western Blot					
Bovine anti-goat IgG linked peroxidase	---	---	1:3000	Jackson ImmunoResearch Laboratories	West Grove, PA
Goat anti-mouse IgG linked peroxidase	---	---	1:3000	Jackson ImmunoResearch Laboratories	West Grove, PA
Mouse anti-rabbit IgG linked peroxidase	---	---	1:3000	Jackson ImmunoResearch Laboratories	West Grove, PA
Antibodies for Immunoprecipitation					
Phosphotyrosine (pY)	mouse	pY20	---	Santa Cruz Biotechnology	Dallas, TX

Table 2: Antibodies used for immunofluorescent staining.

Protein	Species	Clone/Catalog Number	Dilution	Company	Location
Primary antibodies for Immunofluorescence					
Caveolin-1	mouse	7C8	1:100	Santa Cruz Biotechnology	Dallas, TX
Claudin-1	rabbit	51-9000	1:100	ThermoFisher Scientific	Walthan, MA
Claudin-4	mouse	3E2C1	1:100	ThermoFisher Scientific	Walthan, MA
E-Cadherin	rabbit	24E10	1:200	Cell Signaling Technology	Danvers, MA
EphA1	goat	AF638	1:10	R&D Systems	Minneapolis, MN
EphA2	mouse	D7	1:50	Millipore Sigma	Billerica, MA
EphA2	goat	AF3035	1:50	R&D Systems	Minneapolis, MN
Ephrin-A1	mouse	A-5	1:50	Santa Cruz Biotechnology	Dallas, TX
Occludin	mouse	OC-3F10	1:100	ThermoFisher Scientific	Walthan, MA
pY772 EphA2	rabbit	8244	1:50	Cell Signaling Technology	Danvers, MA
ZO-1	rabbit	61-7300	1:100	ThermoFisher Scientific	Walthan, MA
Secondary antibodies for Immunofluorescence					
Donkey anti-goat	---	---	1:300	ThermoFisher Scientific	Walthan, MA
Donkey anti-mouse	---	---	1:300	ThermoFisher Scientific	Walthan, MA
Donkey anti-rabbit	---	---	1:300	ThermoFisher Scientific	Walthan, MA

3. Generation of RHE culture models

RHE cultures were generated as previously described [130, 163-165]. For each 12-well plug, 400,000 J2-3T3 fibroblasts were used. Fibroblasts were pelleted and resuspended in reconstitution buffer (1.1 g NaHCO3, 2.3 g HEPES, resuspended in 50 mL of 0.05 N NaOH), 10X DMEM (Millipore Sigma), 4 mg/mL rat tail collagen type I (ThermoFisher Scientific) and enough 0.5 M NaOH until the color was the same shade of red as DMEM media. 1.5 mL of collagen resuspension was plated into each well and incubated for 30 minutes at 37°C to polymerize. After polymerization, J2-3T3 media containing 4 mM L-glutamine (Millipore Sigma), 10% Newborn Calf Serum (Millipore Sigma), 0.25 μg/ml amphotericin B, 10 μg/ml gentamicin in DMEM High Glucose was added to each well and changed every other day, for up to 4 days, until keratinocytes were ready to be seeded.

NHEKs were expanded and plated at confluence (1.5×10^5 cell/cm^2) on J2-3T3 fibroblast collagen plugs and grown as submerged cultures in E-medium for 3 days. Each liter of E-media contains a 1:1 mix of DMEM High Glucose and DMEM:F12 (Millipore Sigma), 10 mL E-Cocktail Mix (180 μM adenine, 5 μg/mL Bovine pancreatic insulin, 5 μg/mL Human Apo-transferrin, 5 μg/mL triiodothyronine T3; Millipore Sigma), 10 μg/mL Gentamicin, 0.25 μg/mL Amphotericin B, 4 mM L-glutamine, 0.4 μ ug/mL Hydrocortisone (Millipore Sigma), 10 ng/mL Cholera toxin (Millipore Sigma), 50 mL Fetal Bovine Serum (ThermoFisher Scientific) and 5 ng/mL EGF (ThermoFisher Scientific) [165]. These cultures were then lifted to an ALI and grown for the indicated number of days in E-media lacking EGF. Cultures were then processed for morphological analysis, protein extraction, or RNA isolation.

4. Hematoxylin and eosin (H&E) staining and imaging

For histology, formalin-fixed, paraffin-embedded 4 μm tissue sections were stained with H&E by the Skin Disease Research Center, Pathology Core (Northwestern University, Chicago, IL). Images were captured using a digital camera (AxioCam HR; Carl Zeiss, Thornwood, NY) mounted on a light microscope (Axioplan 2; Carl Zeiss).

5. RNA isolation and analysis

Total RNA was collected from cells using a purification kit (RNeasy; Qiagen, Germantown, MD) and cDNA was generated using a reverse transcription kit (Suprscript III; ThermoFisher Scientific). Real-time qPCR was performed (LightCycler 96 System; Roche) using a quantitative FastStart SYBR green PCR kit (Roche). Primer sequences were designed using the PrimerQuest RT-qPCR primer algorithm tool from IDT (IDT, Skokie, IL) and are listed in Table 3.

6. RNA-Sequencing Analysis

After RNA extraction, the RNA quality was evaluated to test for intact ribosomal RNA profiles (18S and 28S) for all of the samples using the Agilent 2100 Bioanalyzer (Agilent Technologies, Santa Clara, CA). Sequencing of the cDNA was performed on the Illumina Genome Analyzer IIx (Illumina, San Diego, CA). The sequence reads were processed as done previously [228]. Filtered reads were mapped to the University of California, Santa Cruz (UCSC) human genome (hg19) using TopHat2 (version 2.0.12) [229]. Cufflinks (version 2.2.1) was used to calculate fragments per kilobase of exon per million fragments mapped (FPKM) for each gene [230]. The counts and FPKM estimates for the samples are available from the Gene Expression Omnibus

Table 3: Primers used for RT-qPCR.

Transcript	Species	Sequence	Company	Location
Ephrin-A1-forward	Human	5'-CGGAGAAGCTGTCTGAGAAGT-3'	Integrated DNA	Skokie, IL
Ephrin-A1-reverse	Human	5'-CTGTGAGTGATTTTGCCACTGA-3'	Integrated DNA	Skokie, IL
RPLPO-forward	Human	5'-CAGATTGGCTACCCAACTGTT-3'	Integrated DNA	Skokie, IL
RPLPO-reverse	Human	5'-GGGAAGGTGTAATCCGTCTCC-3'	Integrated DNA	Skokie, IL
K10-forward	Human	5'-AAACCGCAAAGATGCTGAAGCCTG-3'	Integrated DNA	Skokie, IL
K10-reverse	Human	5'-TCAAGGCCAGTTGGGACTGTAGTT-3'	Integrated DNA	Skokie, IL

(GEO) [231]. The average FPKM value for each gene with an FPKM value over 0.5 was used to generate heatmaps using R statistical software [232]. RNA sequencing analysis was performed by Swindell W.R. and Gudjonsson J.E. (University of Michigan, Department of Dermatology, Ann Arbor, MI) and heatmaps were generated by Ventrella R.

7. Colony growth assay

NHEKs were plated at low density in NHEK growth medium to allow for expansion of individual NHEK colonies. For imagining studies NHEKs were plated at 1000 cell/cm^2 on glass coverslips and for biochemical studies NHEKs were plated on plastic cell culture plates at 5000 cell/cm^2. The following day the medium was changed to 1.2 mM Ca^{2+} containing NHEK media with HKGS along with 1.0 μg/mL of human Fc protein (Jackson ImmunoResearch) or ephrin-A1-Fc (R&D Systems Inc., Minneapolis, MN). The medium with treatments was changed every other day for seven days. After 7 days of treatment, cells were fixed for immunofluorescent analysis or lysates were collected for biochemical analysis. For live cell imaging, keratinocytes were plated on plastic cell culture plates and cells were imaged every 4 hours for 7 days on the Nikon BioStation CT (Nikon Instruments Inc., Melville, NY).

8. Microscopy and image processing

Confluent NHEKs or optimal cutting temperature embedded RHE were fixed and permeabilized in methanol and used for immunofluorescent analysis. Images were captured using a Zeiss AxioImager Z.1 microscope with ApoTome (Carl Zeiss AG, Oberkochen, Germany). Colocalization was analyzed using the Coloc2 plug-in on FIJI [233].

For superresolution microscopy, cells were imaged with SIM (N-SIM; Nikon) with an EM-CCD camera iXon3 DU-897E (Andor Technology, Belfast, UK) and a 100× apo 1.49-NA

objective lens. Image acquisition was completed with the 3D SIM mode and reconstruction of images were prepared using the Nikon NIS Elements software package. Image spot and surface generation and distance quantifications were performed using Imaris Image Analysis Software (Bitplane, Zurich, Switzerland).

9. Western blot analysis

In order to solubilize whole cell proteins, NHEKs were lysed in urea sample buffer (USB; 8 M urea, 1% sodium dodecyl sulfate (SDS), 5 mM β-mercaptoethanol (BME), 10 mM Tris, pH 6.8). A total of 5-25 ug of protein was separated by using SDS-PAGE probed with antibodies to detect proteins as previously described [15]. FIJI imaging software was used to quantify protein band intensities [233].

10. Generation of Chimeras

Chimera 212 contains the extracellular domain (ECD) from EphA2 (amino acids 1-522), transmembrane domain (TMD) from EphA1 (amino acids 544-572), and the cytoplasmic domain (CD) from EphA2 (amino acids 564-976). Chimera 121 contains the ECD from EphA1 (amino acids 1-543), TMD from EphA2 (amino acids 523-563), and CD from EphA1 (amino acids 573-976). In-Fusion cloning (Takara Bio USA, Inc., Mountain View, CA) was used to subclone the chimeras into the pLZRS-Linker vector [80, 234].

11. Retrovirus production

Full-length human EphA1 (Open Biosystems; Dharmacon Inc., Lafayette, CO), EphA2 (a gift from Bing-Cheng Wang; Case Western Reserve University, Cleveland, OH), ephrin-A1 (a gift from Waldemar Debinski; Wake Forest University Medical Center, Winston-Salem, NC) and Chimeras were subcloned into the pLZRS-Linker retroviral vector [80, 234, 235].

In order to generate retroviral supernatents, Phoenix cells, HEK293 cells that stably express viral packaging proteins, were grown in High Glucose DMEM supplemented with 10% Fetal Bovine Serum (Atlanta Biologicals, Flowery Branch, GA), 4 mM L-glutamine, 0.25 μg/ml amphotericin B, and 10 μg/ml gentamicin [236]. When cells were approximately 10-20% confluent, they were transfected overnight in Opti-MEM medium (ThermoFisher Scientific) containing Lipofectamine 2000 Transfection Reagent (ThermoFisher Scientific) and then media was changed back to growth medium lacking antibiotics. The following day retroviral supernatants were generated and concentrated by centrifuging through a 30K filter (ThermoFisher Scientific) at 4°C and then stored at -80°C.

Subconfluent keratinocytes were transduced with the retroviral supernatants containing 4 μg/mL polybrene (Millipore Sigma) for 4 hours at 37°C in NHEK growth medium. Transduced cells were grown for an additional two days before plating for experiments.

12. Generation of lentivirus

Gene silencing of EphA2 was performed using a PLKO-based lentiviral vector containing a short hairpin sequence targeting the 3'-untranslated region of EphA2 (a generous gift from Bingcheng Wang; Case Western Reserve University, Cleveland, OH) [237]. Concentrated lentiviral supernatants were generated from Phoenix packaging cells with help from the SDRC DNA/Gene Delivery research core.

When keratinocytes were 40-60% confluent they were transduced with lentiviral supernatants containing 4 μg/mL polybrene (Millipore Sigma) overnight at 37°C in NHEK growth medium. Transduced cells were puromycin-selected and then plated for an experiment or for subsequent infection with overexpression virus.

13. siRNA transfection

siRNA oligonucleotide duplexes were used to silence ephrin-A1 and EphA1 expression and a GC-matched siRNA was used as a negative control (Sequence information in Table 4) as described before [12]. siRNA complexes were generated by combining with DharmaFECT 1 (ThermoFisher Scientific) transfection reagent at a ratio of 2.25 μL per 1 μL of 20 μM siRNA and incubated at room temperature for 20 minutes. NHEKs were then transfected in suspension with siRNA complexes at a final concentration of 20 nM in 0.07 mM Ca^{2+} NHEK medium containing HKGS, but lacking antibiotics. The following day medium was changed to 0.03 mM Ca^{2+} NHEK medium with HKGS, but without antibiotics. Keratinocytes were grown for an additional 2 days to allow for sufficient knockdown prior to using for an experiment.

14. Sucrose density centrifugation gradients

NHEKs were rinsed and scraped into PBS and spun down at 400g for 3 min to pellet cells. Samples were resuspended in 0.5 M Sodium-carbonate buffer (0.5 M Na-carbonate pH 11, 1 mM sodium orthovanadate, protease/phosphatase inhibitors) [238]. Lysates were homogenized by passing through 18g, 21g, and 26g needles (15X each), and by 30 strokes with a Dounce homogenizer on ice. A subsequent centrifugation at 400g was applied to remove unbroken cells and precipitates. Sucrose solutions were prepared in MESNA buffer (25 mM Mes pH 6.5, 0.15 M NaCl). A 1:1 dilution of 90% sucrose and sample was added to the bottom of the ultracentrifuge tube to create a 45% sucrose mixture. Then, 35% and 5% sucrose buffers were layered on top to create a discontinuous sucrose gradient. These gradients were centrifuged at 44,000 rpm for 18 hours in an ultracentrifuge (Sorvall WX Ultra 80, ThermoFisher Scientific)

Table 4: siRNA target sequences.

Gene	Species	Sequence Information	Company	Catalog Number	Location
EphA1	Human	5'-GGAAGATGAGCAATCAGGAGGTTAT-3'	ThermoFisher Scientific	10620312	Walthan, MA
Ephrin-A1	Human	3 target-specific 19-25 nt siRNA pool	Santa Cruz Biotechnology	sc-39426	Dallas, TX
Negative Control (Stealth RNAi)	---	Medium GC Duplex #2	ThermoFisher Scientific	12935112	Walthan, MA

followed by collection of 12 equal-volume fractions into Laemmli sample buffer. Equal volumes from each fraction were subjected to immunoblotting.

Densitometry was done on all 12 fractions and positive lipid raft fractions were defined as having greater than ten percent of the total amount of either caveolin-1 or flotillin-1. Remaining fractions were then identified as low density or high density relative to the lipid raft fractions [239]. Lipid raft fractions were defined for each sample in order to calculate the lipid raft localization of other proteins tested in that sample.

15. Acyl-biotin exchange (ABE)

ABE protocol was followed as previously described [240, 241]. Cells were lysed and free sulfhydryl groups were blocked with Lysis Buffer (1% TritonX-100, 150 mM NaCl, 50 mM Tris pH 7.4, 5 mM EDTA, 1 mM phenylmethanesulfonyl fluoride (PMSF), 1X protease inhibitor cocktail (PIC)) containing 10 mM *N*-Ethylmaleimide (NEM) for 15 minutes on ice. Cells were scraped off plate and further lysed by passaging through a 25-gauge needle 15 times and then a chloroform-methanol precipitation was done to precipitate the protein from lysis buffer. For this precipitation, 4 volumes of methanol were added to the sample and vortexed. Next, 1.5 volumes of chloroform were added and vortexed followed by 3 volumes of MilliQ water and then vortexed again. Samples were centrifuged at 4,000 g for 30 minutes at room temperature to collect precipitated proteins and aqueous phase was discarded. Precipitated protein pellets were washed with 3 volumes of methanol by inversion followed by centrifugation at 4,000 g for 10 minutes at room temperature. Remaining supernatant was removed and precipitated protein was air-dried. Protein pellets were re-suspended in 400 μL of 4% SDS Buffer (4% SDS, 0.05 M Tris pH 7.4, 5 mM EDTA) containing 10 mM NEM at 70°C for 15 minutes. 1.2 mL of Lysis Buffer

with 10 mM NEM was added to sample. Samples were incubated overnight on a rocker at 4°C to block free thiol groups.

NEM was removed from samples with three sequential chloroform-methanol precipitations: 4.8 mL methanol and vortex, 1.8 mL chloroform and vortex, 3.6 mL MilliQ water and vortex, centrifugation at 4,000 g for 30 minutes at room temp, removal of top aqueous phase, 3.6 mL methanol and inversion, centrifugation at 4,000 g for 10 minutes at room temp, aspiration of supernatant, and air-drying of protein pellet. For the first and second precipitations, 300 μL of 4% SDS Buffer was added and precipitate was re-suspended at 70°C for 15 minutes followed by diluting with 900 μL Lysis Buffer with 0.2% Triton X-100. After last precipitation, protein precipitate was re-suspended in 500 μL 4% SDS Buffer at 70°C for 15 minutes. All free NEM must be removed so it does not react with the newly freed cysteine residues following NH_2OH treatment.

Samples were treated with hydroxylamine (HA) in order to cleave thioester-linked palmitoyl moieties and lack of HA was then used as a negative control. Thus, samples were separated into two equal parts and 960 μL HA+ Buffer (1 mM HPDP-biotin, 0.2% TritonX-100, 0.7 M HA pH 7.4, 1 mM PMSF, 1X PIC) was added to one and 960 μL HA- Buffer (1 mM HPDP-biotin, 0.2% TritonX-100, 0.05 M Tris pH 7.4, 1 mM PMSF, 1X PIC) was added to the other. Samples were incubated on a rotator at room temperature for 1 hour. Residual NH_2OH was removed by three chloroform-methanol precipitation steps as done previously. After first and second precipitations, 300 μL of 4% SDS Buffer was added and precipitate was re-suspended at 70°C for 15 minutes followed by diluting with 900 μL Lysis Buffer with 0.2% Triton X-100. After final precipitation, 240 μL of 4% Triton X Buffer was added with 960 μL

Low-HPDP-biotin Buffer (0.2 mM HPDP-biotin, 0.15 M NaCl, 0.05 M Tris pH 7.4, 0.2% TritonX-100, 1 mM PMSF, 1X PIC) and rotated at room temperature for 1 hour. All unreacted HPDP-biotin was removed with three chloroform-methanol precipitations as done prior. After the first two precipitations, 300 μL of 4% SDS Buffer was added and re-suspended at 70°C for 15 minutes followed by diluting with 900 μL Lysis Buffer with 0.2% Triton X-100. For the last precipitation, each pellet was dissolved in 120 μL of 2% SDS Buffer (2% SDS, 0.02 M Tris pH 7.4, 5 mM EDTA) at 70°C for 15 minutes. Protein was further diluted 20-fold with Lysis Buffer and then centrifuged at 14,000 g for 1 minute to pellet any undissolved protein. Protein particulates were removed and total protein concentration was then determined.

For affinity purification, 300 μg of protein was immunoprecipitated in Lysis Buffer with 50 μL of immobilized streptavidin (SA) beads (Millipore Sigma) while rotating overnight at 4°C. Beads were then washed six times with Lysis Buffer supplemented with 0.0005% SDS and 0.004% Triton X-100, followed by centrifugation at 5,000 rotations per minute for 30 seconds. Following removal of Lysis Buffer after sixth wash, protein was eluted with 2X Laemmli sample buffer supplemented with 5% BME and then separated by SDS-PAGE.

16. Acyl-PEG exchange (APE)

Acyl-PEG exchange (APE) was modified from a previously outlined protocols [241, 242]. NHEKs were collected in a TEA buffer (50 mM triethanolamine pH=7.3, 150 mM NaCl, 5 mM EDTA, 4% SDS). Neutralized tris(2-carboxyethyl)phosphine was added to 200 μg in of protein in TEA buffer to make a total concentration of 10 mM and rotated for 30 minutes at room temperature. Then, NEM was added to make a final concentration of 25 mM and the sample continued to rotate for an additional 2 hours at room temperature to block free thiol groups.

NEM was removed by three sequential rounds of chloroform-methanol precipitations as described: 400 μL methanol and vortex, 150 μL chloroform and vortex, 300 μL MilliQ water and vortex, centrifugation at 20,000 g for 5 minutes at room temp, removal of top aqueous phase, 1 mL methanol and mixing, centrifugation at 20,000 g for 3 minutes at room temp, aspiration of supernatant, 800 μL methanol and mixing, centrifugation at 20,000 g for 3 minutes at room temp, and air-drying of protein pellet. Following the first two precipitations, the protein pellet was re-suspended in 100 μL TEA buffer and heated for 5 minutes at 37°C. After the third precipitation, the protein pellet was re-suspended in 30 μL of TEA buffer containing 0.2% Triton X-100 with 0.75 M HA (+HA) or without HA (-HA) and rotated at room temperature for 1 hour. HA was removed with one chloroform-methanol precipitation followed by resuspension of the protein pellet in 30 μL TEA buffer with 0.2% Triton X-100 supplemented with 1 mM methoxy-Polyethylene glycol-Maleimide (mPEG-Mal) (20 kDa, Millipore Sigma). Samples were rotated for 2 hours at room temperature followed by one chloroform-methanol precipitation in which the final pellet was suspended in 1X Laemmli sample buffer supplemented by 5% BME followed by separation with SDS-PAGE.

17. Cell surface biotinylation

Labelling of cell surface proteins with biotin was modified from a previously described protocol [243]. After washing confluent NHEKs with ice cold PBS, the cultures were labeled on ice with 0.5 mg/mL EZ Link Sulfo-NHS-SS-biotin (ThermoFisher Scientific) for 20 minutes. Biotin was rinsed off with PBS and excess biotin was quenched with 100 mM glycine-PBS on ice for 10 minutes, followed by a final PBS wash. Cell lysates were collected in USB buffer lacking BME. SA-conjugated beads (ThermoFisher Scientific) were added to 400 μg of protein

diluted to equal volumes with Tris-EDTA-Triton X-100 buffer (TEXN; 0.2 M Tris, pH 7.5, 0.005 M EDTA, 0.15 M NaCl, 1% Triton X-100) and a SA-biotin immunoprecipitation was done overnight at 4°C while rotating. Beads were pelleted, washed, and eluted by boiling with 2X Lamelli buffer supplemented with 5% BME. Samples were separated by SDS-PAGE along with whole cell lysates.

18. Phosphotyrosine (pY) immunoprecipitation in HEK293 cells

HEK293 cells were transfected as previously described for Phoenix cells and then maintained in High Glucose DMEM growth medium containing 10% Fetal Bovine Serum, 4 mM L-glutamine, 0.25 μg/ml amphotericin B, and 10 μg/ml gentamicin. After treatment, protein lysates from HEK293 cells were collected in RIPA buffer (50 mM Tris pH 7, 150 mM NaCl, 2 mM EDTA, 1% Na Deoxycholate, 1% NP-40, 0.1% SDS, 50 mM NaF, 200 μM Na-Vanadate). 100 μg of protein lysate was immunoprecipitated overnight at 4°C in RIPA buffer containing 10 μL of pY antibody (pY20; Santa Cruz Biotechnology). Protein A/G PLUS Agarose beads (Santa Cruz Biotechnology) were used to immunoprecipitate proteins bound to pY20 antibody at 4°C for 2 hours. Protein beads were then washed three times by centrifuging at 7,500 rotations per minute for 2 minutes at 4°C in RIPA buffer. Protein was eluted from agarose beads in Lamelli Sample Buffer containing 5% BME then separated by SDS-PAGE along with whole cell lysates.

19. Silicone chamber confrontation coculture assay

Silicone chambers with a 500 μm separation (Ibidi, Fitchburg, WI) were used to prevent intermixing of cell populations as previously described [60]. NHEKs were plated to confluency in each chamber (70 μL of 0.9 million NHEKs/mL) in NHEK growth medium. On one side of the silicone chamber ephrin-A1 overexpressing NHEKs were plated and on the other side wild

type EphA2 overexpressing or Chimera 212 expressing NHEKs were plated. After 24 hours, the silicone chamber was removed and medium was changed to 0.2 mM Ca^{2+} medium. Then, 48 hours after initiation of confrontation, NHEKs were fixed and permeabilized in methanol.

20. Scratch wound healing assay

Confluent NHEKs were kept in 0.2 mM Ca^{2+} containing NHEK Complete medium for 24 hours prior to scratch wound assays that were done as previously described [14, 244]. A single scratch was made through the center of each well. Following wounding, 1.0 μg/mL of human Fc protein (Jackson ImmunoResearch, West Grove, PA) or ephrin-A1-Fc (R&D Systems Inc.) were added to the 0.2 mM Ca^{2+} NHEK Complete media. Images of wound closure were captured using a digital camera (AxioCam MR; Carl Zeiss) mounted on an inverted light microscope (Axiovert 40 CFL; Carl Zeiss). The percentage of wound closure was calculated for each condition by comparing the cell-free surface area 24 hours after wounding normalized to the respective wound area at 0 hours. For every replicate, scratch wounds were performed in triplicates for each condition. To rule out possible contributions of proliferation to keratinocyte migration, we also performed scratch wound healing assays with a two hour 0.4 μg/mL mitomycin C (Millipore Sigma) pretreatment prior to scratching for some replicates.

21. RHE punch biopsy wound closure

3-D RHE cultures were generated on J2-3T3 fibroblast-containing collagen plugs that were plated on transwell inserts with a transparent polyethylene terephthalate (PET) membrane and 3 μm pores (Corning Incorporated, Corning, NY). They were lifted to an air-liquid interface by removing the media above the submerged culture. Seven days after airlifting the RHE, 4-mm punch biopsy apparatus was used to generate a wound in the center of the maturing RHE.

Another set of J2-3T3 fibroblast-containing collagen plugs were polymerized in cell culture plates two days before epidermal wounds were generated in the RHE. The wounded RHE was removed from the transwell and placed on top of the new collagen plug. RHE were treated with 1 μg/mL Fc or ephrin-A1-Fc recombinant protein and allowed to migrate into the wound bed for an additional five days. Wounded RHE cultures were processed for morphological analysis twelve days after being airlifted. Formalin-fixed, paraffin-embedded 4 μm tissue sections were stained with H&E by the Skin Disease Research Center, Pathology Core (Northwestern University, Chicago, IL). H&E sections were used to quantify percent wound closure by comparing the remaining length between the unclosed epidermis and the original wound length determined by the length of the wound site in the collagen.

22. Crystal Violet assay

NHEKs were seeded at a low density of 2500 cell/cm^2. NHEKs were fixed at the indicated time points in 10% neutral-buffered formalin for 10 minutes and then stored at 4°C. After the final day, 0.5% crystal violet in 20% methanol was added to each well and incubated for 20 minutes. Following staining, plates were washed, air-dried, and eluted with 10% acetic acid for 20 minutes. Absorbencies was read at 490 nm on a multilabel plate reader (VICTOR X5; PerkinElmer, Waltham, MA).

23. Hoechst Dye DNA assay

Keratinocytes were plated at a low density of 2500 cell/cm^2. NHEKs were stained at indicated days with 20 μM Hoechst dye (ThermoFisher Scientific) in M154 media lacking supplements for 1 hour at 37°C. Absorbencies was immediately read at 490 nm on a VICTOR X5 multilabel plate reader.

24. Statistics

Data are expressed as the mean ± Standard Deviation (SD) and significance was determined when $p \leq 0.05$. A paired two-tailed student t-test was used to determine significant differences when two groups were compared. When comparing two or more variables, an analysis of variance (ANOVA) with a post hoc test was used to determine significance between groups. Specific post hoc tests used and number of replicates are described in corresponding figure legends. Statistical analyses were performed using GraphPad Prism 7 (La Jolla, CA, USA).

III. EPHA2 TRANSMEMBRANE DOMAIN IS UNIQUELY REQUIRED FOR KERATIONCYTE MIGRATION BY REGULTING EPHRIN-A1 LEVELS

1. EphA1 and EphA2 have distinct expression and localization patterns during epidermal morphogenesis

Eph/ephrin signaling has been shown to be important for maintaining epidermal homeostasis [10, 11]. We have previously shown that EphA2 is the predominant Eph receptor transcript in subconfluent keratinocytes and its expression level decreases during calcium-induced differentiation. The other prevalent Eph receptors expressed in keratinocytes, EphA1 and EphA4, remain relatively stable and increase during calcium-induced differentiation, respectively [15]. Similarly, in RNA sequencing analysis, EphA2 is the predominant Eph receptor expressed in subconfluent keratinocytes (Figure 4). However, EphA2 transcription is downregulated during keratinocyte differentiation resulting in EphA1 being the most highly expressed Eph receptor in fully differentiated RHE cultures. EphA4 expression is also upregulated during keratinocyte differentiation. Moreover, the transcripts for the major ephrin-A ligands, Ephrin-A1 and Ephrin-A3, are both increased during keratinocyte differentiation. Transcript levels for the spliced isoform of EphB6 (EphB6[2]) is also increased during keratinocyte differentiation and the full length EphB6 is not expressed until the final stages of 3-D epidermal differentiation, but has a low abundance in skin. The predominant ephrin-B ligand is Ephrin-B1, which is decreased during differentiation. Ephrin-B2 and Ephrin-B3 are both expressed to a lesser extent than Ephrin-B1 and remain relatively unchanged during differentiation. Although mRNA expression level does not always directly correlate with protein

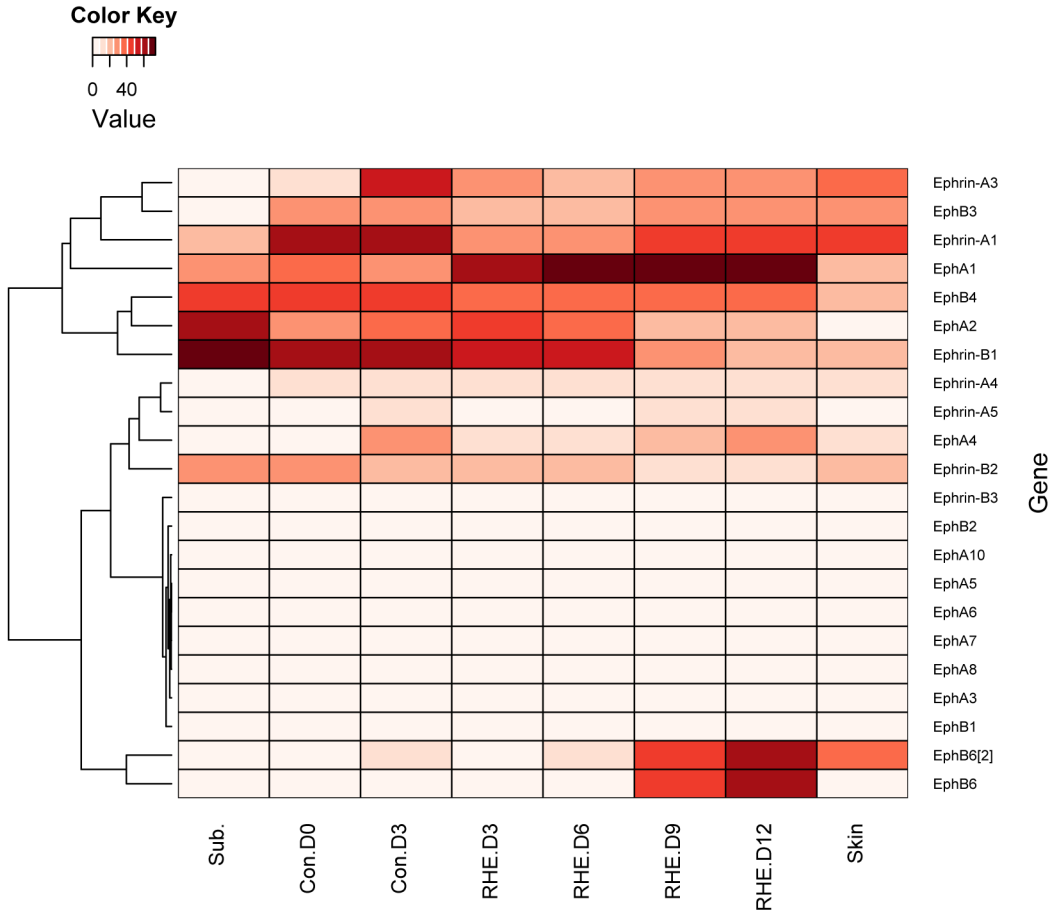

Figure 4: Eph/ephrin RNA transcript changes during different stages of keratinocyte differentiation.

RNA-sequencing heatmap analysis showing the change in Eph/ephrin fragments per kilobase of transcript per million mapped read (FPKM) during differentiation as indicated by the color key. Dendrogram shows the clustering of genes with similar expression profiles. (Sub.=subconfluent, Con.D0=confluent day 0 before addition of high Ca^{2+}, Con.D3=confluent day 3 in 1.2 mM Ca^{2+}, RHE D3, D6, D9, D12=RHE days after airlifting).

expression level, the alterations in transcript levels of EphA1 and EphA2 are similar to changes in protein expression levels during keratinocyte differentiation [15, 245]. Both transcript and protein levels for EphA2 decrease, whereas EphA1 remains unchanged during keratinocyte differentiation.

Even though EphA1 and EphA2 have different expression patterns in keratinocytes they have similar localization patterns at cell-cell contacts in the suprabasal layers of differentiated RHE (Figure 5). Furthermore, in the basal layers, where ephrin-A ligands are concentrated, EphA1 and EphA2 exhibit a diffuse cytoplasmic localization (Figure 5) [15]. However, during calcium-induced cell-cell contact stabilization and differentiation in 2-D NHEK cultures, EphA1 and EphA2 display different localization patterns (Figure 6). Prior to a calcium switch, when NHEKs are confluent, some EphA2 is localized at cell-cell contacts, whereas EphA1 has a diffuse localization pattern that lacks cell border localization. One and 24 hours after addition of high calcium (1.2 mM), EphA2 is predominantly localized to cell-cell contacts, whereas EphA1 continues to have a diffuse localization pattern throughout the cell with cell-cell contact localization. Therefore, although EphA1 and EphA2 have similar localization patterns in 3-D RHE cultures, they likely have differential dynamics to cell-cell contacts in keratinocytes, which can be visualized during 2-D cell-cell contact calcium-induced differentiation.

The ability of EphA1 and EphA2 to localize to cell-cell contacts corresponds with their capability to be tyrosine phosphorylated during calcium-induced cell-cell contact stabilization. EphA1 lacks tyrosine phosphorylation after the addition of high calcium whereas EphA2 is abundantly phosphorylated at its tyrosine residues. However, both EphA1 and EphA2 are tyrosine phosphorylated following ephrin-A1-Fc treatment (Figure 7). This suggests that surface

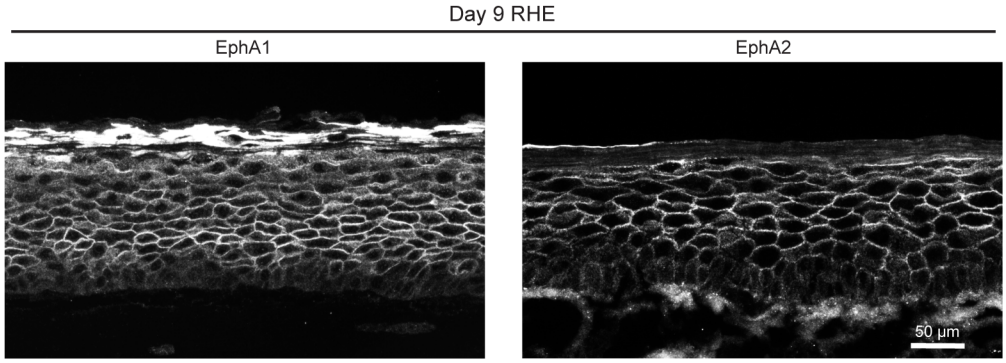

Figure 5: EphA1 and EphA2 have similar distribution patterns in 3-D RHE.
Immunofluorescent images of EphA1 and EphA2 in Day 9 RHE. (Scale bar=50 µm).

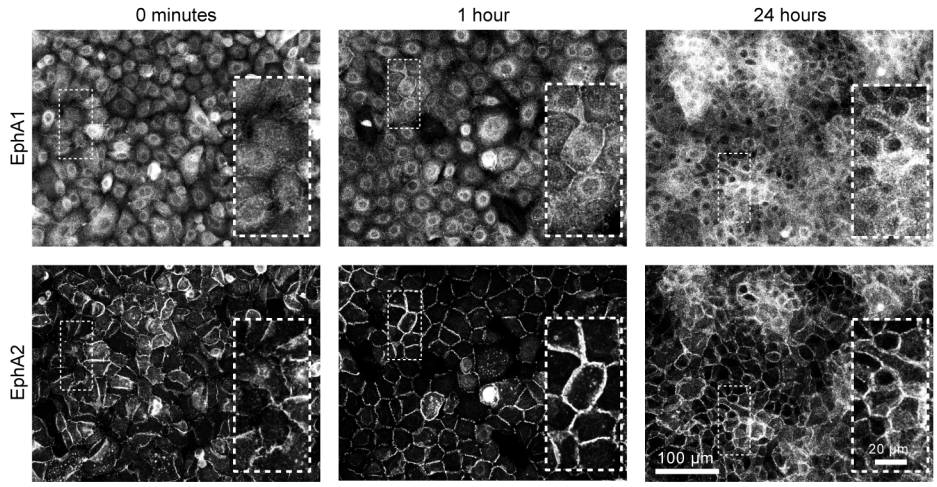

Figure 6: EphA1 and EphA2 have different localization patterns during 2-D calcium-induced differentiation.

Immunofluorescent staining of EphA1 and EphA2 during calcium-induced keratinocyte differentiation. Images are shown one hour after addition of high (1.2 mM) calcium during cell-cell contact stabilization and 24 hours after addition of high calcium when keratinocytes have differentiated. (Scale bar=100 μm and 20 μm for magnified insets).

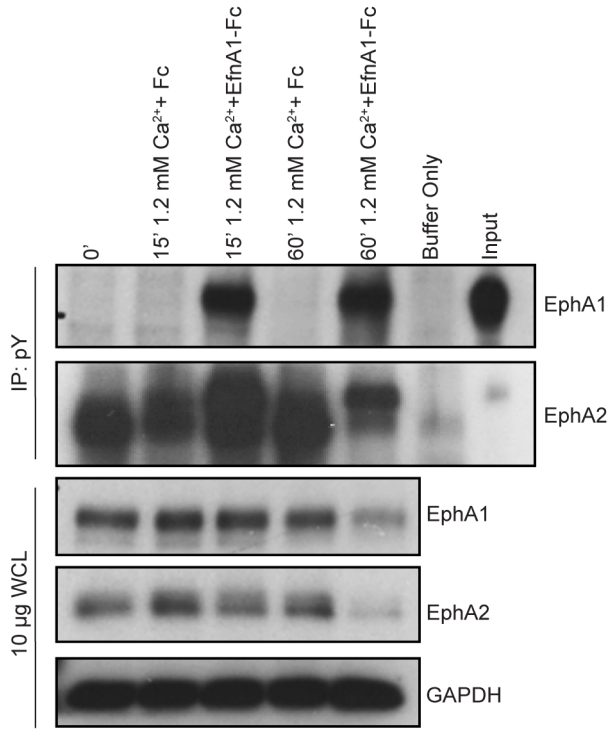

Figure 7: EphA1 and EphA2 have different phosphotyrosine activation statuses during calcium-induced differentiation.

Tyrosine phosphorylated proteins were immunoprecipitated from NHEKs that were in low (0.03 mM) calcium medium or changed to high (1.2 mM) calcium medium for 15 or 60 minutes with Fc or Ephrin-A1-Fc (EfnA1-Fc) recombinant protein (1.0 µg/mL). Immunoprecipitated proteins were separated by SDS-PAGE and then probed for EphA1 and EphA2. Buffer Only was used as a negative control. Whole cell lysates (WCL) show total protein expression levels. GAPDH was used as a protein loading control.

EphA1 can be activated by ephrin-A1-Fc, but lack of cell-cell contact localization of EphA1 limits its activation by endogenous ephrin-A1. The cell-cell contact and surface localization of EphA2 likely gives it the ability to be activated by both endogenous and ectopic ephrin-A1, respectively.

2. Ephrin-A1-induced forward signaling through EphA2 promotes late stage differentiation in keratinocytes

EphA2 forward signaling can be studied in keratinocytes by pharmacological delivery of a soluble ephrin-A1-Fc recombinant protein [12, 246]. Ephrin-A1-Fc enhances apical-basal polarity and early differentiation markers in MDCK cells and keratinocytes, respectively [12, 73]. Since TJ complexes form in the stratum granulosum and are formed during the late stages of epidermal differentiation we questioned whether delivery of ephrin-A1-Fc would have an effect on tight junction formation [131].

To test this, we chronically delivered ephrin-A1-Fc to subconfluent keratinocytes for 7 days. Long-term live cell imaging showed that treatment with ephrin-A1-Fc promoted a lateral expansion of keratinocyte colonies, whereas control treated cultures continued to proliferate as a monolayer (Figure 8). After seven days of treatment, ephrin-A1-Fc-induced colonies expressed tight junction proteins claudin-1, claudin-4, occludin, and ZO-1 at cell-cell contacts in the upper layers (Figure 9). This corresponded to a significant increase in total protein levels of claudin-4 and occludin (Figure 10). These proteins were also localized to cell-cell borders suggesting that ephrin-A1 delivery enhances the formation of the TJ protein complexes and likely corresponds to a better barrier formed in the stratified layers of the keratinocytes.

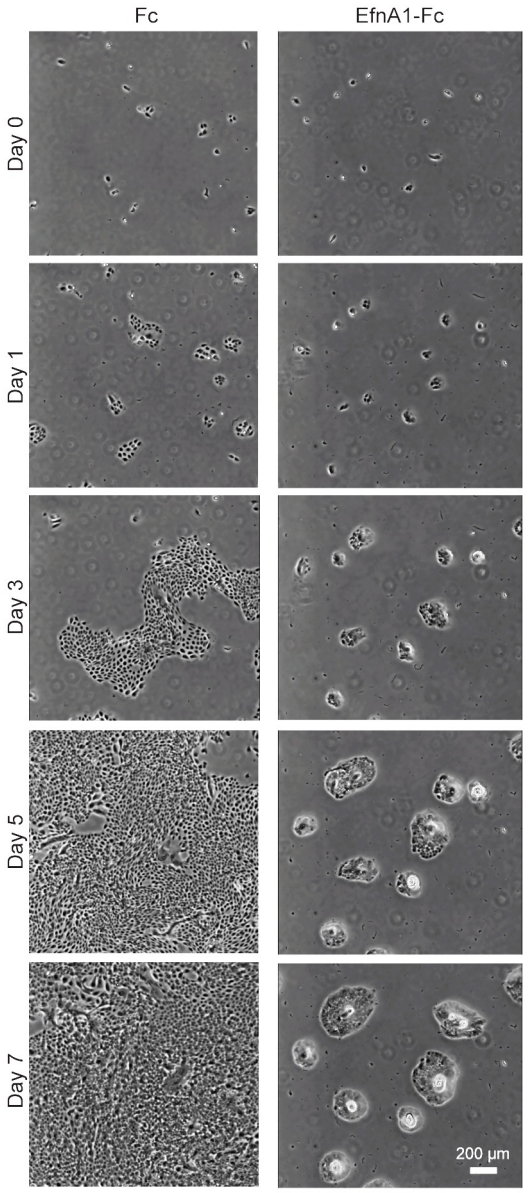

Figure 8: Ephrin-A1-Fc recombinant protein promotes NHEK stratification and colony formation.

NHEKs were plated at low cell density and then treated for 7 days with Fc or Ephrin-A1-Fc (EfnA1-Fc) recombinant protein (1.0 µg/mL) in high (1.2 mM) calcium medium. Images were taken every 4 hours on the Nikon BioStation CT and still-images are shown for Days 0, 1, 3, 5 and 7. (Scale bar=200 µm).

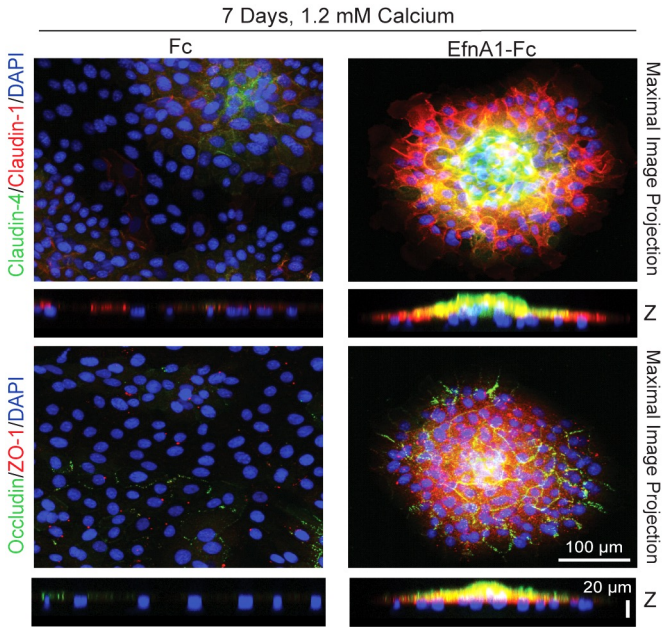

Figure 9: Forward signaling through Eph receptors promotes expression of tight junction proteins in NHEK colonies.

Immunofluorescent staining of subconfluent NHEK colonies after they were treated for 7 days with Fc or Ephrin-A1-Fc (EfnA1-Fc) recombinant protein (1.0 µg/mL) in high (1.2 mM) calcium medium. NHEK colonies were stained for the tight junction proteins claudin-1, claudin-4, occludin, and ZO-1. (Scale bar=100 µm for Maximal Image Projection and 20 µm for Z cross section).

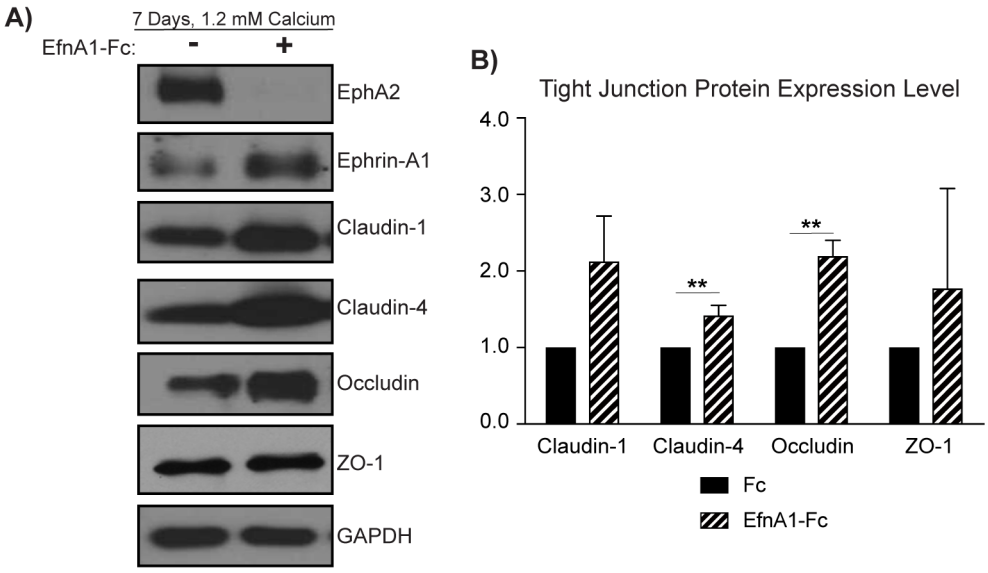

Figure 10: Ephrin-A1-Fc treatment increases the expression of tight junction proteins.
(A) Western blot analysis of protein lysates after subconfluent NHEKs had been treated in high (1.2 mM) calcium medium with Fc or Ephrin-A1-Fc (EfnA1-Fc) recombinant protein (1.0 μg/mL) for 7 days. This is quantified in **(B)**. (Error bars represent SD; **p≤0.01; t-test for each protein, n=3-4).

3. Ligand-induced activation of EphA2 increases tyrosine 772 (Y772) and decreases serine 897 (S897) phosphorylation

To better understand forward signaling elicited by ephrin-A1, we used this ephrin-A1-Fc agonist-based approach in NHEKs to determine how this treatment affects EphA2 activation. We monitored phosphorylation of the Y772 residue in the EphA2 kinase domain and the S897 residue between the kinase and SAM domain of EphA2 [97]. When NHEKs were treated with ephrin-A1-Fc in growth media there was increased pY772 activation of EphA2 15 and 60 minutes after treatment (Figure 11). Similarly, when NHEKs were placed under confluent culture conditions, basal activation of EphA2 was detected and then pY772 EphA2 was further stimulated 60 minutes after a calcium switch (Figure 12). Conversely, as ligand-activated pY772 EphA2 increased with ephrin-A1-Fc treatment or addition of high calcium, the ligand-independent pS897 form of EphA2 was decreased (Figure 11; Figure 12). During calcium-induced cell-cell contact stabilization, total EphA2 was increased, but for all of the other treatments, total EphA2, EphA1, and ephrin-A1 remained unchanged. This implies that the Y772 residue and S897 residue of EphA2 can be used to monitor the ligand-dependent and ligand-independent forms of EphA2, respectively [247].

4. Lipid raft domain association of EphA2 and ephrin-A1 in human keratinocytes

Lipid rafts contribute to keratinocyte differentiation and migration through mechanisms that include regulation of desmosome dynamics and EGFR signaling, respectively [248, 249]. Since ephrin-A1 is a negative regulator of keratinocyte migration largely through action on EphA2, we characterized the lipid raft localization of this ligand/receptor combination [14]. One defining feature of lipid rafts is that they are resistant to solubilization in non-ionic detergents or

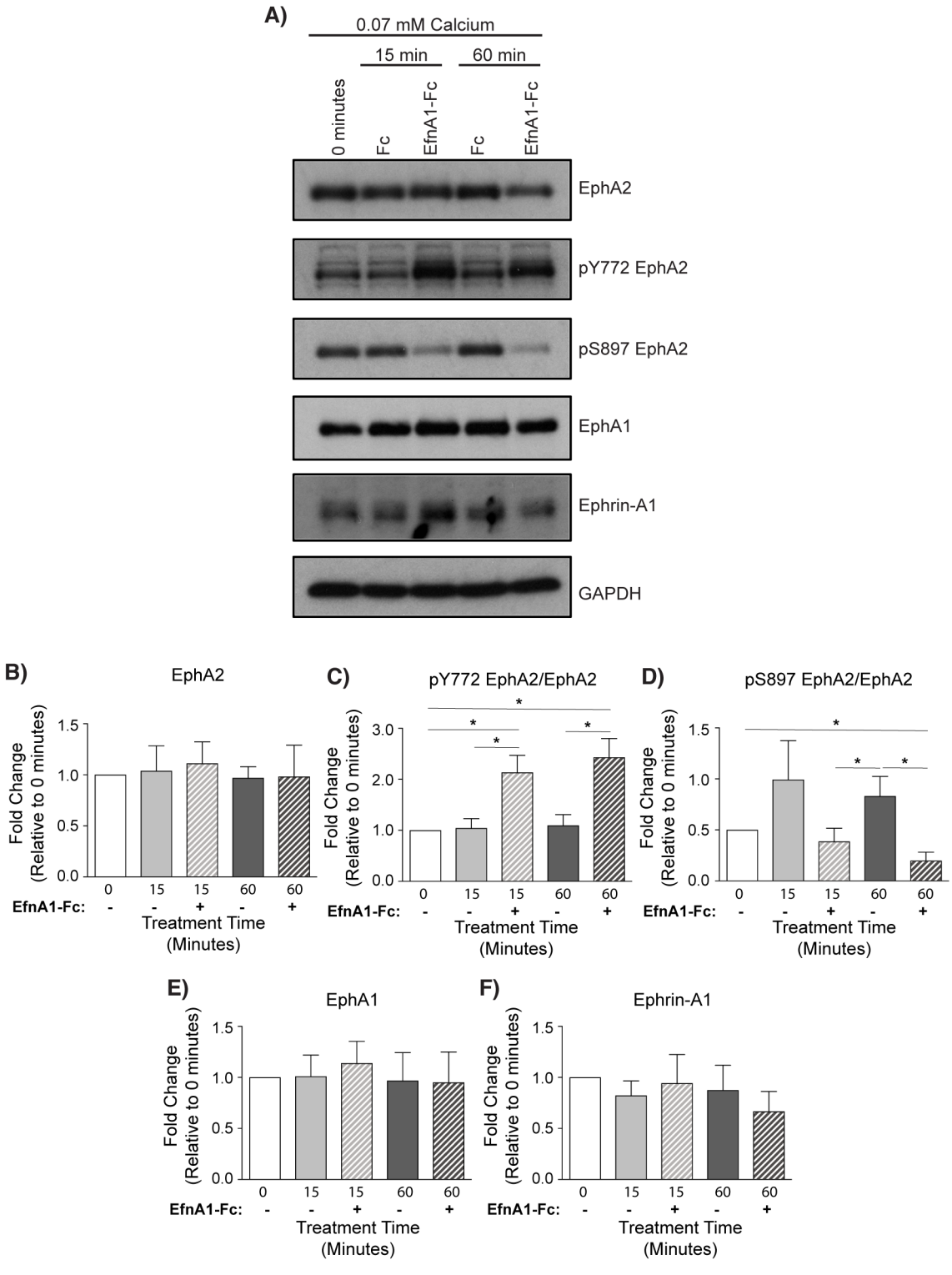
A)
0.07 mM Calcium
15 min
60 min
0 minutes
Fc
EfnA1-Fc
Fc
EfnA1-Fc
EphA2
pY772 EphA2
pS897 EphA2
EphA1
Ephrin-A1
GAPDH
B)
EphA2
C)
pY772 EphA2/EphA2
D)
pS897 EphA2/EphA2
Fold Change (Relative to 0 minutes)
EfnA1-Fc:
Treatment Time (Minutes)
E)
EphA1
F)
Ephrin-A1

Figure 11: Ephrin-A1-Fc treatment increases ligand-dependent and decreases ligand-independent EphA2 activation.
(A) Western blot analysis of EphA2, pY772 EphA2, pS897 EphA2, EphA1, and ephrin-A1 in keratinocytes that were treated with Fc or ephrin-A1-Fc (EfnA1-Fc) recombinant protein (1.0 μg/mL) in growth media for 0, 15 or 60 minutes. GAPDH was used as a protein loading control. This is quantified for total EphA2 **(B)**, relative pY772 EphA2/total EphA2 **(C)**, relative pS897 EphA2/total EphA2 **(D)**, EphA1 **(E)**, and ephrin-A1 **(F)**. (Error bars represent SD; *p≤0.05; paired one-way ANOVA with Tukey post hoc test, n=5).

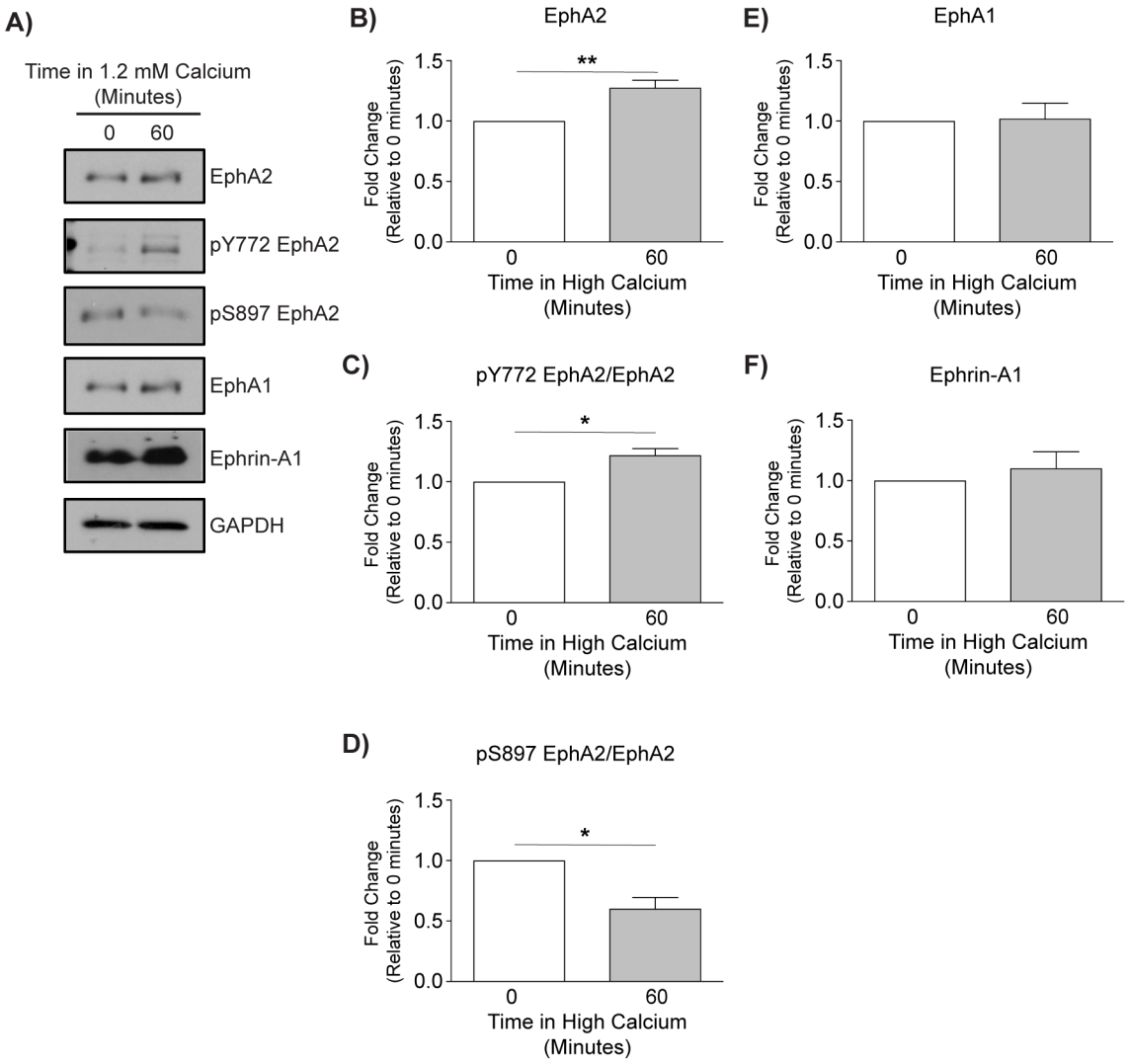

Figure 12: Calcium-induced cell-cell contact stabilization promotes pY772 EphA2 activation and inhibits pS897 EphA2 activation.

(A) Western blot analysis of EphA2, pY772 EphA2, pS897 EphA2, EphA1, and ephrin-A1 in NHEKs that were maintained in low (0.03 mM) Ca^{2+} medium and then switched into high (1.2 mM) Ca^{2+} medium for 60 minutes. GAPDH was used as a control for protein loading. This is quantified for total EphA2 **(B)**, relative pY772 EphA2/total EphA2 **(C)**, relative pS897 EphA2/total EphA2 **(D)**, EphA1 **(E)**, and ephrin-A1 **(F)**. (Error bars represent SD; *p≤0.05; paired t-test, n=4-6).

sodium carbonate buffer. After homogenization, insoluble detergent resistant membranes (DRMs) can be isolated by flotation as a low-density membrane fraction in a sucrose density gradient [204, 238, 250]. Lipid raft-containing fractions can be identified by lipid-raft-associated proteins caveolin-1 and flotillin-1. It has been previously shown that compared to the non-ionic detergent Triton X-100, sodium carbonate can provide a more sensitive solubilization of membrane domains and is not affected by the amount of cellular membrane mass extracted [251]. Therefore, sodium carbonate extraction was used for assessment of DRMs in keratinocytes. For this purpose, we took advantage of the decreased density and insolubility of lipid rafts in sodium carbonate buffer to assess Eph/ephrin lipid raft distribution in keratinocytes.

When keratinocytes were in low calcium medium, EphA2 and pY772 EphA2 were present in lipid raft domains along with ephrin-A1 (Figure 13 A). 60 minutes after a calcium switch, EphA2 distribution was increased in lipid raft domains whereas, pY772 EphA2 was more prevalent outside of these lipid raft fractions (Figure 13 A-C). This movement was specific to the ligand-activated form of EphA2 because there was lack of distribution change for the ligand-independent pS897 form of EphA2 (Figure 13 A, D). Also, EphA1 was localized to lipid raft domains but remained steady in these membrane regions during cell-cell contact stabilization (Figure 13 A, E). The relative abundance of ephrin-A1 outside of lipid raft domains increased as cell-cell contacts were stabilized following the pattern of ligand- activated EphA2 (Figure 13 A, F). Changes in protein lipid raft concentration were likely not dependent on how lipid raft fractions were being molecularly defined in our biochemical study since concentrations of caveolin-1 and flotillin-1 in lipid raft defined membrane fractions remained unchanged between samples (Figure 14).

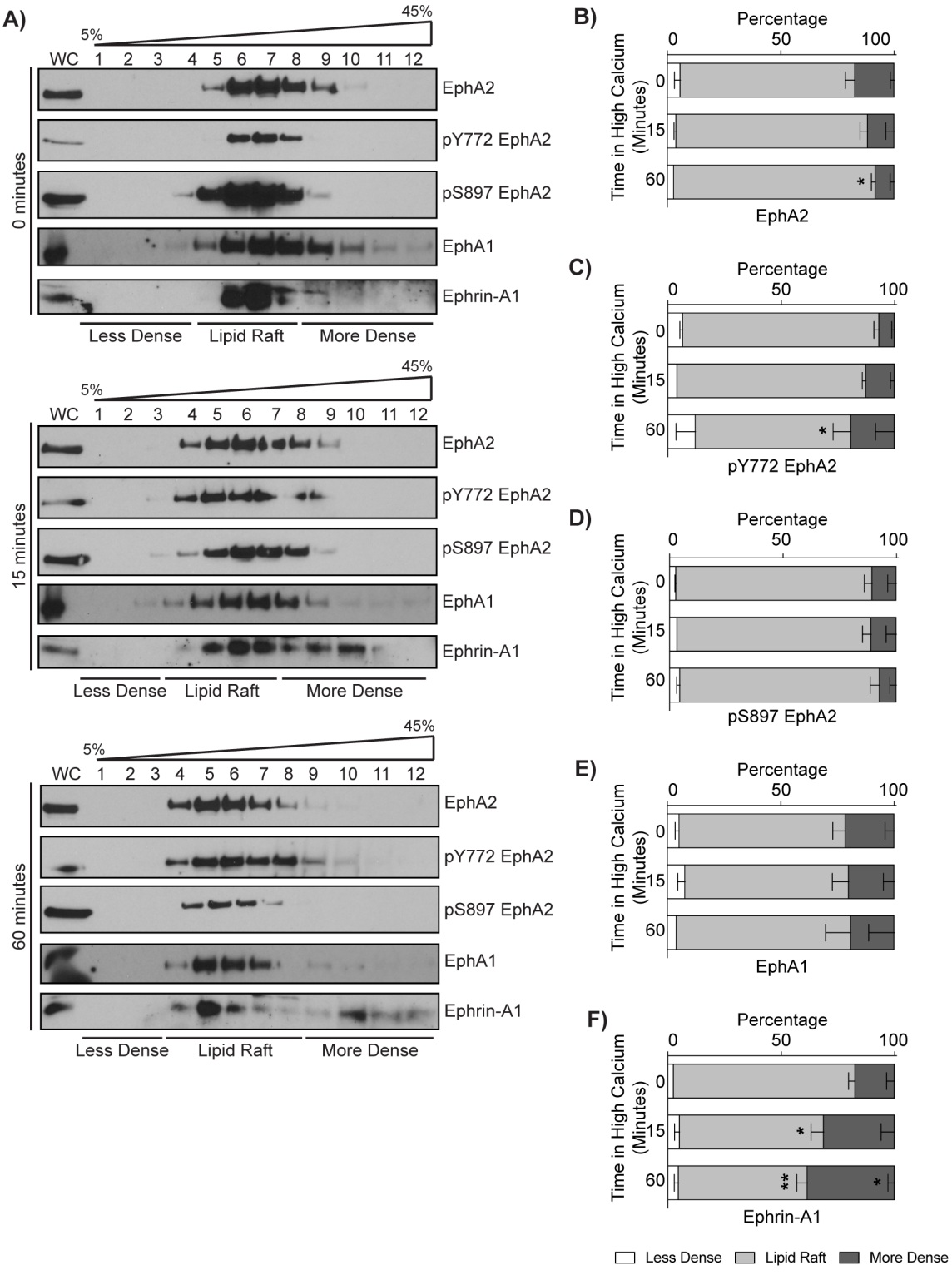
A)
5%
45%
WC 1 2 3 4 5 6 7 8 9 10 11 12
0 minutes
EphA2
pY772 EphA2
pS897 EphA2
EphA1
Ephrin-A1
Less Dense
Lipid Raft
More Dense
15 minutes
60 minutes
B)
C)
D)
E)
F)
Percentage
0
50
100
Time in High Calcium (Minutes)
0
15
60
EphA2
pY772 EphA2
pS897 EphA2
EphA1
Ephrin-A1
Less Dense
Lipid Raft
More Dense

Figure 13: Ephrin-A1 and ligand activated EphA2 are increased outside of lipid raft domains during calcium-induced cell-cell contact stabilization.
(A) Sucrose density gradients of EphA2, pY772 EphA2, pS897 EphA2, EphA1, and ephrin-A1 in keratinocytes maintained in low Ca^{2+} (0.03 mM) or switched to high Ca^{2+} (1.2 mM) medium for 15 and 60 minutes. Densitometry is quantified for EphA2 **(B)**, pY772 EphA2 **(C)**, pS897 EphA2 **(D)**, EphA1 **(E)**, and ephrin-A1 **(F)** as less dense, lipid raft, and more dense fractions. Location of these fractions were determined by flotillin-1 and caveolin-1 for each time point. (WC=Whole cell lysate; Error bars represent SD; *p≤0.05, **p≤0.01; paired two-way ANOVA with Dunnett post hoc test compared to 0 minutes, n=4).

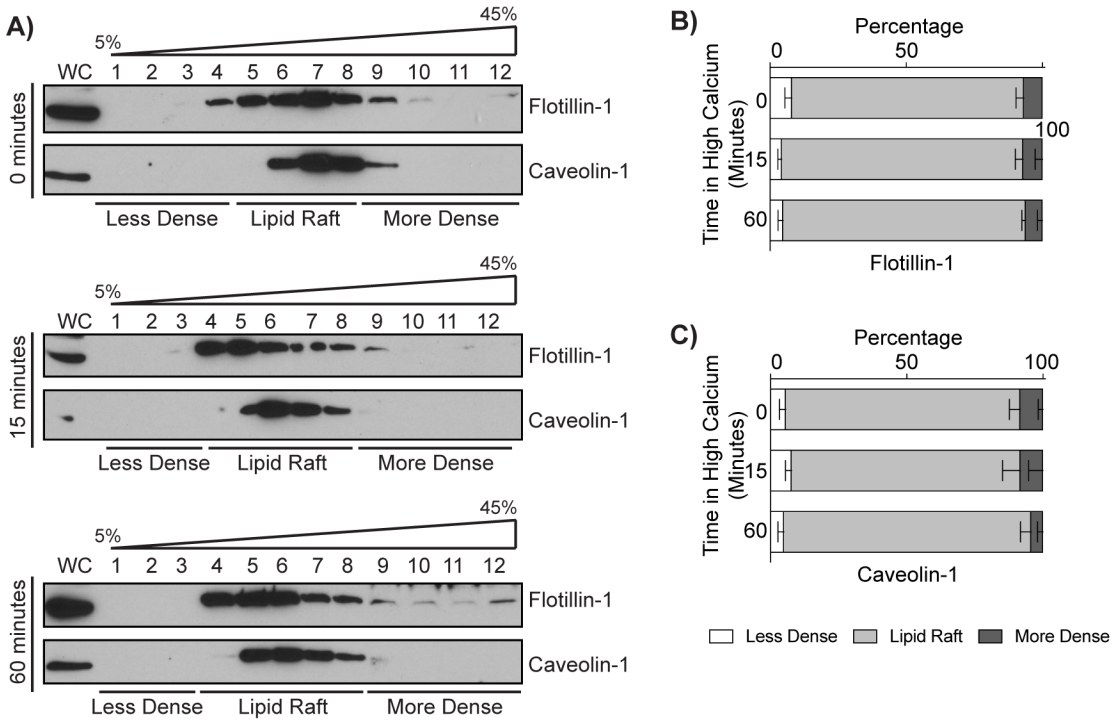

Figure 14: Calcium-induced cell-cell contact stabilization does not alter lipid-raft associated proteins in defined membrane microdomains.
(A) Sucrose density gradients of flotillin-1 and caveolin-1 in keratinocytes maintained in low Ca^{2+} (0.03 mM) or switched to high Ca^{2+} (1.2 mM) medium for 15 and 60 minutes. Densitometry is quantified for flotillin-1 **(B)** and caveolin-1 **(C)** as less dense, lipid raft, and more dense fractions. Lipid raft fractions were defined as having at least 10% of total flotillin-1 or caveolin-1 for each time point. Less dense and more dense fractions were then labelled accordingly once lipid raft fractions were defined (WC=Whole cell lysate; Error bars represent SD; paired two-way ANOVA with Dunnett post hoc test compared to 0 minutes, n=4).

Prior to cell-cell contact stabilization in high calcium, EphA2, as well as a basally active pY772 EphA2, were localized to cell borders and lipid raft domains (Figure 15). As cell-cell contacts mature in response to a calcium switch, the colocalization of pY772 EphA2 in caveolin-positive lipid raft domains was decreased as defined by Mander's coefficient analysis (Figure 15 A, B) matching the pattern of lipid raft depletion observed biochemically in sucrose density gradients (Figure 13 A, C). However, colocalization between total EphA2 and caveolin-1 remained unchanged (Figure 15 A, C). Additionally, the average distance between pY772 EphA2 spots and caveolin-1 positive surfaces, as identified by structured illumination microscopy (SIM) reconstruction, increased after NHEKs were placed in high calcium (1.2 mM) medium for 60 minutes (Figure 16). Collectively, these data suggest that a portion of EphA2 is present in lipid rafts along with ephrin-A1 and an activated form of this receptor is preferentially depleted out of these membrane domains along with its ligand upon cell-cell contact stabilization. Alternatively, ligand-activated EphA2 can be accumulating with ephrin-A1 outside of lipid-raft domains after the addition of high calcium.

We then used ephrin-A1-Fc to further assess how activation of EphA2 causes redistribution of this receptor to different membrane microdomains. Recombinant ephrin-A1-Fc treatment correlated with a redistribution of pY772 EphA2, but not total EphA2, out of lipid raft domains (Figure 17 A-C). Again, molecularly defined fractions containing caveolin-1 or flotillin-1 remained unchanged between samples (Figure 17 D, E). These observations further imply that ephrin-A1-induced activation of EphA2 triggers movement or an accumulation of this receptor in non-lipid raft domains.

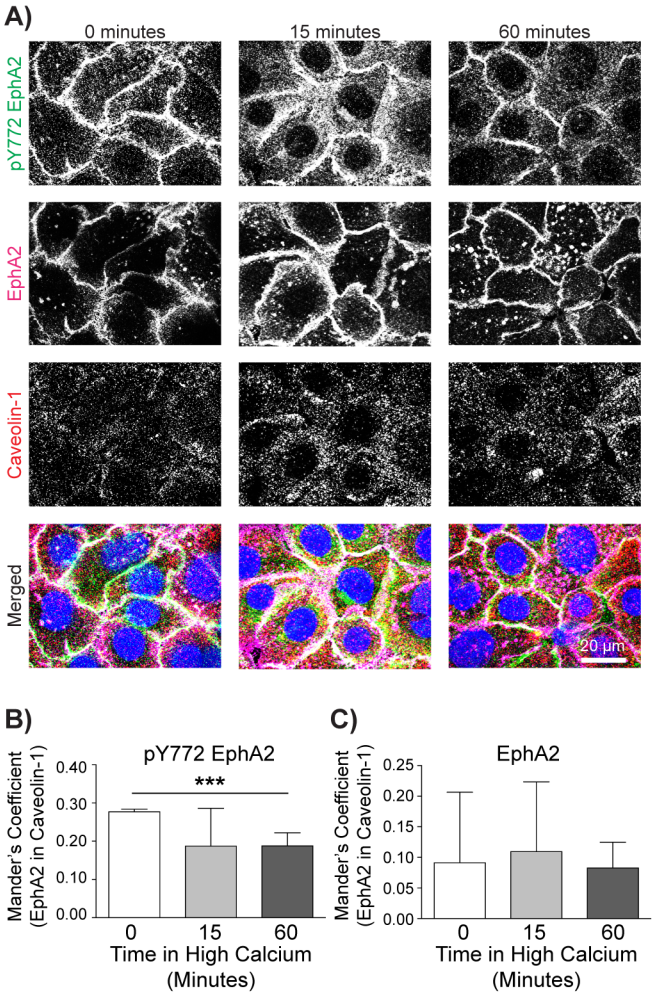

Figure 15: Decreased colocalization of caveolin-1 with ligand-activated pY772 EphA2 during calcium-induced cell-cell contact stabilization.
(A) Representative pY772 EphA2, EphA2, and caveolin-1 immunofluorescent images of NHEKs maintained in low Ca^{2+} (0.03 mM) medium and then switched into high Ca^{2+} (1.2 mM) medium for the indicated time points. DAPI was used to stain nuclei. (Scale bar=20 µm). Colocalization analysis of pY772 EphA2 in caveolin-1 and EphA2 in caveolin-1 is quantified as Mander's coefficients in **(B)** and **(C)**, respectively. (Error bars represent SD; ***p≤0.001; paired one-way ANOVA with Tukey post hoc test, n=4).

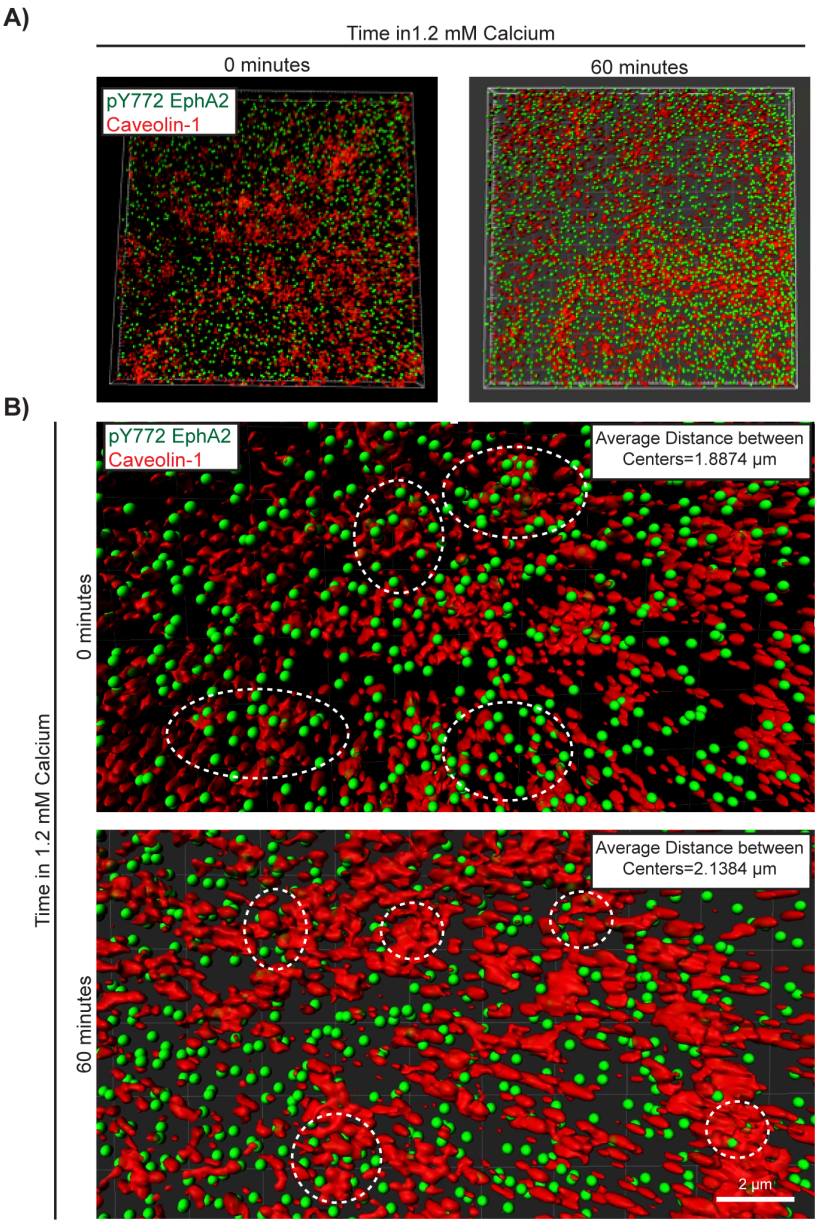

Figure 16: Ligand-active pY772 EphA2 moves away from caveolin-positive lipid raft domains during cell-cell contact stabilization.
(A) 3-D reconstructed images of caveolin-positive surfaces and pY772 EphA2 spots at 0 and 60 minutes after addition of high (1.2 mM) Ca^{2+}. Zoomed-in images are shown in **(B)** with white dotted lines highlighting areas of pY772 EphA2 embedded in caveolin-1 surfaces. Average distance between the center of pY772 EphA2 spots and caveolin-1 surfaces were calculated and shown in top right corners. (Scale bar=2 µm).

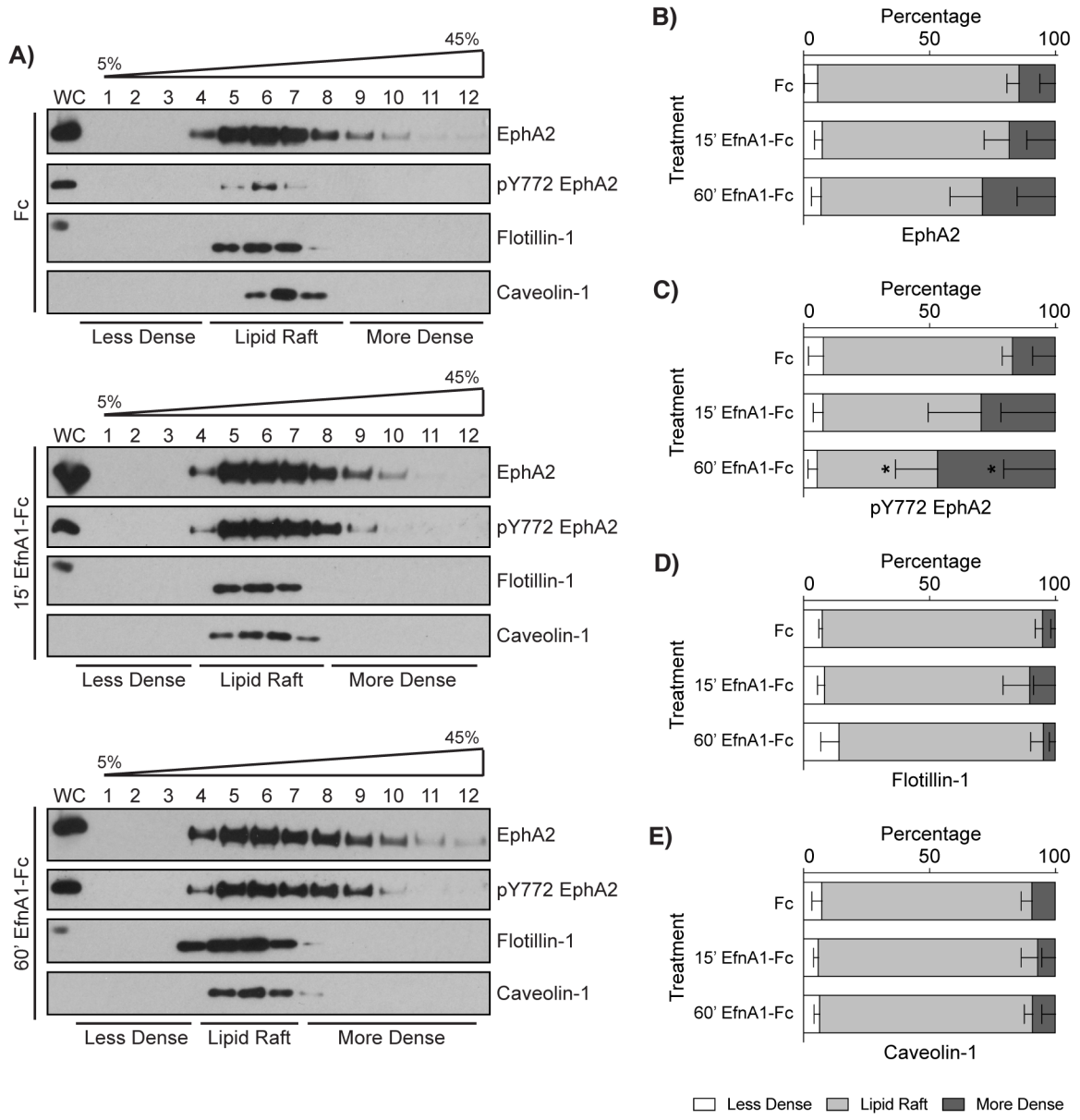

Figure 17: Recombinant ephrin-A1-Fc treatment depletes ligand-activated pY772 EphA2 from lipid raft domains.

(A) Sucrose density gradients after NHEKs were treated with Fc or Ephrin-A1-Fc (EfnA1-Fc) recombinant protein (1.0 μg/mL) for 15 and 60 minutes in growth medium. Densitometry is quantified for EphA2 **(B)**, pY772 EphA2 **(C),** flotillin-1 **(D)**, and caveolin-1 **(E)** as less dense, lipid raft, and more dense fractions as defined by flotillin-1 and caveolin-1. (Error bars represent SD; *p≤0.05; paired two-way ANOVA with Dunnett post hoc test compared to Fc treatment, n=3).

5. EphA2 palmitoylation is undetectable in keratinocytes

Protein palmitoylation can target proteins to lipid raft domains through the addition of a covalently-linked palmitate on specific cysteine residues [200, 201]. EphA2 contains three predicted cysteine palmitoylation sites in its ECD that are proximal to the TMD (C247, C376, C612). Additionally the PAT enzyme ZDHHC5 was recently identified to be part of the EphA2 interactome in keratinocytes [159]. This led us to hypothesize that EphA2 trafficking to lipid rafts could be modulated by protein palmitoylation.

Palmitoylation status can be tested by performing an ABE. In this procedure, palmitoylated cysteine residues are exchanged for biotin allowing for immunoprecipitation of all proteins that contain a palmitate. This only occurs in the presence of HA, which cleaves thioester-linked palmitoyl moieties. Therefore, lack of HA represents a negative control for non-specifically purified proteins [252]. Ras is an abundantly palmitoylated protein therefore can be used as a positive control for protein palmitoylation [202]. In NHEKs, Ras was palmitoylated in proliferating and differentiated keratinocytes (Figure 18). However, there was lack of evidence for palmitoylation of EphA2 (Figure 18). Alternative to ABE, palmitoylation status can be tested by APE mass tag labeling. Similarly, HA is required for palmitate cleavage, but instead of labelling with biotin, mPEG-Mal binds to previously palmitoylated cysteine residues. APE allows for identification of different palmitoylation isoforms and stoichiometric levels of these isoforms [242]. When NHEKs were switched to high calcium (1.2 mM) medium for different time points, Ras and Dsg1/2 both displayed mobility shifts in which there was an additional one or two isoforms, respectively (Figure 19). However, there was lack of additional protein species identified for EphA2, again signifying that EphA2 lacks palmitate-containing

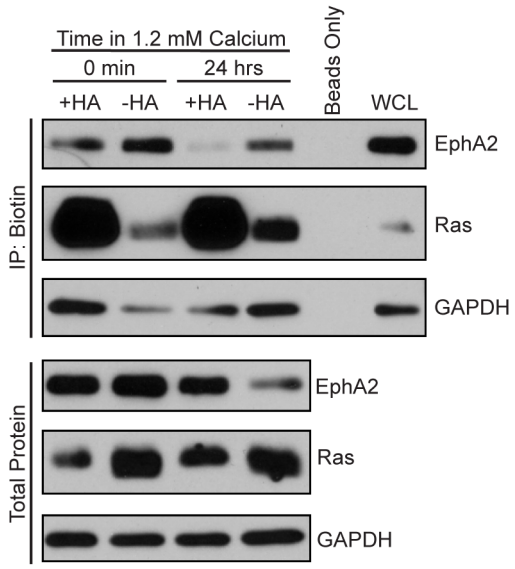

Figure 18: EphA2 palmitoylation in NHEKs is undetectable with ABE.
Palmitoylated proteins were labeled with biotin in NHEKs that were in low (0.03 mM) or high (1.2 mM) calcium medium for 24 hours. Biotinylated proteins were immunoprecipitated, separated by SDS-PAGE, and blotted for EphA2 and Ras (positive control). Lack of HA was used as a negative control. Total protein and whole cell lysates (WCL) were run to determine protein levels in each sample and GAPDH was used as a protein loading control.

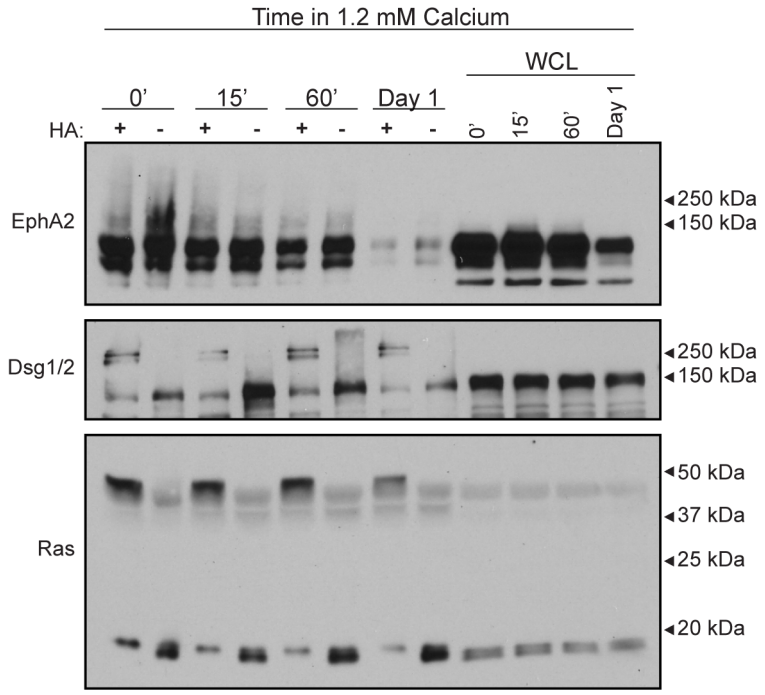

Figure 19: EphA2 palmitoylation in NHEKs is undetectable with APE.
NHEKs that were in high calcium (1.2 mM) for 0 minutes, 15 minutes, 60 minutes, or one day were labelled with 20 kDalton (kDa) mPEG-Mal. Proteins were immunoprecipitated, separated by SDS-PAGE, and blotted for EphA2, Dsg1/2 (positive control) and Ras (positive control). Palmitoylated proteins display a molecular weight mobility-shift due to addition of mPEG-Mal on each cysteine that contains a palmitate moiety. Lack of HA was used as a negative control. Whole cell lysates (WCL) were run to determine total protein levels in each sample. Molecular weights for reference are displayed on the right.

moieties (Figure 19). Although these results do not rule out the possibility that EphA2 is palmitoylated, it does suggest that EphA2 is not palmitoylated at these time points and conditions to a similar extent of Ras or Dsg.

Moreover, to further verify that palmitoylation is not playing a significant role in EphA2 cell-cell contact localization, we made putative palmitoylation-deficient mutants where the three predicted cysteine residues in the extracellular domain closest to the TMD were mutated to serine residues (EphA2.3CS), as previously done for plakophilin-2, plakophilin-3, and Dsg2 [240, 241]. EphA2.3CS was expressed in control (pLKO) or EphA2 knockdown NHEKs (shEphA2.pLKO) (Figure 20). When compared to endogenous EphA2 (LZRS), EphA2.3CS still retained its ability to localize to cell-cell contacts suggesting that even if EphA2 has the potential to be palmitoylated it likely doesn't regulate its trafficking to cell-cell contacts. Thus, after examining the palmitoylation status of EphA2 by three different protocols, ABE, APE, and generation of putative palmitoylation-deficient mutants, there is still lack of evidence for EphA2 palmitoylation.

6. The EphA2 TMD is required for receptor localization at cell-cell contacts

During cell-cell contact stabilization, EphA2 is localized to borders where it is likely activated by ephrin ligands [12]. At a calcium concentration of 0.2 mM, AJs proteins are recruited to cell-cell contacts but there are a lack of desmosome proteins thus providing us the ability to determine Eph receptor localization to stable junctions with minimal differentiation effects [161, 253]. After cell-cell contacts were stabilized in 0.2 mM calcium for 24 hours, EphA2 and EphA1 exhibited distinct localization patterns (Figure 21). Specifically, EphA2 was concentrated at sites of cell-cell contact whereas EphA1 had a diffuse localization pattern,

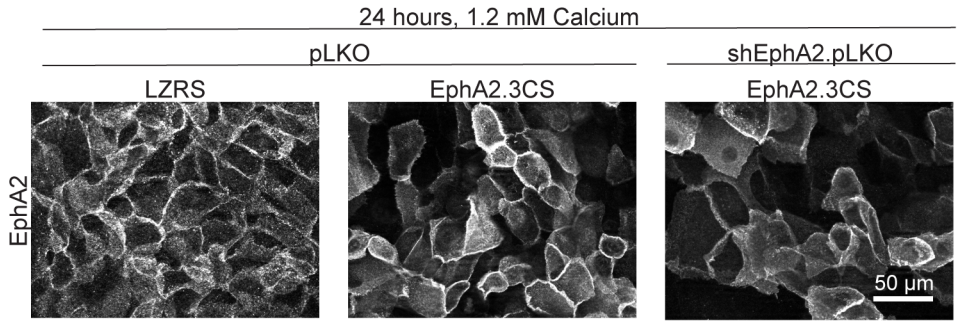

Figure 20: Putative palmitoylation-deficient EphA2 mutant localizes to cell-cell contacts. Immunofluorescent staining of EphA2 that contains the three predicted palmitoylated cysteines residues mutated to serines (EphA2.3CS) compared to empty vector control (LZRS) in both control (pLKO) and EphA2 knockdown (shEphA2.pLKO) NHEKs. NHEKs were switched to 1.2 mM Ca^{2+} medium for 24 hours. (Scale bar=50 μm).

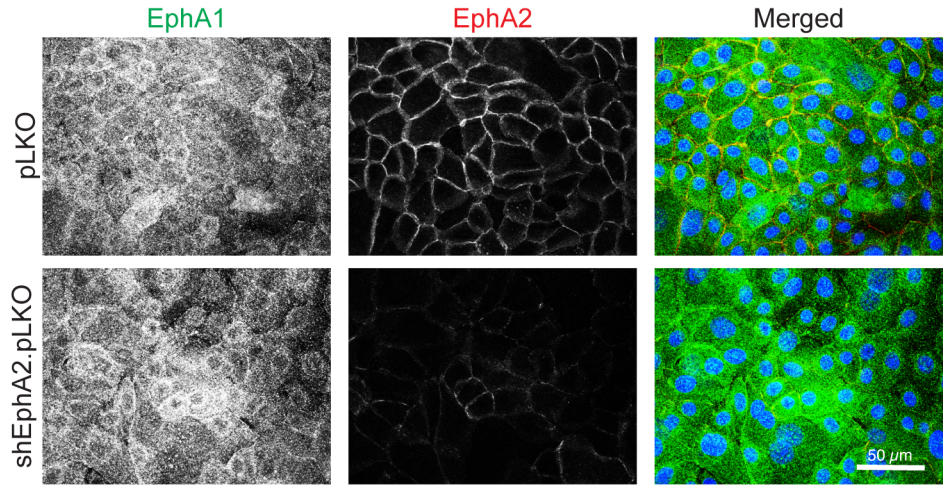

Figure 21: shRNA efficiently knocks down EphA2 expression.
Immunofluorescent images of EphA1 and EphA2 in control (pLKO) and EphA2 knockdown (shEphA2.pLKO) NHEKs with stable cell-cell contacts formed in 0.2 mM calcium for 24 hours. DAPI was used to stain nuclei. (Scale bar=50 μm).

similar to EphA1 and EphA2 localization patterns during calcium-induced keratinocyte differentiation (Figure 6). Although these two receptors have high amino acid sequence homology (approximately 65 percent), the sequence homology of their TMD is much lower (approximately 36 percent) (Figure 22) [92, 254]. Since TMD length and amino acid sequence impact membrane localization, we hypothesized that the unique properties of the EphA2 TMD may play a role in this RTKs cell-cell contact localization and dynamics out of lipid raft domains following cell-cell contact stabilization [103].

To assess the functional significance of the EphA1 and EphA2 TMDs in keratinocytes, the TMD of each EphA receptor was exchanged with the corresponding amino acid sequence of the other to generate chimeras; Chimera 121 contains the EphA1 ECD, EphA2 TMD, and EphA1 CD and Chimera 212 contains the EphA2 ECD, EphA1 TMD, and EphA2 CD (Figure 22). In order to compare the localization of Chimera 212 to that of EphA2, these ectopic proteins were expressed in keratinocytes when cell-cell contacts were stabilized (0.2 mM Ca^{2+} for 24 hours) where endogenous levels of EphA2 were knocked down (shEphA2.pLKO) (Figure 21). EphA1 was knocked down in NHEKs using siRNA to confirm specificity for EphA1 localization patterns (Figure 23). In contrast to endogenous EphA1, overexpressed EphA1 localized to cell-cell contacts, similar to that of EphA2 (Figure 24). This was also the case for Chimera 121 (Figure 24). Since overexpression of EphA1 was sufficient to cause cell border localization it cannot be determined if the EphA2 TMD had an effect on the localization of Chimera 121 to cell-cell contacts. However, unlike wild-type (WT) EphA2, Chimera 212 failed to localize to cell borders when cell-cell contacts were stabilized (Figure 24). Interestingly, the localization pattern of Chimera 212 more closely resembled that of EphA1 than EphA2 suggesting that the TMD

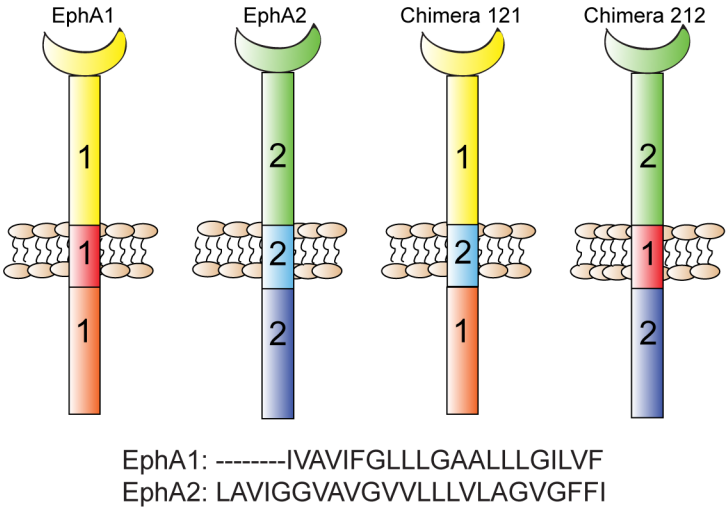

Figure 22: Diagram of transmembrane domain swaps to generate Chimera 121 and Chimera 212.

Diagram depicting Chimera 121 that contains the extracellular domain from EphA1 (amino acids 1-543), transmembrane domain from EphA2 (amino acids 523-563), and cytoplasmic domain from EphA1 (amino acids 573-976) and Chimera 212 that contains the extracellular domain from EphA2 (amino acids 1-522), transmembrane domain from EphA1 (amino acids 544-572), and cytoplasmic domain from EphA2 (amino acids 564-976). The differences in the predicted amino acid sequences of the transmembrane domain between EphA1 and EphA2 are shown below.

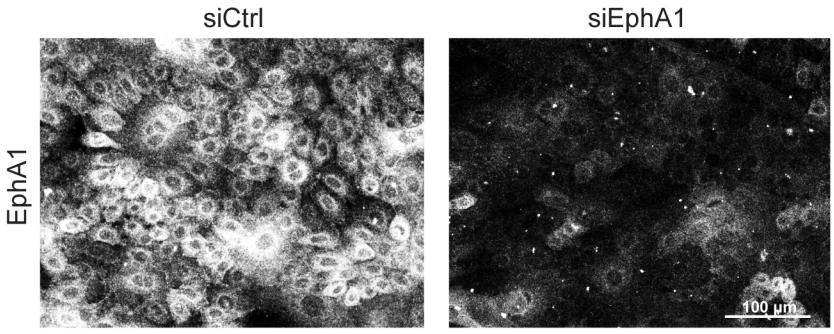

Figure 23: EphA1 expression is decreased in NHEKs expression siRNA targeting EphA1. Immunofluorescent images of EphA1 control (siCtrl) and EphA1 knockdown (siEphA1) NHEKs with stable cell-cell contacts formed in 1.2 mM calcium for 24 hours. DAPI was used to stain nuclei. (Scale bar=100 μm).

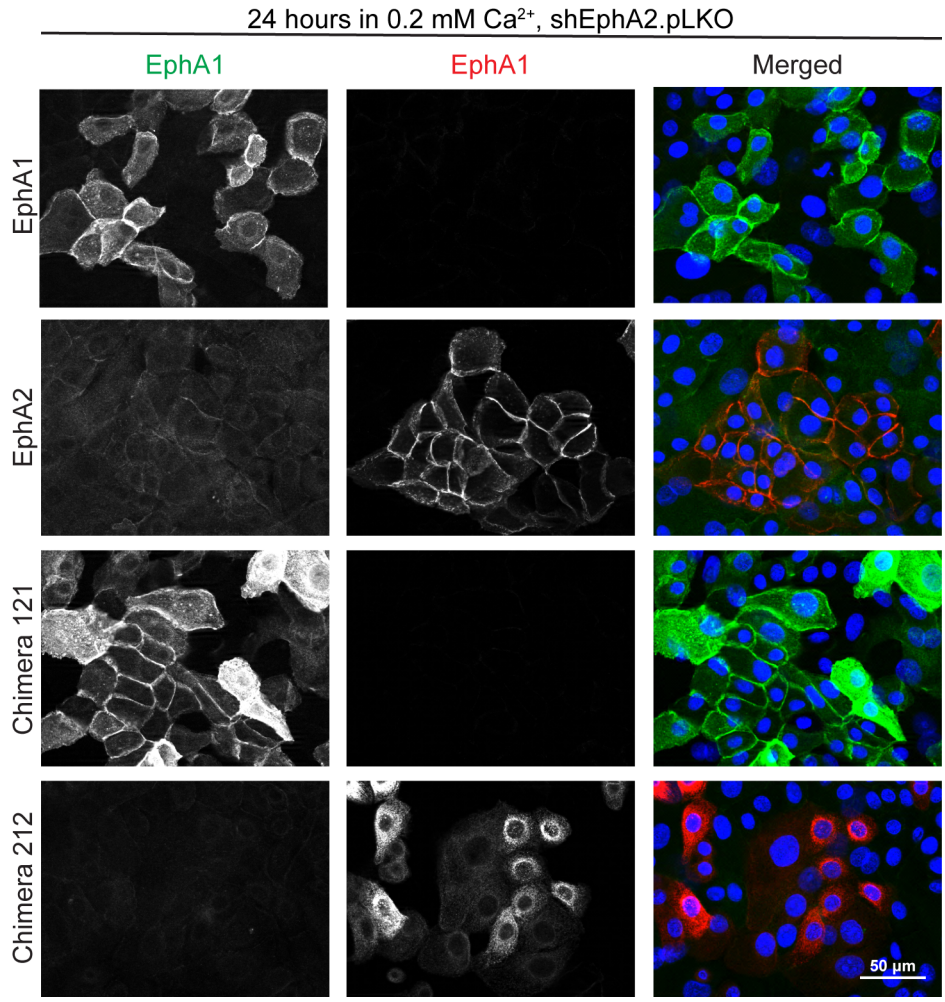

Figure 24: The EphA2 transmembrane domain is required for cell-cell contact localization.

Immunofluorescent staining of EphA1 and EphA2 in NHEKs that are overexpressing wild type EphA1, wild type EphA2, Chimera 121, or Chimera 212 on an EphA2 knockdown background (shEphA2.pLKO). NHEKs were maintained in 0.2 mM Ca^{2+} for 24 hours to allow for stabilization of cell-cell contacts. DAPI was used to stain nuclei. (Scale bar=50 µm).

plays an important role in these distinct localization patterns. Although Chimera 212 did not concentrate at cell borders, a limited but detectable portion of Chimera 212 was present at cell-cell contacts as junctions were being stabilized in high calcium (1.2 mM) for 15 minutes (Figure 25). Moreover, when cell surface proteins were labeled with biotin, Chimera 212 was biotinylated at the cell surface (Figure 26). Taken together, these findings suggest that Chimera 212 retains the ability to be trafficked to the cell surface but is poorly stabilized at regions of cell-cell contact.

Epidermal junctions are arguably more reflective of the in vivo state when studied in 3-D RHE models [130, 164]. In this culture model, when LZRS, EphA1, EphA2, Chimera 121, or Chimera 212 were expressed in NHEKs expressing (pLKO) or lacking endogenous EphA2 (shEphA2.pLKO) there were lack of significant morphological alterations (Figure 27). Also, EphA2 exhibited a junctional localization pattern whereas Chimera 212 remained mostly intracellular emulating its localization pattern during 2-D cell-cell contact stabilization (Figure 28; Figure 24). Collectively, these data add weight to the idea that the EphA2 TMD contributes to the stabilization of this RTK at cell-cell borders.

In order to verify that Chimera 212 has active kinase activity we utilized 293NT cells that lack endogenous Eph receptors. EphA2 and Chimera 212 were introduced into 293NT cells and forward signaling was activated with ephrin-A1-Fc treatment. Then, tyrosine phosphorylated proteins were immunoprecipitated from cell lysates. Following activation, there was an increase in proteins that were tyrosine phosphorylated with WT EphA2 and Chimera 212 (Figure 29). Additionally, there was enhanced tyrosine phosphorylation at the molecular weight of EphA2 (140 kDa), likely representing receptor autophosphorylation (Figure 29). Therefore, it is likely

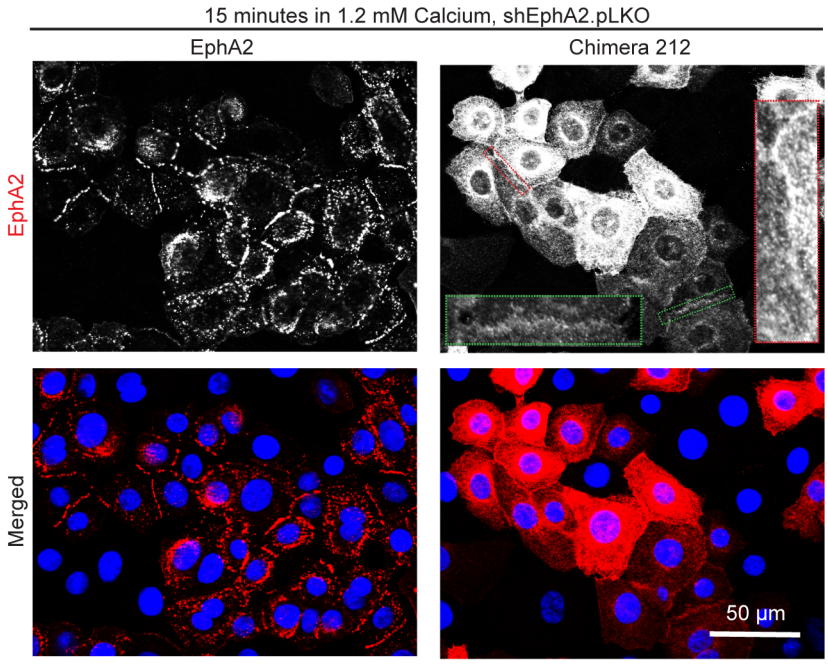

Figure 25: Chimera 212 has the ability to localize to cellular junctions during calcium-induced cell-cell contact stabilization.
Immunofluorescent images of EphA2 in NHEKs expressing EphA2 or Chimera 212 on an EphA2 knockdown (shEphA2.pLKO) background. NHEKs were grown in 0.03 mM calcium medium then switched to 1.2 mM calcium medium for 15 minutes to stabilize cell-cell contacts. Enlarged images correspond to cell-cell contacts where Chimera 212 was localized (Scale bar=50 µm).

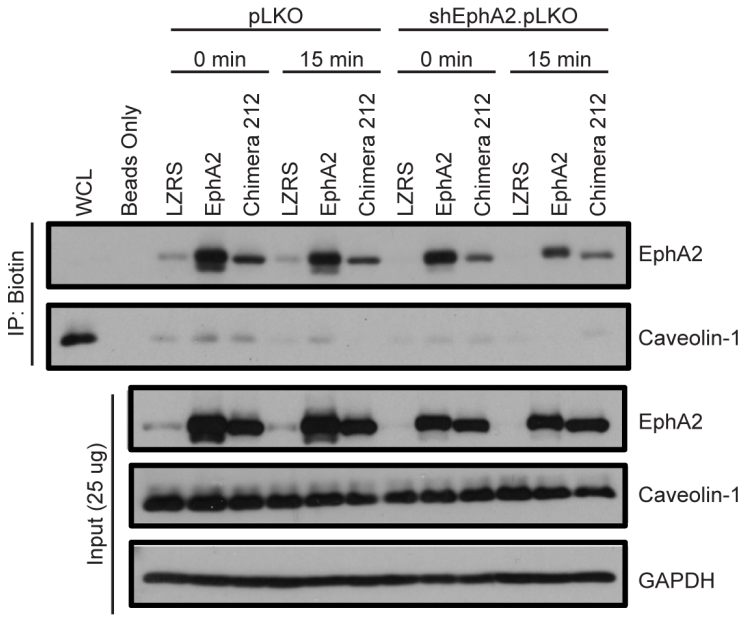

Figure 26: Chimera 212 can localize to the cell surface of NHEKs.
Cell surface proteins were labeled with biotin at 0 and 15 minutes after changing medium from 0.03 mM to 1.2 mM Ca^{2+} in NHEKs expressing LZRS, EphA2, or Chimera 212 on a control (pLKO) or EphA2 knock down (shEphA2.pLKO) background. Caveolin-1 was used as a negative control for cell surface biotinylation and GAPDH was used as a protein loading control. (WCL=Whole cell lysate; Beads Only=Streptavidin beads in buffer, IP negative control).

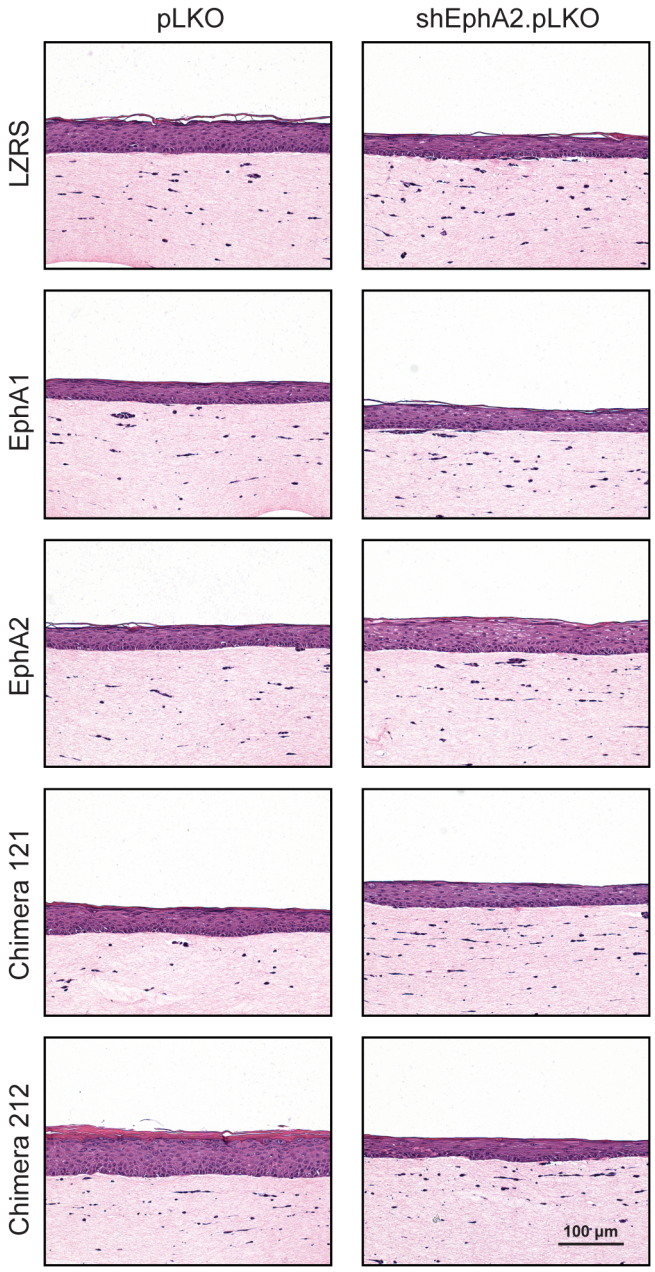

Figure 27: RHE cultures expressing wild type EphA1, wild type EphA2, Chimera 121, and Chimera 212 can stratify and differentiate.
LZRS, EphA1, EphA2, Chimera 121, and Chimera 212 were expressed in NHEKs on a control (pLKO) or EphA2 knockdown (shEphA2.pLKO) background. NHEKs were plated onto fibroblast-containing collagen plugs and lifted to an ALI. H&E staining of RHE culture 9 days after lifting to an ALI. (Scale bar=100 µm).

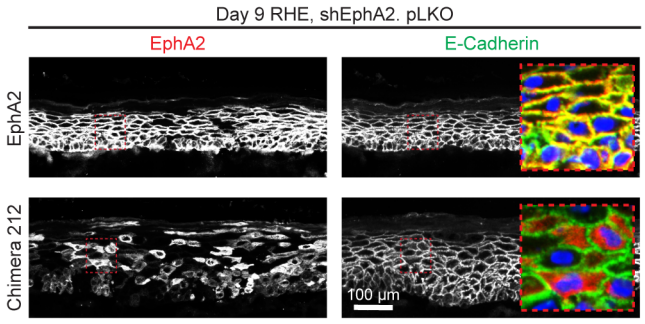

Figure 28: Chimera 212 lacks cell border localization in RHE.
Representative EphA2 and E-cadherin immunofluorescent images of RHE overexpressing EphA2 or Chimera 212 in EphA2 knockdown (shEphA2.pLKO) NHEKs 9 days after being lifted to an ALI. DAPI was used to stain nuclei. Magnified images show colocalization between EphA2 and E-cadherin (Scale bar=100 µm).

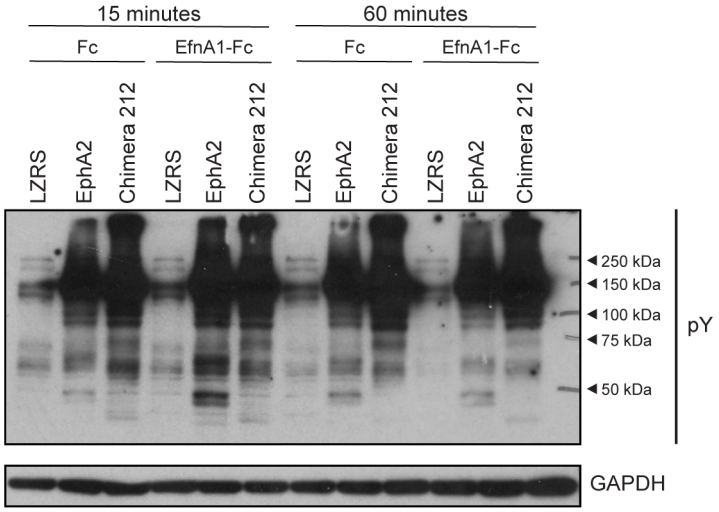

Figure 29: Chimera 212 can promote tyrosine phosphorylation of proteins.
LZRS, EphA2, and Chimera 212 vectors were expressed in 293NT cells and then treated with Fc or Ephrin-A1-Fc (EfnA1-Fc) recombinant protein (1.0 μg/mL) for 15 or 60 minutes. Tyrosine phosphorylated proteins were immunoprecipitated, separated by SDS-PAGE, and blotted for all tyrosine phosphorylated proteins (pY). GAPDH was used as a protein loading control. Molecular weights for reference are displayed on the right.

that Chimera 212 does have autophosphorylation and kinase activity even though it lacks the ability to be stabilized at cell-cell contacts.

7. Ephrin-A1 levels are regulated by EphA2 in a manner that depends on its TMD

Differences in receptor localization at cell-cell contacts between EphA2 and Chimera 212 led us to investigate the ability of Chimera 212 to localize to lipid raft domains. Sucrose gradients were performed 24 hours after cell-cell contacts were stabilized when endogenous EphA2 is normally concentrated at cell borders. When EphA2 and Chimera 212 were expressed in keratinocytes lacking endogenous EphA2 (shEphA2.pLKO) they both localized to lipid raft domain fractions at similar percentages, despite differences in localization patterns (Figure 30 A). These differences suggest that Chimera 212 may localize to lipid raft domains in endosome, Golgi apparatus, and cell surface membranes, rather than cell-cell contact membranes [255]. Exogenous expression of these receptors did not alter the relative abundance of flotillin-1 or caveolin-1 in lipid raft fractions (Figure 30 D, E). Thus, this chimera allowed for us to determine how loss of cell-cell contact stabilized EphA2 affects keratinocyte behaviors, without altering the ability of this receptor to localize to the cell surface and lipid raft domains. Although, EphA2 and Chimera 212 localized to lipid raft domains to a similar extent, the distribution of pY772 EphA2 and ephrin-A1 had differential localization to lipid raft fractions. Chimera 212 caused an increase in pY772 EphA2 outside of lipid raft domains despite having increased ephrin-A1 in lipid raft domains (Figure 30 B, C). This suggests that activated Chimera 212 may not localize to lipid raft domains with ephrin-A1 as was demonstrated by endogenous pY772 EphA2 during calcium-induced differentiation.

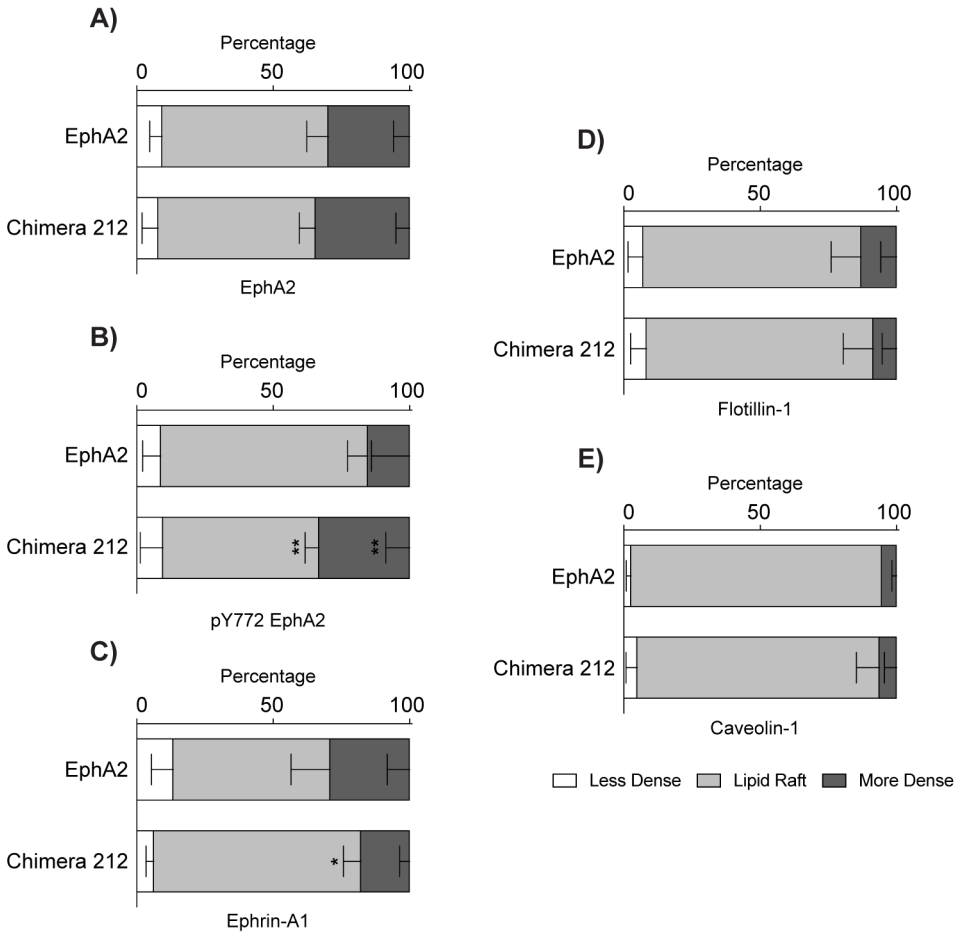

Figure 30: Chimera 212 alters pY772 EphA2 and ephrin-A1 lipid raft distribution. Quantification of sucrose density gradients for percentage of EphA2 **(A)**, pY772 EphA2 **(B)**, and ephrin-A1 **(C)** in less dense, lipid raft, and more dense fractions. Endogenous EphA2 was knocked down (shEphA) and wild type EphA2 or Chimera 212 were expressed and then NHEKs were switched to 0.2 mM calcium medium for 24 hours. Lipid raft fractions were defined by flotillin-1 and caveolin-1, which are quantified in **(D)** and **(E),** respectively. (Error bars represent SD; *p≤0.05, **p≤0.01; paired two-way ANOVA with Bonferroni post hoc test, n=3).

In order to understand how uncoupling of pY772 EphA2/ephrin-A1 movements affect endogenous EphA2, both EphA2 and Chimera 212 were expressed in NHEKs that still express endogenous EphA2. This led to a decrease in the percentage of this chimeric receptor and endogenous EphA2 from lipid raft fractions whereas ectopic expression of EphA2 had less impact on EphA2 membrane microdomain localization (Figure 31 A, B). Also, overexpression of EphA1 did not affect the lipid raft localization of endogenous EphA2 (Figure 31 A, B). Exogenously expressed EphA proteins did not alter the percentage of caveolin-1 or flotillin-1 in defined lipid raft fractions (Figure 31 C, D). These observations demonstrate that Chimera 212 also impairs endogenous EphA2 localization to lipid raft domains, likely including those located at cell-cell contacts where ephrin-A1 ligands are concentrated.

Following ephrin-induced activation of EphA2 at cell-cell contacts, Eph/ephrin complexes are internalized and degraded or recycled back to the cell surface [83]. This clearing of ephrins from the plasma membrane likely relies on the ability of Eph receptors to engage ligand in trans within specialized membrane domains, possibly including lipid rafts. Ultimately, this results in a down-modulation of ephrin ligand levels when EphA2 is prominently expressed in cells [188]. Therefore, we hypothesized that lack of Chimera 212 stabilization at cell-cell contacts and the depletion of endogenous EphA2 from lipid rafts would impact the ability of this chimeric receptor to regulate ephrin-A1 levels in keratinocytes. Interestingly, total ephrin-A1 protein levels were markedly increased when Chimera 212 was expressed in control (pLKO) and EphA2 knockdown keratinocytes (shEphA2.pLKO) under conditions where cell-cell contacts were stabilized (0.2 mM Ca^{2+} for 48 hours) (Figure 32). Also, expression of Chimera 212 resulted in smaller protein species as detected by immunoblotting, likely representing ephrin-A1

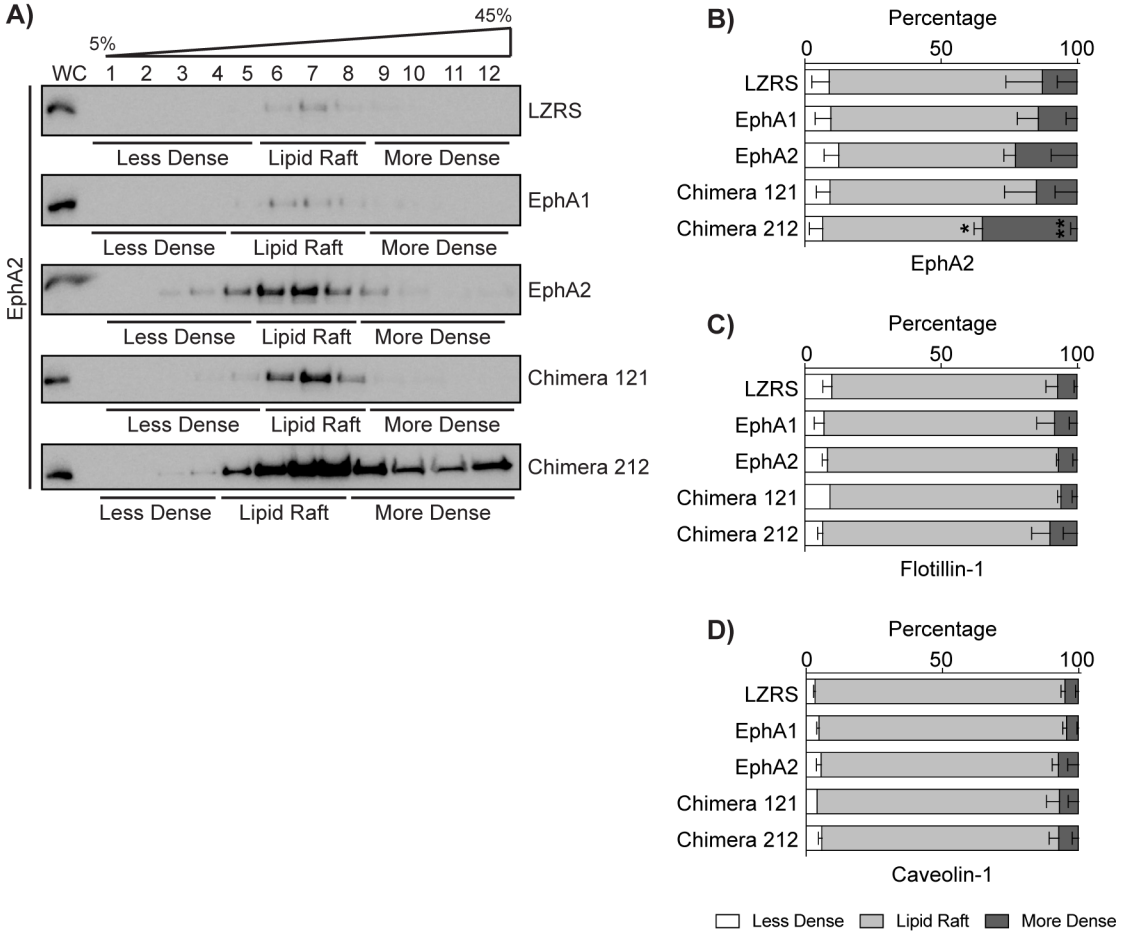

Figure 31: Chimera 212 causes an accumulation of endogenous EphA2 and Chimera 212 outside of lipid raft domains.

(A) Sucrose density gradients for EphA2 in NHEKs expressing control vector (LZRS), EphA1, EphA2, Chimera 121, or Chimera 212 after being maintained in 0.2 mM calcium medium for 24 hours. The percentage of EphA2 in less dense, lipid raft, and more dense fractions are quantified in **(B)**. Lipid raft fractions were defined by flotillin-1 and caveolin-1, which are quantified in **(C)** and **(D),** respectively. (Error bars represent SD; *p≤0.05, **p≤0.01; paired two-way ANOVA with Dunnett post hoc test compared to LZRS control, n=3).

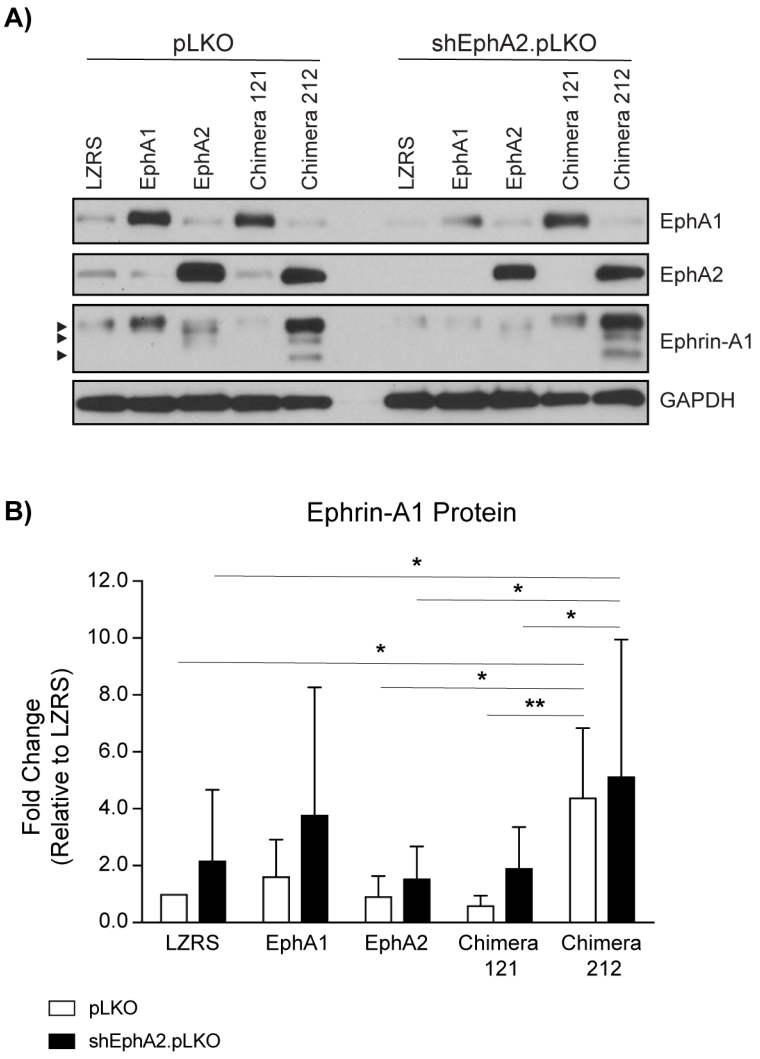

Figure 32: Chimera 212 leads to an accumulation of ephrin-A1.
(A) Western blot analysis of EphA1, EphA2, and ephrin-A1 in NHEKs that have been maintained in 0.2 mM calcium for 48 hours and express LZRS, EphA1, EphA2, Chimera 121, or Chimera 212 in control (pLKO) or EphA2 knockdown (shEphA2.pLKO) NHEKs. Processed ephrin-A1 fragments are indicated by arrowheads. GAPDH was used as a protein loading control. The expression level of ephrin-A1 is quantified in **(B).** (Error bars represent SD; *p≤0.05, **p≤0.01; paired two-way ANOVA with Bonferroni post hoc test between two groups and Tukey post hoc test between multiple groups, n=4).

fragments generated by protease cleavage as previously described in human glioblastoma and mammary adenocarcinoma cells [256-258]. Ectopic expression of EphA1, EphA2, or Chimera 121 had minimal impact on ephrin-A1 protein levels (Figure 32). Also, we failed to detect significant changes in ephrin-A1 mRNA transcript levels among these cultures suggesting that these alterations in ephrin-A1 protein expression does not reflect altered transcriptional regulation (Figure 33). Therefore, Chimera 212 increased expression of ephrin-A1 protein, possibly due to loss of EphA2 lipid raft association and cell-cell contact localization of this receptor.

Alterations in ephrin-A1 protein levels led us to hypothesize that ephrin-A1 internalization at cell-cell contacts may be altered when Chimera 212 was expressed. To test this a silicone chamber coculture confrontation assay was used [60]. The silicone chamber allowed for separation of two different NHEK populations; one population overexpressing ephrin-A1 and the other population either overexpressing wild type EphA2 or expressing Chimera 212. After removal of the silicon chamber, keratinocytes migrated until they confronted the other cell population thus forming a heterotypic confrontation interface. This interface allowed for an ephrin-A1/EphA2 boundary predominantly controlled by EphA2 trans-activation due to lack of ephrin-A1 co-expression in the EphA2 overexpressing cells. When ephrin-A1 confronted EphA2 overexpressing NHEKs, both the receptor and ligand exhibited a colocalized pattern in discrete puncta into the EphA2 overexpressing cells, likely due to trans-endocytosis of ephrin-A1 at cell-cell contacts (Figure 34 A). However, when ephrin-A1 overexpressing cells encountered Chimera 212 expressing cells there was lack of ephrin-A1 puncta in the Chimera 212 expressing cells, likely from lack of ligand trans-endocytosis (Figure 34 B). Also, Chimera 212 expressing

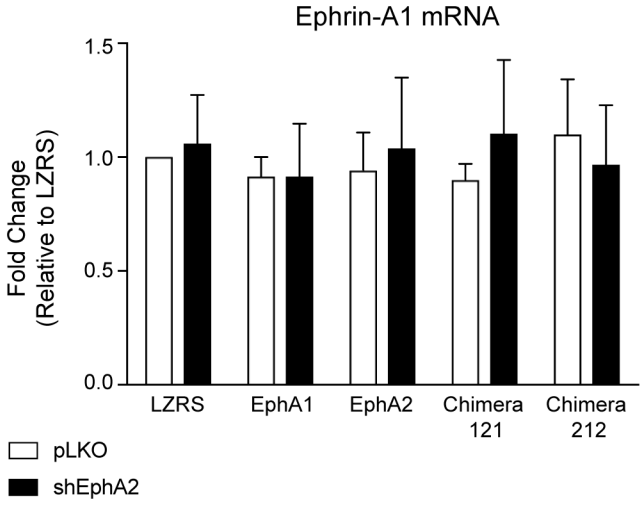

Figure 33: Overexpression of wild type EphA1 and EphA2 or Chimeras does not alter ephrin-A1 transcript levels.
q-RT-PCR analysis of ephrin-A1 mRNA levels in NHEKs expressing LZRS, EphA1, EphA2, Chimera 121, or Chimera 212 after 48 hours in 0.2 mM calcium medium in control (pLKO) or EphA2 knockdown (shEphA2.pLKO) background (Error bars represent SD; paired two-way ANOVA with Bonferroni post hoc test between two groups and Tukey post hoc test between multiple groups, n=3).

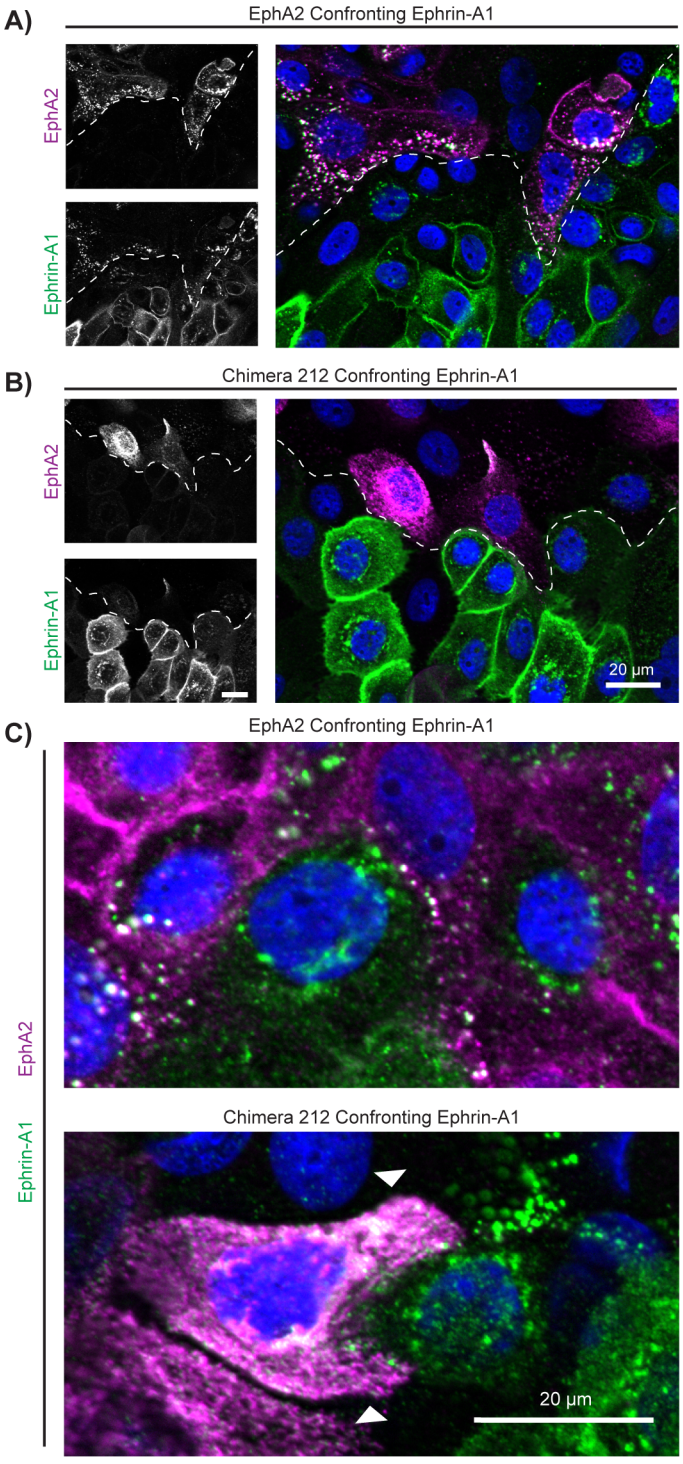
A)
EphA2 Confronting Ephrin-A1
EphA2
Ephrin-A1
B)
Chimera 212 Confronting Ephrin-A1
EphA2
Ephrin-A1
20 µm
C)
EphA2 Confronting Ephrin-A1
EphA2
Chimera 212 Confronting Ephrin-A1
Ephrin-A1
20 µm

Figure 34: Chimera 212 alters ephrin-A1 internalization at cell-cell contacts.
Immunofluorescent staining of ephrin-A1 overexpressing NHEKs confronting either EphA2 overexpressing NHEKs **(A)** or Chimera 212 expressing NHEKs **(B)**, 48 hours in 0.2 mM Ca^{2+} medium after removal of the silicon coculture chamber. White dashed lines show confrontation area and DAPI was used to stain nuclei. **(C)** Magnified image of a confrontation area between an ephrin-A1 overexpressing cell confronting an EphA2 overexpressing cell (top) or Chimera 212 expressing cell (bottom). Arrowheads indicate abnormal cellular processes at the heterotopic boundary. (Scale bar=20 μm).

cells contain abnormal cellular process that surround the ephrin-A1 overexpressing cells at the Chimera 212-Ephrin-A1 boundary (Figure 34 C). This is opposed to the linear boundary that is formed at the EphA2-Ephrin-A1 interface. Collectively, these data suggest that Chimera 212-induced increases in ephrin-A1 are possibly due to inability of this receptor to efficiently internalize ephrin-A1 at cell-cell contacts.

8. EphA2 TMD is required for efficient keratinocyte migration

Ligand targeting of EphA2 by ephrin-A1 negatively regulates migration of keratinocytes [14, 80, 259]. In view of the observed increase in ephrin-A1 levels in keratinocytes expressing Chimera 212, we investigated how replacement of the EphA2 TMD with that of EphA1 would impact cell migration. We anticipated that the migratory response of Chimera 212 and wild type EphA2 expressing keratinocytes would be different due to enhanced availability of ephrin-A1 ligand in the cellular microenvironment in the latter condition. To test this possibility, scratch-wounds were made in confluent keratinocyte cultures with cell-cell contacts stabilized at 0.2 mM calcium for 24 hours.

As a positive control and consistent with previous studies, treatment with an ephrin-A1-Fc recombinant protein (1 μg/mL) at the time of wounding inhibited keratinocyte migration [14, 80] (Figure 35 A). Furthermore, keratinocytes overexpressing EphA1, EphA2, or Chimera 121 showed reduced migration when treated with ephrin-A1-Fc while overexpression of the respective receptor alone had minimal impact (Figure 35 A). Strikingly, expression of Chimera 212 significantly inhibited keratinocyte migration to a similar extent as recombinant ephrin-A1-Fc treatment (Figure 35 A). Knockdown of endogenous EphA2 (shEphA2), although not significant, decreased wound closure (Figure 35 B). However, treatment of shEphA2

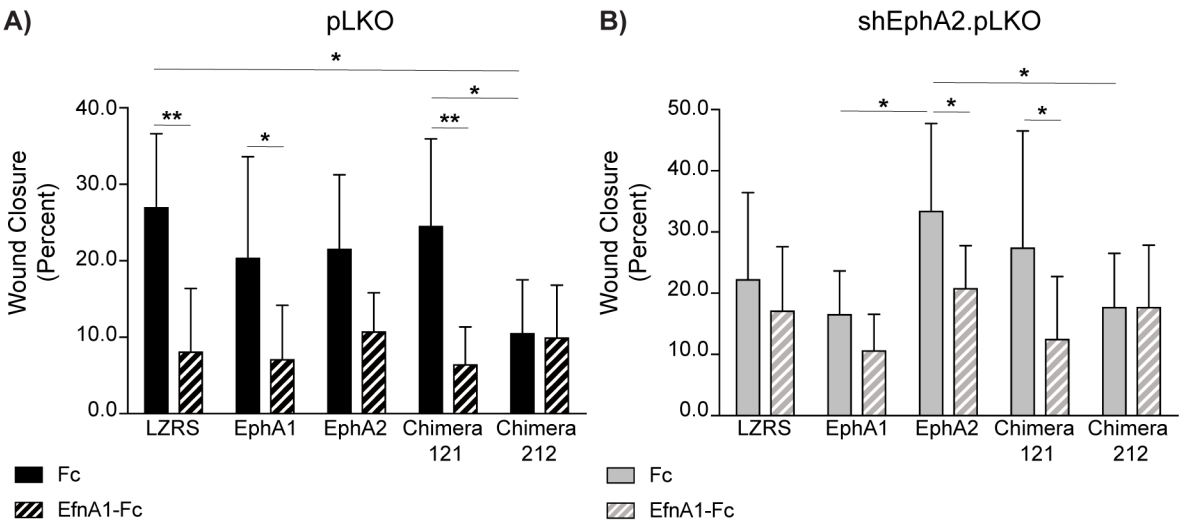

Figure 35: The EphA2 TMD is required for efficient keratinocyte migration.
Scratch wound assays were performed in NHEKs expressing LZRS, EphA1, EphA2, Chimera 121, or Chimera 212 in a control (pLKO; **A**) or EphA2 knockdown (shEphA2.pLKO; **B**) background. NHEKs were in 0.2 mM Ca^{2+} for 24 hours prior to wounding and then then treated with Fc or ephrin-A1-Fc (EfnA1-Fc) recombinant protein (1.0 μg/mL) in 0.2 mM Ca^{2+} at the time of scratching and allowed to migrate into the wound area for 24 hours. Percent wound closure was then calculated. (Error bars represent SD; *p≤0.05, **p≤0.01; paired two-way ANOVA with Bonferroni post hoc test between two groups and Tukey post hoc test between multiple groups, n=3).

keratinocytes with ephrin-A1-Fc did not further inhibit migration. When EphA2 and Chimera 121 were overexpressed in shEphA2 keratinocytes migration was increased and this response could be inhibited with ephrin-A1-Fc treatment (Figure 35 B). However, migration was not increased in shEphA2 NHEKs when EphA1 or Chimera 212 were overexpressed suggesting that the EphA2 TMD is required to promote migration in keratinocytes lacking endogenous EphA2 (Figure 35 B).

In addition to 2-D NHEK cultures, we can test keratinocyte migration potential in 3-D RHE by generating an epidermal wound in the center of the RHE with a punch biopsy. This allows for cells at the leading edge to migrate and close the epidermal wound [167]. The wounds were generated seven days after lifting to an air-liquid interface and then keratinocytes were given five days to migrate into the wound bed. Percent wound closure was determined relative to the initial punch biopsy area (Figure 36). In control (LZRS) and EphA2 overexpressing NHEKs, an epidermal tongue migrated into the wound area. But, ephrin-A1-Fc treatment (1 μg/mL) not only caused an inhibition of migration, but actually caused an increase in the wound area likely due to ephrin-A1-induced contraction of the epidermis. Similarly, expression of Chimera 212 caused a significant decrease in percent wound closure, similar to that of ephrin-A1-Fc treatment. Therefore, cumulative with 2-D migration studies, it suggests that the EphA2 TMD is required for efficient wound closure and lack of its endogenous TMD causes a migratory phenotype analogous to ephrin-A1-Fc treatment.

Chimera 212-induced inhibition of migration led us to question if these keratinocytes lack the ability to proliferate. To test this, we utilized Crystal Violet (Figure 37) and Hoechst (Figure 38) dyes to stain DNA of viable cells as keratinocytes are undergoing exponential growth. When

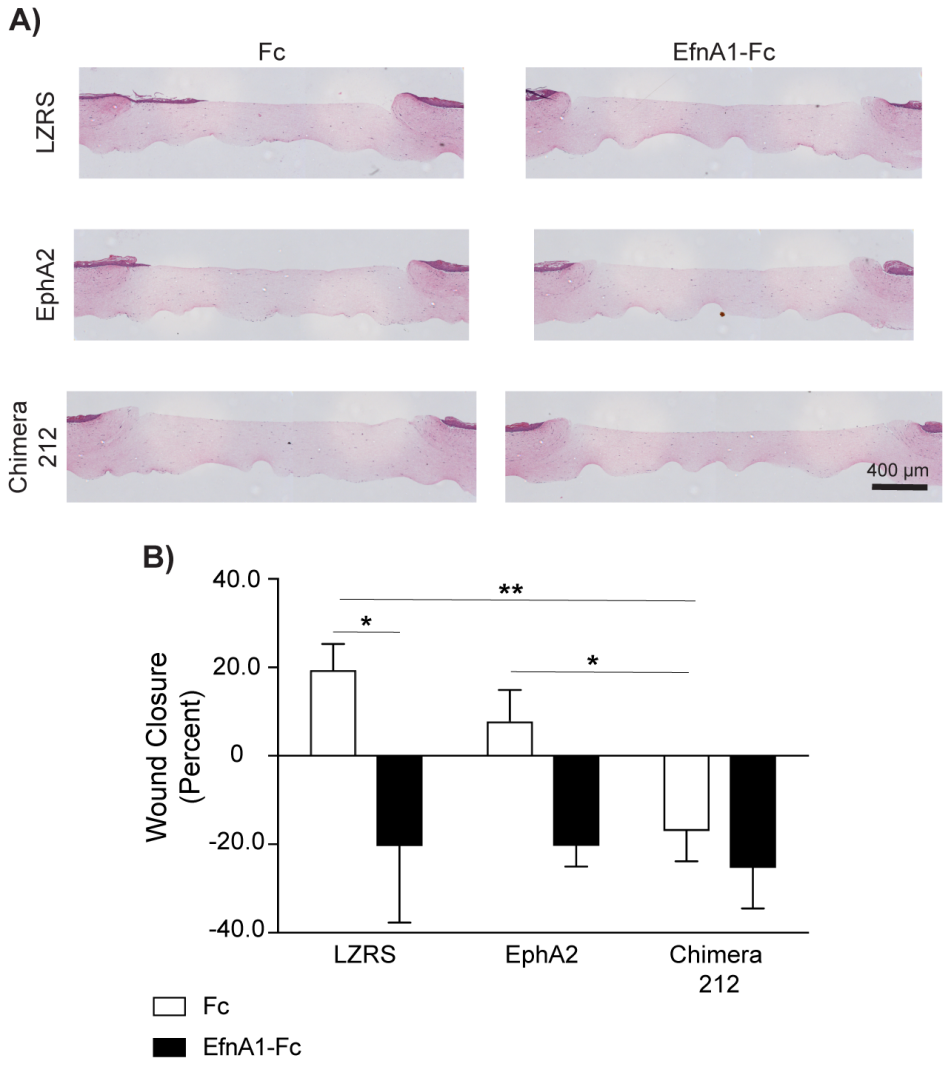

Figure 36: The EphA2 TMD is required for wound closure in RHE.
(A) H&E images of RHE expressing LZRS, EphA2, or Chimera 212 five days after being wounded and treated with Fc or EfnA1-Fc (1.0 μg/mL). Percent wound closure is quantified in **(B).** (Error bars represent SD; *p≤0.05, **p≤0.01; paired two-way ANOVA with Bonferroni post hoc test between two groups and Tukey post hoc test between multiple groups, n=2-3).

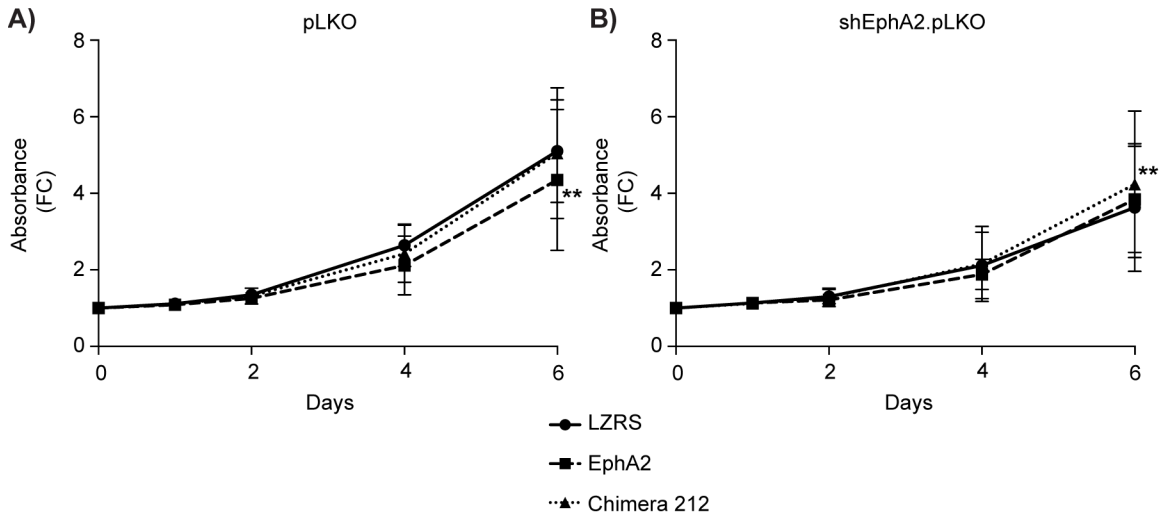

Figure 37: NHEKs expressing Chimera 212 retain the ability to proliferate when assessed with Crystal Violet staining.

Crystal violet assays were performed over a course of 6 days in control (pLKO) **(A)** and EphA2 knockdown (shEphA2.pLKO) NHEKs **(B)** that were expressing LZRS, wild type EphA2, or Chimera 212. NHEKs were plated to be subconfluent and allowed to proliferate for 6 days. Fold change (FC) in absorbance was compared to day 0. (Error bars represent SD; **p≤0.01; paired two-way ANOVA with Bonferroni post hoc test, n=4).

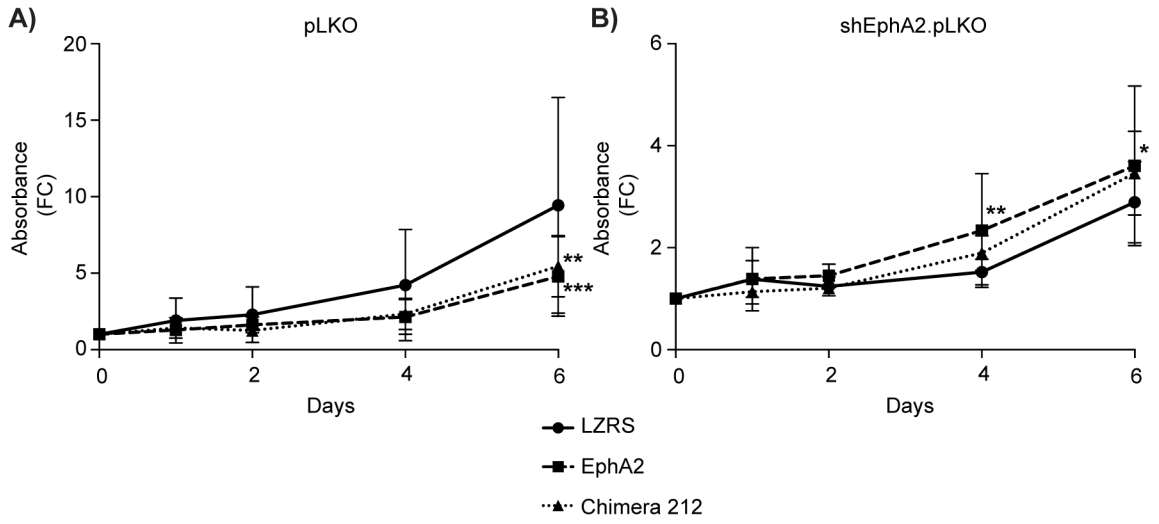

Figure 38: Chimera 212 expressing NHEKs proliferate to a similar extent as wild type EphA2 when evaluated with Hoechst staining.
Hoechst dye assays were completed in control NHEKs (pLKO) or NHEKs lacking endogenous EphA2 (shEphA2.pLKO) and reconstituted with LZRS, wild type EphA2, or Chimera 212. NHEKs were plated to be subconfluent and allowed to proliferate for 6 days. Fold change (FC) in absorbance was compared to day 0. (Error bars represent SD; *p≤0.05, **p≤0.01, ***p≤0.001; paired two-way ANOVA with Bonferroni post hoc test, n=3).

NHEKs were stained with Crystal Violet, overexpression of EphA2 caused a significant decrease in proliferation, but this was normalized when wild type EphA2 was expressed in NHEKs lacking endogenous EphA2 (shEphA2). But, when Chimera 212 was expressed in shEphA2 NHEKs proliferation was increased (Figure 37). However, when NHEKs were stained with Hoechst dye, both EphA2 and Chimera 212 overexpression decreased proliferation, but these affects were eliminated in shEphA2 NHEKs; reconstitution of wild type EphA2 and Chimera 212 in shEphA2 NHEKs actually increased cell number (Figure 38). Hence, Chimera 212 expressing cells still have the ability to proliferate similar to that of control (LZRS) NHEKs. These results further support migration results showing that lack of migration in Chimera 212 expressing cells is likely not due to alterations in cell proliferation.

In order to determine the effect that proliferation has on migration, mitomycin C (MMC; 0.4 μg/mL) was used prior to scratching therefore inhibiting keratinocyte proliferation. Chimera 212 decreased keratinocyte migration irrespective of the presence of MMC (Figure 39). However, inhibition of proliferation alters keratinocyte migration. In control (LZRS) or EphA2 overexpressing NHEKs, addition of MMC promotes migration, but this effect was diminished by knocking down endogenous EphA2 (shEphA2; Figure 39). Also, addition of MMC decreased migration between control and shEphA2 NHEKs. However, these migration defects were not normalized by reconstitution with WT EphA2 (Figure 39). Therefore, proliferation inversely affects keratinocyte migration. Also, EphA2 knockdown reduces keratinocyte migration when proliferation is inhibited.

Since Chimera 212 increased ephrin-A1 levels in keratinocytes, we hypothesized that inhibition of migration would be normalized by preventing the induction in ephrin-A1 levels,

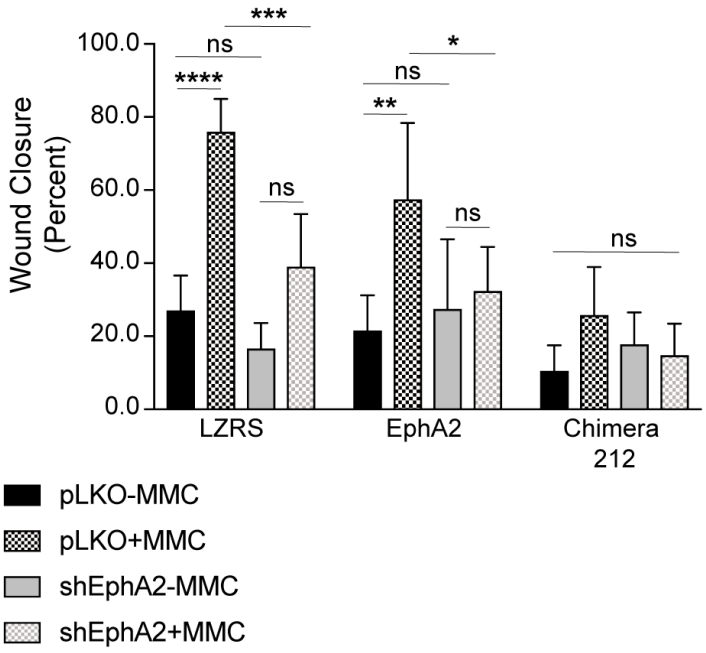

Figure 39: Cell proliferation prevents keratinocyte migration.
Scratch wound assay were completed in control (pLKO) and EphA2 knockdown (shEphA2) NHEKs that were also expressing LZRS, EphA2, or Chimera 212. NHEKs were switched to 0.2 mM Ca^{2+} medium for 24 hours. Then, 2 hours prior to scratching NHEKs were treated with control or MMC (0.4 μg/mL) in 0.2 mM Ca^{2+} medium to inhibit cell proliferation. Following scratching, NHEKs were allowed to migrate into the scratch wound for 24 hours and then percent wound closure was calculated. (Error bars represent SD; *p≤0.05, **p≤0.01, ****p≤0.0001; paired two-way ANOVA with Tukey post hoc test, n=3).

which we achieved via siRNA-mediated knockdown (Figure 40 A). Consistent with its role in restricting migration, reducing ephrin-A1 levels by itself led to more efficient closure of linear scratch wounds in vitro (Figure 40 B). Moreover, when ephrin-A1 was knocked down in keratinocytes expressing Chimera 212, keratinocyte migration was normalized to control levels, consistent with the notion that this EphA2 mutant deficient in lipid raft association and cell-cell contact localization inhibited migration largely as a consequence of increased ephrin-A1 levels (Figure 40 B). Collectively, our data suggest that the EphA2 TMD has important functions in regulating ephrin-A1 levels in order to allow for efficient keratinocyte migration.

As opposed to migration, ephrin-A1 is a positive regulator of keratinocyte differentiation [12]. When EphA1, EphA2, Chimera 121, or Chimera 212 were overexpressed in keratinocytes, K10 mRNA levels remained unaltered (Figure 41). Also, protein expression levels of differentiation-associated proteins like K10, Dsg1, and Dsc1 were not significantly changed (Figure 42). Therefore, it is likely that modifications in signaling from expression of Chimera 212 are relatively specific to anti-migratory pathways. Also, these data suggest that increased expression of ephrin-A1 is not sufficient to enhance keratinocyte differentiation.

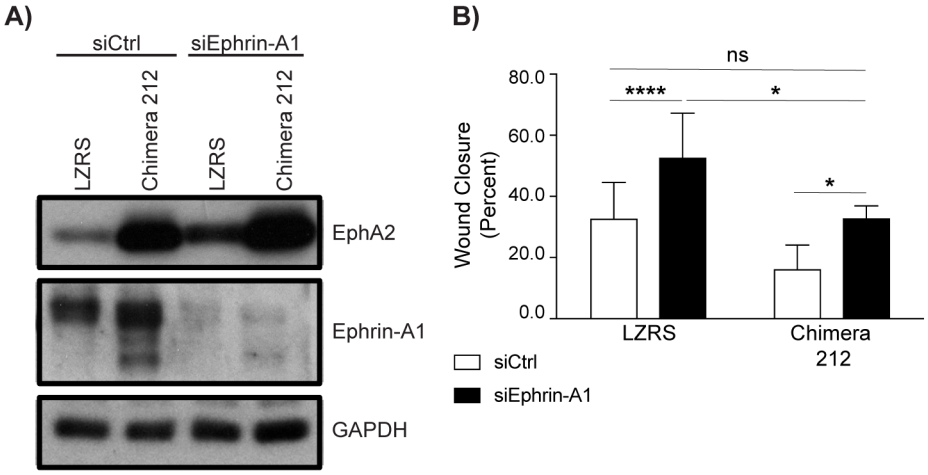

Figure 40: Ephrin-A1 knockdown normalizes Chimera-212-induced inhibition of keratinocyte migration.

(A) Western blot analysis of EphA2 and ephrin-A1 in keratinocytes that have been treated with control or ephrin-A1 siRNA. GAPDH was used as a protein loading control. **(B)** Keratinocytes expressing LZRS or Chimera 212 were treated with control or ephrin-A1 and allowed to migrate for 24 hours after generation of a linear scratch wound closure. Percent wound closure was then calculated. (Error bars represent SD; ns=not significant, *p≤0.05, **p≤0.01, ****p≤0.0001; paired two-way ANOVA with Bonferroni post hoc test, n=4).

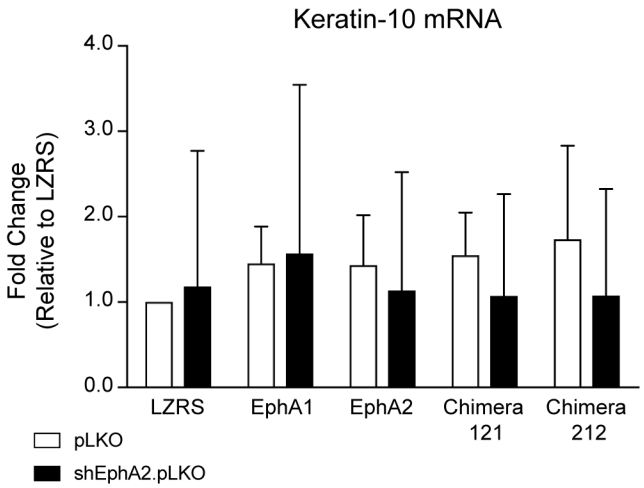

Figure 41: Expression of EphA1, EphA2, Chimera 121, or Chimera 212 do not affect the expression of K10 transcripts.

RT-qPCR analysis of K10 mRNA levels in NHEKs expressing LZRS, EphA1, EphA2, Chimera 121, or Chimera 212 in control (pLKO) or EphA2 knockdown (shEphA2.pLKO) NHEKs. RNA was harvested after NHEKs were maintained in 0.2 mM calcium medium for 48 hours. (Error bars represent SD; paired two-way ANOVA with Tukey post hoc test compared between conditions, n=3).

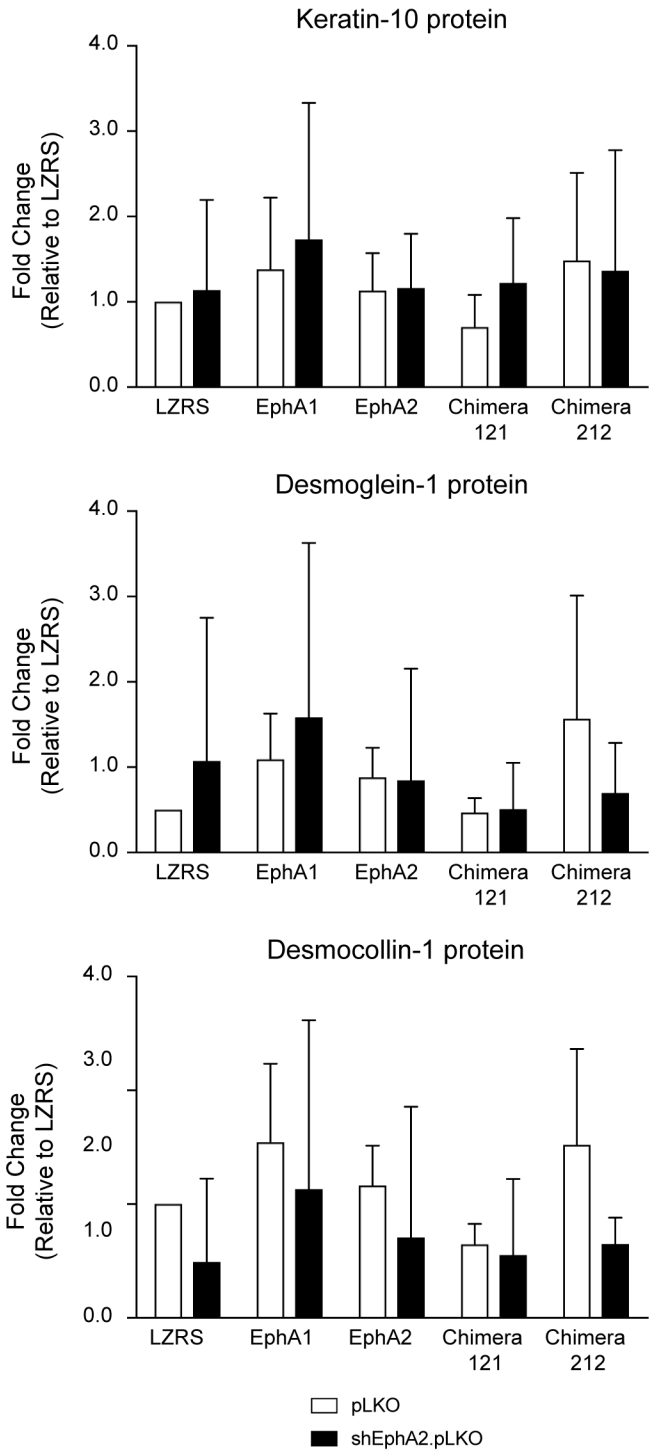
Keratin-10 protein
Fold Change (Relative to LZRS)
4.0
3.0
2.0
1.0
0.0
LZRS
EphA1
EphA2
Chimera 121
Chimera 212
Desmoglein-1 protein
Fold Change (Relative to LZRS)
4.0
3.0
2.0
1.0
0.0
LZRS
EphA1
EphA2
Chimera 121
Chimera 212
Desmocollin-1 protein
Fold Change (Relative to LZRS)
4.0
3.0
2.0
1.0
0.0
LZRS
EphA1
EphA2
Chimera 121
Chimera 212
pLKO
shEphA2.pLKO

Figure 42: Expression of EphA1, EphA2, Chimera 121, or Chimera 212 do not significantly affect keratinocyte differentiation.
Protein analysis of differentiation-associated proteins K10, Dsg1, and Dsc1 in NHEKs expressing LZRS, EphA1, EphA2, Chimera 121, or Chimera 212 in control (pLKO) or EphA2 knockdown NHEKs (shEphA2.pLKO). Lysates were collected after 48 hours in 0.2 mM calcium medium (Error bars represent SD; paired two-way ANOVA with Tukey post hoc test compared between conditions, n=3).

IV. SUMMARY AND FUTURE DIRECTIONS

1. The EphA2 lipid raft model

Eph/ephrin signaling relies on the ability of this receptor/ligand pair to localize to cell-cell contacts in order to balance ligand-induced cis-inhibition and trans-activation. Modulation of this balance can lead to diverse signaling outcomes [260]. Although an extensive body of work has contributed to our understanding of downstream Eph/ephrin signaling, specifically in embryogenesis, neuronal patterning, and cancer cells, our knowledge of how this receptor/ligand pair localizes to specific membrane microdomains allowing for receptor activation is still incomplete [22, 261]. Here, we have shown that in addition to early stages of keratinocyte differentiation, forward signaling elicited by ephrin-A1 can promote late stages of epidermal differentiation (Figure 9; Figure 10) [12]. During the initial stages of calcium-induced differentiation, when cell-cell contacts begin to stabilize, EphA2 and ephrin-A1 have dynamic localization patterns in different membrane microdomains (Figure 13; Figure 15; Figure 16).

This led us to suggest a model in which membrane microdomain localization of EphA2 and ephrin-A1 is important for its downstream signaling behaviors (Figure 43). In this model, EphA2 and ephrin-A1 are localized to lipid raft domains in proliferating keratinocytes. Due to this localization pattern, EphA2 is likely prevented from autonomous activation due to cis-inhibition from ephrin-A1. However, as cell-cell contacts mature during calcium-induced differentiation, formation of cadherin-based junctions promotes the stabilization of EphA2 at cell borders. This promotes the removal of ligand-activated pY772 EphA2 along with ephrin-A1 into non-lipid raft domains. Alternatively, cell-cell contact stabilization can preferentially promote ephrin-A1-induced activation of EphA2 in non-lipid raft membrane domains. When

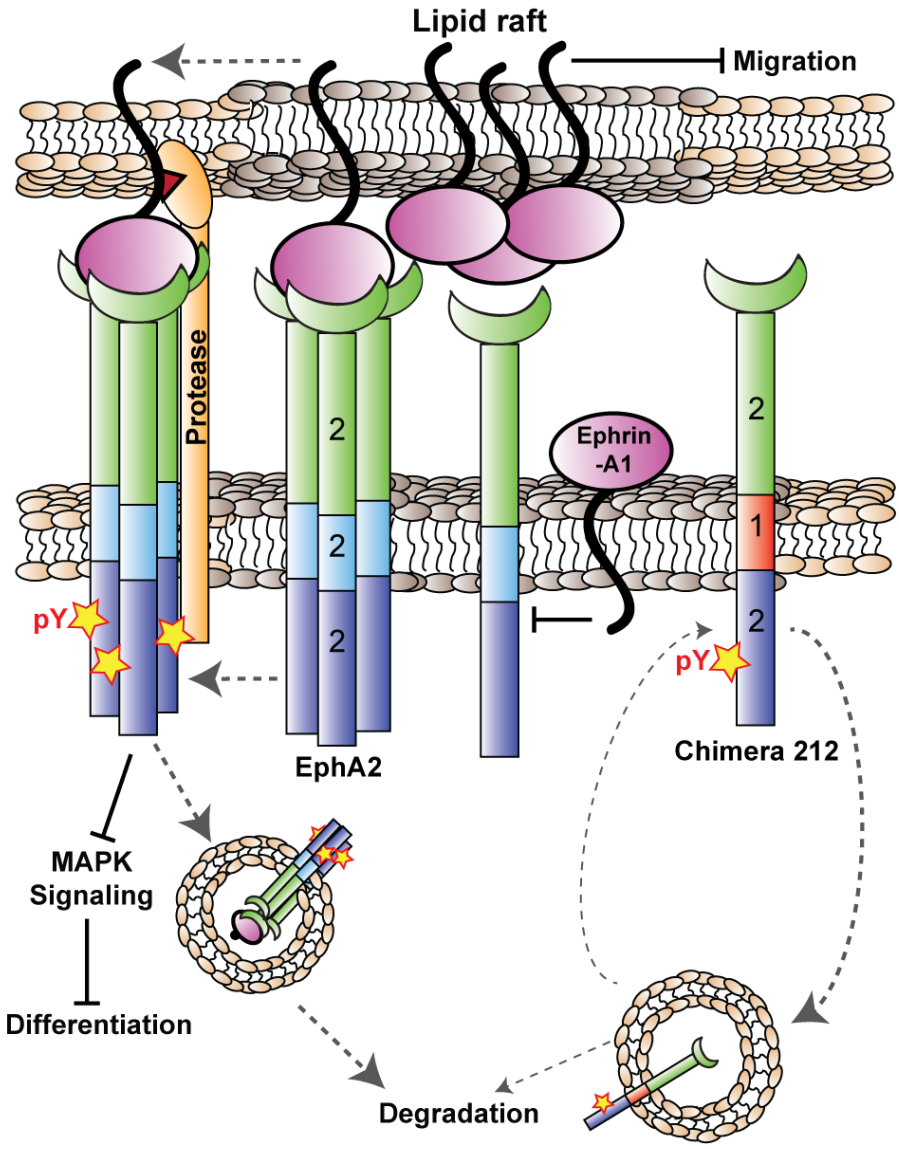

Figure 43: EphA2 and ephrin-A1 dynamics at cell-cell contacts.
EphA2 and ephrin-A1 are localized to lipid raft domains at cell-cell contacts. During cell-cell contact stabilization EphA2 engages with ephrin-A1 promoting EphA2 tyrosine phosphorylation. Ligand-induced activation of EphA2 results in pY772 EphA2 accumulation in non-lipid raft domains, protease cleavage of ephrin-A1, and transendocytosis. Forward signaling through EphA2 promotes keratinocyte differentiation, due to inhibition of MAPK signaling, and prevents keratinocyte migration. Exchange of the EphA2 TMD with that of EphA1 causes loss of receptor cell-cell contact localization. This results in decreased ligand-active EphA2 from lipid raft domains, while causing an accumulation of ephrin-A1 in these membrane domains. Ephrin-A1 accumulation prevents keratinocyte migration, suggesting that the EphA2 TMD is required for efficient wound closure.

ligand-induced activation of EphA2 by ephrin-A1 occurs, it can then inhibit keratinocyte migration.

EphA2 regulation of ephrin-A1 at cell-cell contacts is important for its role in controlling keratinocyte migration (Figure 43). This is demonstrated by the ability of Chimera 212 to inhibit NHEK migration in an ephrin-A1-dependent manner (Figure 35; Figure 36; Figure 40). Chimera 212 can localize to the cell surface as well as lipid raft domains (Figure 26; Figure 30). It also possesses autophosphorylation abilities and the capability to tyrosine phosphorylate other proteins (Figure 29). However, Chimera 212 lacks localization to cell-cell contacts in 2-D and 3-D keratinocyte culture models (Figure 24; Figure 28). This results in an accumulation of ephrin-A1 protein levels and subsequent inhibition of keratinocyte migration, similar to that of ephrin-A1-Fc recombinant protein treatment (Figure 35; Figure 36). Chimera 212-induced inhibition of migration is in part due to increased ephrin-A1 protein levels since silencing of ephrin-A1 normalizes keratinocyte migration (Figure 40). Lack of Chimera 212 localization to cell-cell contacts where ephrin-A1 is localized implies that increased ephrin-A1 protein negatively regulates migration directly through activation of another Eph receptor or indirectly through alternative mechanisms. It is likely that this ephrin-A1-induced inhibition is occurring through EphA1 or EphA4, both of which are expressed in keratinocytes (Figure 4) [15]. Alternatively, ephrin-A1 could be interacting in cis with other adhesion or signaling receptors at the cell membrane that can alter migratory behavior, similar to ephrin-A5-induced activation of β1 integrin [40]. Collectively, this suggests that localization of EphA2 to cell-cell contacts is important in regulating ephrin-A1-induced signaling outputs, and therefore affects keratinocyte behavior.

2. Eph/ephrin interaction interfaces in the epidermis

In the epidermis, lipid rafts are enriched in the transit amplifying population of keratinocytes in the basal layer of the epidermis. Since lipid rafts are important for cell-cell interactions in skin, as well as many other cellular processes, it suggests membrane microdomains may be required to promote epidermal morphogenesis [5, 6, 204, 211]. However, the mechanisms utilized by lipid rafts to contribute to epidermal homeostasis remain relatively unknown.

In psoriatic lesions where keratinocyte differentiation is perturbed there is a loss of ephrin-A1 and an increase in EphA2 mRNA transcripts. Also, in a RHE model that has characteristics of inflammatory skin disease including altered EphA2 and ephrin-A1 expression levels, treatment with ectopic ephrin-A1-Fc can normalize differentiation defects [15]. This signifies the importance of ephrin-A1-induced forward signaling in keratinocyte differentiation. Forward-induced signaling is likely initiated in the basal layer of the epidermis, where ephrin-A ligands are concentrated. EphA receptors are expressed throughout all the layers, which allows for forward signaling to occur between adjacent basal cells as well as along the basal/suprabasal interface [10, 15]. Therefore, along these boundaries lipid rafts could be playing a vital role in transit amplifying cells to organize the distribution of Eph/ephrins in order to maintain proliferative signaling in basal cells and pro-differentiation signaling in suprabasal cells (Figure 44). Consequently, alterations in lipid rafts or Eph/ephrin expression and localization could then lead to skin diseases where epidermal homeostasis is perturbed.

When considering the basal/suprabasal interface there is an asymmetrical distribution of Eph/ephrins, in which basal cells express both EphA2 and ephrin-A1 and suprabasal cells mainly

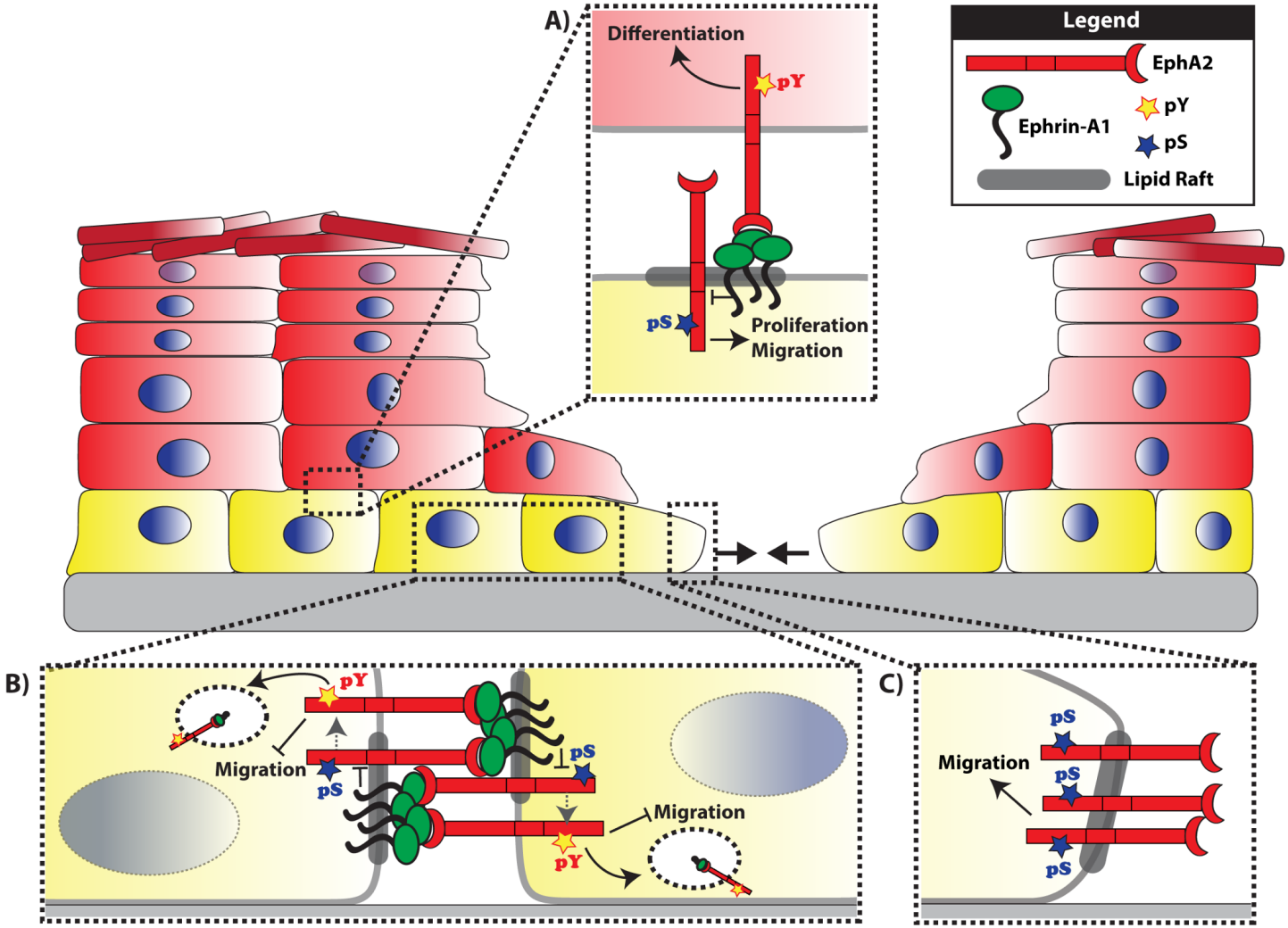
A)
Differentiation
pY
pS
Proliferation
Migration
Legend
EphA2
Ephrin-A1
pY
pS
Lipid Raft
B)
pY
Migration
pS
pS
pS
Migration
pY
C)
pS
Migration
pS
pS

Figure 44: EphA2 and ephrin-A1 localization to different epidermal interfaces alters signaling outputs.
(A) At the basal/suprabasal interface ephrin-A1 is asymmetrically divided, where the ligand in concentrated in the basal cell layer relative to the suprabasal layer. In the basal layer, localization of ephrin-A1and EphA2 to lipid raft domains causes ephrin-A1-induced cis-inhibition of EphA2 thus maintaining proliferative signaling. However, lack of ephrin in suprabasal cells promotes forward signaling through EphA2 resulting in keratinocyte differentiation. **(B)** In basal cells, EphA2 and ephrin-A1 are coexpressed. This results in ephrin-A1-induced cis inhibition of EphA2 in lipid rafts domains. However, once trans-activation of EphA2 can overcome its cis-inhibition, EphA2 is removed from lipid raft domains and prevents keratinocyte migration. **(C)** However, at the leading edge of a wound, lack of ephrin-A1-induced trans-activation causes ligand-independent pro-migratory signaling through EphA2 allowing for effective wound closure.

express EphA2 (Figure 44 A) [15]. Therefore, ephrin-A1-induced forward signaling through EphA2 can help to initiate the initial stages of epidermal differentiation in suprabasal cells as seen with ephrin-A1-Fc treatment [12]. Since there is less ephrin-A1 in suprabasal cells there would be lack of cis-inhibition resulting predominantly in trans-activation of EphA2. Lipid rafts at these asymmetric boundaries likely position ephrin-A1 to allow for this asymmetric forward signaling to take place.

Conversely, in the basal layer of the epidermis, both ephrin-A ligands and EphA2 are present [15, 204, 211]. Therefore, lipid rafts could play a vital role in organizing Eph/ephrin complexes in this progenitor layer (Figure 44 B). One possible outcome of this overlapping expression pattern is the continual ligand-induced activation of EphA2 in basal keratinocytes that leads to EphA2/ephrin-A1 removal from lipid raft domains. The diffuse cytoplasmic localization patterns of EphA2 and ephrin-A1 in the basal layer of the epidermis are consistent with the possibility that there is the continual ligand-induced activation of EphA2 that removes receptor/ligand pair from cell-cell contacts and lipid raft domains [15]. Similar EphA2 dynamics have been seen on an artificial membrane functionalized with mobile ephrin-A1; following ligand binding, ephrin-A1 and active EphA2 undergo radial transport in a manner that is inversely correlated with a known lipid raft protein, CD44 [262-264]. This removal of ligand-activated EphA2 from lipid raft domains in basal cells may limit keratinocyte migration under homeostatic conditions. Furthermore, ligand-induced activation of EphA2 in the basal layer likely promotes keratinocyte cell polarization thus promoting stratification and differentiation [73].

Forward signaling through EphA2 in the basal layer does not, however, promote premature keratinocyte differentiation. Therefore, additional mechanisms must be present to maintain proliferation in the basal layer. Since, EphA2 is a transcriptional target of the MAPK pathway, which is active in proliferative cells, it suggests that MAPK activation may allow for continual EphA2 transcription [176]. Consequently, EphA2 would constantly be delivered to lipid raft domains at cell-cell contacts allowing for ephrin-A1-induced cis-inhibition and subsequent ligand-independent proliferative signaling. Once ephrin-A1-induced trans-activation of EphA2 can overcome its cis-inhibition it would likely result in receptor/ligand internalization and degradation. This homeostatic state of EphA2 likely prevents sufficient forward signaling from occurring thus not allowing for pre-mature keratinocyte differentiation.

However, EphA2 homeostasis in the basal layer is likely disturbed when an epidermal wound occurs (Figure 44 C). The keratinocyte at the leading edge is no longer attached to a cell along its anterior surface resulting in asymmetric adhesive anchoring. Furthermore, this keratinocyte at the leading edge would have an asymmetric distribution of EphA2 activation in which there is a lack of ligand-active pY772 EphA2 and an accumulation of ligand-independent pS897 EphA2 at the membrane proximal to the wound-site. Conversely, there would be continual ligand-induced activation of EphA2 at its posterior cell-cell contact. Therefore, this leading cell would have an increase in ligand-independent pro-migratory EphA2 signaling at its leading edge promoting keratinocyte migration into the wounded area. Similarly, in psoriasis, a lack of ephrin-A1 would not only remove cis-inhibitory cues, but also lead to the deficiency of forward signaling through EphA2. This would likely cause an accumulation of ligand-independent pro-proliferative signaling via EphA2 throughout all the epidermal layers.

3. Cell-cell contact localization of EphA2 is likely required for boundary formation

Eph/ephrins are important for creating tissue boundaries during embryogenesis [8]. For example, in embryos 10.5 days post coitum (dpc) in a developing limb, ephrin-A ligands are expressed in the central limb bud region and EphA receptors are expressed in the surrounding proximal and distal limb bud areas. As the limb continues to develop at 13.5 dpc, ephrin-A ligands are expressed in the interdigital zone, whereas EphA receptors are expressed in the opposing digit regions. Similar complementary patterns between EphA receptor and ephrin-A ligands are seen during embryogenesis in the midbrain, branchial arches, and trunk regions [114]. Specifically, during *Xenopus* gastrulation, opposing expression of EphA4 in the involuting mesoderm and ephrin-A1 in the non-involuting ectoderm is required to mediate repulsive interactions for tissue separation [265]. Although EphA2 is not as abundantly expressed in the *Xenopus* embryo as EphA4, it is expressed at variable levels in different tissue regions throughout embryogenesis and EphA2 has a higher affinity for ephrin-A1 ligand relative to EphA4 [24, 31]. Therefore, even though EphA2 is less abundant than EphA4, it may also play an important role in boundary formation during gastrulation. During *Xenopus* gastrulation ephrin-A1 is highly expressed in the ectoderm relative to the mesoderm, whereas EphA2 is expressed at similar levels in both compartments [68]. This expression profile is similar to that of the basal/suprabasal interface in epidermis, in which basal cells abundantly express EphA2 and ephrin-A1, and suprabasal cells predominantly express EphA2. This suggests that similar mechanisms governing receptor and ligand distribution as well as downstream signaling elicited by EphA2 and ephrin-A1 at the basal/suprabasal epidermal interface may be analogous to the ectoderm/mesoderm boundary during gastrulation [10, 15].

In addition to embryogenesis, ephrin-A1 and EphA2 gradients are important for creating boundaries between progenitor cell populations and their differentiated progeny. This is exemplified in cardiac stem cells and cardiomyocytes and the limbus and cornea, which upon injury is altered to enhance wound healing [59, 60]. When high ephrin-A1 expressing cells confront high EphA2 expressing cells, E-cadherin is destabilized at the heterotypic boundary and ephrin-A1 induces a "push" response resulting in a reversal of migration of the EphA2 expressing cells. This response is dependent on the countergradient of EphA2 and ephrin-A1 at the boundary [60]. Also, at this boundary ephrin-A1 is internalized into EphA2 expressing cells (Figure 34 A, B). Therefore, one would predict that cell-cell contact localization of EphA2 is required for this ephrin-A1-induced forward signaling response. Additionally, when Chimera 212 expressing NHEKs interact with ephrin-A1 overexpressing NHEKs it results in abnormal extended processes interacting with the ephrin-A1 overexpressing cells (Figure 34 C). This suggests that EphA2 cell-cell contact localization is required to elicit ephrin-A1-induced forward signaling in order to form a stable, adhesive boundary between cells.

EphA2/ephrin-A1 boundary formation is mediated by disintegrin and metalloproteinase domain-containing protein 10 (ADAM10)-dependent shedding of EGFR ligand to destabilize E-cadherin at the boundary [60, 266]. Inhibition of ADAM10 and EGFR prevents ephrin-A1-induced reversal of cell migration through EphA2 and E-cadherin destabilization at the boundary. Since Chimera 212 expression alters cellular boundaries it suggests that the lack of cell-cell contact localization of Chimera 212 could result in a loss of its interaction with ADAM10, thus altering ADAM10 proteolytic activity. Interaction between the LBD of EphA2 and ADAM10 can result in ephrin-A5 ligand cleavage and transendocytosis of the ligand [257,

267]. Therefore, loss of boundary formation as well as keratinocyte migration, from Chimera 212 may be from a combination of decreased ephrin-A1 cleavage and transendocytosis, and shedding of EGFR ligands. This yields the possibility that the EphA2 TMD is important for interacting with other transmembrane receptors and adhesion molecules at the cell membrane. A similar mechanism is seen with the TMD of vascular endothelial (VE)-cadherin which binds to vascular endothelial growth factor (VEGFR)-2 and VEGFR3 to allow for endothelial cells to signal in response to alterations in fluid flow [268].

4. EphA2 cell-cell contact localization maintains ephrin-A1 homeostasis

The TMD of EphA2 is required for its proper localization to cell-cell junctions. Deviations in this localization pattern likely impairs the potential of these receptors to engage with ephrin-A1 ligands at cell-cell contacts and thus limit ephrin-A1 in lipid raft domains. Under homeostatic conditions, ephrin-A1 levels are maintained at a steady-state with a balance of transcriptional up-regulation and ligand turnover that is governed by the presence of receptors like EphA2 [83, 188]. However, aberration in EphA2 localization to ephrin-A1 interfaces likely perturbs this balance.

Following ligand binding to receptor, ephrins can be cleaved by ADAM or matrix metallopeptidase (MMP) proteases allowing for ephrin transendocytosis or proteolysis [256, 257, 269]. Since Chimera 212 led to a decrease in total levels of EphA2 from lipid raft domains and disrupted the balance of ephrin-A1 and pY772 EphA2 in lipid raft domains, we speculate that this altered localization impedes ephrin-A1 transendocytosis and turnover. Interestingly, processed ephrin-A1 fragments were seen with Chimera 212 expression providing evidence for altered ephrin-A1 internalization and degradation under these conditions. Alternatively, these

processed fragments may be due to an accumulation of ephrin-A1, thus causing an increase in both full length and processed forms, but at the same ratio as endogenous conditions.

Even though Chimera 212 lacks cell-cell contact localization, ephrin-A1 still maintains its ability to inhibit keratinocyte migration. This suggests that ephrin-A1 is likely working through another EphA receptor, possibly EphA1 or EphA4. In order to better understand this mechanism, EphA1 and/or EphA4 gene silencing studies can be done in NHEKs expressing Chimera 212. Knockdown of the EphA receptor that contributes to ephrin-A1-induced inhibition of migration will normalize these migration defects similar to knockdown of ephrin-A1 (Figure 40) or indicate that a non-Eph receptor mechanism governs this phenotypic response in keratinocytes.

Since Chimera 212 increases ephrin-A1 fragments, the EphA receptor contributing to inhibition of migration is likely also playing a role in ephrin-A1 processing. However, it is not known how processed forms of ephrin-A1 contribute to migration. In order to determine the requirement of ephrin-A1 processing, an ephrin-A1 cleavage mutant can be expressed in keratinocytes [256]. If ephrin-A1 cleavage is required to inhibit keratinocyte migration, reconstitution of this mutant in NHEKs lacking endogenous ephrin-A1 would normalize Chimera 212-induced migration defects. A variety of MMPs, including MMP-1, MMP-2, MMP-9, and MMP-13, as well as ADAM10 can cleave ephrin-A ligands [256, 257, 269]. MMP and ADAM inhibitor and knockdown studies would help determine the contribution of individual proteases to the ephrin-A1 migratory response. If ephrin-A1 fragments are important for inhibition of keratinocyte migration, then loss of the protease responsible for its cleavage would normalize the Chimera 212-induced migratory response. Collectively, these results would prove

useful in identifying other EphA receptors and proteases that can be therapeutically targeted to promote keratinocyte migration during wound healing when ephrin-A1 levels and proteolytic fragments are increased [14, 60].

5. TMD features that control lipid raft domain association

Lipid rafts play an important role in organizing adhesion complexes and signaling receptors at cell-cell contacts to modulate keratinocyte behavior [206, 207, 248]. The ability of a single-pass transmembrane receptor to localize to a lipid raft domain is dependent on several factors including its TMD length, the surface area of the amino acid side chains in its TMD, and palmitoylation proximal to the cytoplasmic side of the TMD. These protein properties can be altered to increase or decrease lipid raft affinity, as has been previously done for LAT [199]. Even though EphA1 has a TMD that is three amino acids shorter than EphA2, they both have similar amino acid side chain surface areas (~615 Angstroms), which is slightly lower than that of LAT (~690 Angstroms), which is a lipid raft preferring protein [199, 270]. However, unlike LAT, EphA1 and EphA2 lack cysteine residues proximal to the cytoplasmic side of their TMD suggesting that they lack palmitoylation sites that would increase lipid raft affinity. Since both surface area and palmitoylation status are similar between EphA1 and EphA2 it is likely that TMD length is the main factor contributing to their differences in lipid raft dynamics and ability to localize to cell-cell contacts.

The number of amino acids in a receptor's TMD is important in determining its length through a membrane. However, a protein can alter its membrane spanning length by changing the angle that it crosses through the membrane. Similar to many other RTKs, the TMD spanning length of EphA1 and EphA2 are dependent on their ligand binding status. Following ligand-

induced-activation and subsequent oligomerization, EphA1 and EphA2 increase their membrane crossing angles from 15° to 45° therefore shortening their membrane spanning length [92, 93]. This would lead one to hypothesize that EphA1 and EphA2 dynamics in different membrane microdomains is dependent on their ability to bind ligand. Intriguingly, EphA2 has a higher binding affinity for ephrin-A1 ligand than EphA1 suggesting that EphA2 has a greater ability to shorten its membrane spanning length [24, 31]. This mechanism is corroborated by our data in which calcium-induced cell-cell contact stabilization and ephrin-A1-Fc-induced activation of EphA2 results in pY772 EphA2 accumulation in non-lipid raft fractions, possibly due to alterations in the TMD crossing angle elicited by ligand-induced receptor dimerization. Furthermore, because EphA1 has a lower affinity for ephrin-A1 is likely retains a small crossing angle causing it to have a long membrane spanning length resulting in constitutive localization to lipid raft domains.

In order to better understand the importance of the EphA2 TMD to lipid raft localization and resultant ephrin-A1 dynamics, mutations can be made to the EphA2 TMD amino acid sequence. It has previously been shown that the specific amino acid sequence of a receptor's TMD does not affect lipid raft localization [199]. For example, when the TMD amino acid sequence of LAT is scrambled it does not alter lipid raft affinity compared to wild type LAT. However, exchange of its TMD to exclusively leucines, which are hydrophobic but contains a larger aliphatic side chain (~142 Angstroms) compared to alanine (~55 Angstroms), significantly decreases LAT's lipid raft affinity [270]. Alternatively, one would predict that decreasing the amino acid surface area of the TMD by mutating the residues to alanines would increase lipid raft affinity. Therefore, these findings and predictions can be utilized to generate EphA2 mutants

with decreased and increased lipid raft affinities to further delineate how lipid raft localization affects downstream signaling.

Furthermore, our model suggests that ligand-induced active EphA2 is excluded from lipid raft domains. Therefore, it is likely that an EphA2 mutant that is constitutively active would have decreased affinity for lipid raft domains. One such mutant that could be tested is an EphA2 mutant that lacks its SAM domain (EphA2ΔSAM). EphA2ΔSAM has increased oligomerization and autophosphorylation activity [271]. Interestingly, EphA2ΔSAM promotes receptor dimerization, which would likely result in removal from lipid raft domains due to shortening of the transmembrane spanning regions. Moreover, EphA2ΔSAM inhibits cell migration, which is similar to that of Chimera 212 expression in keratinocytes [272]. Lastly, EphA2 monomers make a significant contribution to pro-tumorigenic signaling. Therefore, promoting EphA2 dimerization and removal from lipid raft domains presents a therapeutic approach that may be beneficial to inhibit proliferative and migratory signaling pathways [247].

6. Eph/ephrin membrane trafficking

When EphA2 is localized to the cell membrane it can be trafficked to different membrane domains depending on its activation status which can ultimately lead to c-cbl-dependent ubiquitination pathways [188]. Our findings extend these observations to the possibility that lipid rafts may be playing an important role in EphA2 receptor endocytic trafficking pathways. Nevertheless, the precise mechanism by which EphA2 is trafficked between different membrane domains remains to be determined. Utilization of live-cell imaging techniques would give insight into the endocytic pathways employed by EphA2 following ligand-induced activation in keratinocytes.

Although the specific endocytic mechanisms of EphA2 and ephrin-A1 in keratinocytes are unknown, an EphA2 interactome analysis in 2-D differentiated NHEKs and 3-D RHE determined that EphA2 has many potential interactors that could be playing a role in trafficking EphA2 between membrane microdomains [159]. Additionally, in PANTHER database gene ontology classification of protein class and KEGG pathway analysis, membrane traffic proteins and endocytosis were identified as top pathways, respectively, for EphA2-interacting proteins. One of the significant proteins identified as an EphA2 interactor in both 2-D and 3-D cultures was caveolin-1, further confirming the ability of EphA2 to localize to caveola-enriched lipid raft domains. Also, identified in both models of keratinocyte differentiation was the adaptor protein epsin. Epsin contains a phospholipid-binding domain and ubiquitin-interacting motifs at its C-terminal end as well as clathrin and adaptor complex AP2 binding sites at its N-terminal region. This structure allows for epsins to act as endocytic adaptor protein [273]. For EGFR, epsin can traffic EGFR through a ubiquitin-dependent CIE pathway causing receptor degradation. But, when there is lack of ubiquitination epsin directs EGFR through CDE resulting in signal transduction and receptor recycling [274-276]. One could envision epsin functioning in a similar manner at the cell membrane to control EphA2 recycling and degradation.

Other identified membrane trafficking proteins in the EphA2 interactome that may be important in EphA2 endocytosis were synaptosomal-associated proteins 23 and 29 (SNAP23/29) [159]. SNAP proteins are a specific type of snap receptor (SNARE) that drive membrane fusion in secretory and endocytic pathways by facilitating tethering, docking, and fusion of vesicles [277]. Interestingly, SNAP23 has been shown to be attached to the cytoplasmic leaflet of lipid raft domains in the plasma membrane through protein palmitoylation and plays an important role

in trafficking MMPs to lipid raft domains allowing for invadopodium formation and cell invasion [278-280]. Potentially, SNAP23 plays a similar role in membrane fusion of EphA2 into lipid raft membrane domains during EphA2 endocytic recycling pathways.

It is interesting to note that RHE cultures contain more trafficking and endocytosis proteins identified in the EphA2 interactome, possibly suggesting additional pathways utilized by EphA2 once keratinocytes stratify [159]. Some trafficking proteins that were exclusively identified in RHE cultures that may be playing a role in EphA2 membrane trafficking include: 1) EHD1, which is a trafficking protein in 'pre-sorting endosomes' that transports the GPI-containing and lipid-raft localized protein CD-59 [281]. 2) Rab13, which is found in recycling and late endosomes. Rab13 has been shown to play a role in the trafficking of integrins, tight junctions, and EGFR [282]. 3) The epithelial-specific Rab25 (also known as Rab11c) that associates with apical recycling endosomes in polarized cells [283]. Additional studies will be required to fully understand how EphA2 is transported between membrane microdomains resulting in receptor recycling and degradation. Elucidation of these mechanisms will help to better understand possible points of intervention to selectively regulate the fate of EphA2 trafficking and consequent signaling outputs.

7. Temporal regulation of TJ function by EphA1/ephrin-A1

In endothelial cells and other types of epithelial cells, ephrin-A1 treatment negatively regulates the functionality of the TJ barrier, which opposes what we see in epidermal keratinocytes [15, 159, 170-172]. These opposing effects of ephrin-A1 and TJ formation is likely due to treatment in different cell-types or the length of treatment. Negative regulation of the TJ barrier by ephrin-A1 has previously been shown to be kinase-dependent and attributed to protein

modifications of TJ proteins [170, 172]. EphA2 can associate and phosphorylate claudin-4, preventing claudin-4 from incorporating into TJ complexes [170]. Also, tyrosine phosphorylation of occludin can enhance or reduce barrier function depending on cell type [284].

Although there have been extensive studies on the acute regulation of EphA2/ephrin-A1 signaling in TJ barrier function, the effect of chronic modulation of this signaling axis in the formation of the epidermal barrier remains elusive. Our findings show that forward signaling elicited by ephrin-A1 enhanced the expression of TJ proteins (Figure 9; Figure 10). Ephrin-A1-induced EphA2 activation could enhance the formation of the tight junction barrier by two non-mutually exclusive mechanisms: promoting cytoskeletal reorganization and driving planar cell polarity. Eph receptors have been shown to modulate activity of the Rho family of GTPases leading to alterations in cytoskeletal dynamics. In turn the cytoskeleton can regulate TJ assembly and function [285, 286]. EphA2 can also promote cellular polarization and enhance AJ stability thereby indirectly promoting the formation of TJs [73].

There is a variety of human skin diseases where the epidermal barrier is compromised, including atopic dermatitis and psoriasis [132]. Specifically, in psoriatic plaques there is a decrease in the gene expression and protein level of ephrin-A1 accompanied by upregulation of EphA2 compared to normal non-lesional skin. Also, forward signaling through EphA2 by ephrin-A1-Fc treatment can promote keratinocyte differentiation and normalize differentiation defects in a cytokine-induced RHE resulting in decreased protein levels of EphA2 [12, 15]. When EphA2 is increased in psoriatic epidermis it exhibits enhanced cell-cell contact localization in the basal layer, in which ephrin-A1 protein levels are reduced. Thus, these receptors are likely available for binding to ephrin-A1-Fc upon treatment [15]. Therefore, ephrin-

A1-Fc can bind to the unliganded EphA2 causing receptor activation, inhibition of pro-proliferative MAPK signaling, transendocytosis of the ligand with EphA2, and subsequent receptor downregulation. Inhibition of MAPK signaling will then allow for initiation of keratinocyte differentiation ultimately leading to late differentiation and formation of the TJ barrier. These findings further highlight the importance of both ligand and receptor localization to cell-cell contacts in order to maintain epidermal homeostasis.

In addition to psoriasis and atopic dermatitis, other epithelial diseases where the TJ barrier is compromised include inflammatory diseases like Crohn's disease, ulcerative colitis, asthma, and sinusitis [287-289]. Even though previous studies suggest that activation of EphA2 by ephrin ligands negatively regulates TJs in an acute setting, our current findings support the hypothesis that chronic ephrin-A1 treatment may prove useful to ameliorate barrier defects. Moreover, 12-mer EphA2-targeting peptides have been identified that specifically bind to the ephrin-binding domain of EphA2 initiating the receptor's activation, albeit not as strongly as ephrin-A1-Fc treatment [290, 291]. Recombinant ephrin-A1-Fc treatment and these peptides may prove valuable as a therapeutic intervention in inflammatory diseases where EphA2 is upregulated. These 12-mer peptides may be specifically suitable when using full length ephrin-A1 is difficult. These potential treatments also possess much opportunity for skin diseases where treatments can be applied to localized areas through topical application.

8. Misregulation of EphA2 and ephrin-A1 in cancer cell signaling

In addition to these inflammatory diseases, Eph2 and ephrin-A1 are often misregulated in cancer. Although EphA2 has tumor suppressive functions, it is often upregulated in non-melanoma skin cancers, likely because activation of the Ras/Raf/Erk1/2-MAPK signaling

pathway can stimulate EphA2 expression. Cancers often also exhibit a loss or mislocalization of ephrin-A1 leading to ligand-independent EphA2 signaling [168, 176]. Combined with our data, one can speculate that this would cause an accumulation of the pS897 EphA2 in lipid raft domains. This active form of EphA2 results in increased migration and invasion [80]. Ligand-independent EphA2-induced migration can be inhibited by restoring ligand in the microenvironment with recombinant ephrin-A1-Fc [80]. Interestingly, it has been shown that there is a preferential activation of Akt in lipid raft domains [292]. Therefore, one would predict that in a tumor with hyperactive Akt there would be further enhancement of ligand-independent pro-oncogenic signaling of EphA2 in lipid raft membrane microdomains.

Cancer cells have been shown to have increased levels of cholesterol-rich lipid raft domains [250, 293]. According to our model, lipid rafts inhibit ephrin-A1-induced activation of EphA2 due to ligand-induced cis-inhibition. Therefore, accumulation of lipid rafts in the cell membrane would likely enhance ligand-independent pS897 EphA2 in the plasma membrane. Increased pS897 EphA2 would increase migration and proliferation, which are all characteristic of pro-oncogenic signaling [9, 80].

9. Conclusions

The mechanisms that are exploited by cancer cells to promote tumor invasion are similar to those utilized by cells for migration during tissue patterning and wound healing. These redundant molecular mechanisms are seen in Eph/ephrin signaling [8]. When wound healing is delayed, like in the diabetic corneal epithelium, ephrin-A1 expression is increased which is opposite of what is seen in tumors [14, 175]. Therefore, low protein expression of ephrin-A1 is required for wound healing, similar to tumor migration, suggesting that there is a narrow range

of ephrin-A1 protein levels that must be maintained to allow for efficient, but not excessive, keratinocyte migration. Our studies provide additional support for the notion that ephrin-A1 abundance is a key determinant of cell migration (Figure 40). We now extend these findings to include the importance of the EphA2 TMD and lipid raft association as a new mechanism in regulating ephrin-A1 levels in epithelial cells.

The ability of ephrin-A1 to decrease keratinocyte migration provides more weight to the argument that recombinant ephrin-A1-Fc treatment or other EphA2 targeting approaches that disrupt the receptor's lipid raft localization can be used to reduce tumor cell migration. Additionally, studies to better understand EphA2/ephrin-A1 endocytic trafficking and degradation pathways following removal from lipid raft domains may prove useful in identifying potential therapeutic targets to decrease ephrin-A1 levels and promote keratinocyte migration during cutaneous wound healing.

Due to the vast array of signaling outcomes that are modulated by Eph/ephrin signaling, our findings will be useful in understanding how Eph/ephrins are organized at cellular boundaries to control tissue morphogenesis. Our studies in keratinocytes can be extended to a variety of other cell types where cell-cell communication is required for controlling cellular behaviors. This research highlights the importance of Eph/ephrin localization to cell-cell contacts to allow for proper juxtracrine signaling to occur. Aberrations in Eph/ephrin localization perturbs the balance of bidirectional signaling, ultimately disrupting tissue homeostasis.

REFERENCES

1. Goldsmith, L.A., *My organ is bigger than your organ.* Arch Dermatol, 1990. **126**(3): p. 301-2.
2. Simpson, C.L., D.M. Patel, and K.J. Green, *Deconstructing the skin: cytoarchitectural determinants of epidermal morphogenesis.* Nat Rev Mol Cell Biol, 2011. **12**(9): p. 565-80.
3. Munro, S., *Lipid rafts: elusive or illusive?* Cell, 2003. **115**(4): p. 377-88.
4. Capozza, F., et al., *Absence of caveolin-1 sensitizes mouse skin to carcinogen-induced epidermal hyperplasia and tumor formation.* Am J Pathol, 2003. **162**(6): p. 2029-39.
5. Ma, W.Y., et al., *Inverse correlation between caveolin-1 expression and clinical severity in psoriasis vulgaris.* J Int Med Res, 2012. **40**(5): p. 1745-51.
6. Mathay, C., et al., *Transcriptional profiling after lipid raft disruption in keratinocytes identifies critical mediators of atopic dermatitis pathways.* J Invest Dermatol, 2011. **131**(1): p. 46-58.
7. Sezgin, E., et al., *The mystery of membrane organization: composition, regulation and roles of lipid rafts.* Nat Rev Mol Cell Biol, 2017(.Sezgin, 2017 #147). **18**(6): p. 361-374.
8. Ventrella, R., N. Kaplan, and S. Getsios, *Asymmetry at cell-cell interfaces direct cell sorting, boundary formation, and tissue morphogenesis.* Exp Cell Res, 2017. **358**(1): p. 58-64.
9. Pasquale, E.B., *Eph receptors and ephrins in cancer: bidirectional signalling and beyond.* Nat Rev Cancer, 2010. **10**(3): p. 165-80.
10. Lin, S., B. Wang, and S. Getsios, *Eph/ephrin signaling in epidermal differentiation and disease.* Semin Cell Dev Biol, 2012. **23**(1): p. 92-101.
11. Perez White, B.E. and S. Getsios, *Eph receptor and ephrin function in breast, gut, and skin epithelia.* Cell Adh Migr, 2014. **8**(4): p. 327-38.
12. Lin, S., et al., *Ligand targeting of EphA2 enhances keratinocyte adhesion and differentiation via desmoglein 1.* Mol Biol Cell, 2010. **21**(22): p. 3902-14.
13. Walsh, R. and M. Blumenberg, *Specific and shared targets of ephrin A signaling in epidermal keratinocytes.* J Biol Chem, 2011. **286**(11): p. 9419-28.
14. Kaplan, N., et al., *EphA2/Ephrin-A1 signaling complexes restrict corneal epithelial cell migration.* Invest Ophthalmol Vis Sci, 2012. **53**(2): p. 936-45.
15. Gordon, K., et al., *Alteration of the EphA2/Ephrin-A signaling axis in psoriatic epidermis.* J Invest Dermatol, 2013. **133**(3): p. 712-22.
16. Hirai, H., et al., *A novel putative tyrosine kinase receptor encoded by the eph gene.* Science, 1987. **238**(4834): p. 1717-20.
17. Holzman, L.B., R.M. Marks, and V.M. Dixit, *A novel immediate-early response gene of endothelium is induced by cytokines and encodes a secreted protein.* Mol Cell Biol, 1990. **10**(11): p. 5830-8.
18. Bartley, T.D., et al., *B61 is a ligand for the ECK receptor protein-tyrosine kinase.* Nature, 1994. **368**(6471): p. 558-60.
19. Kozlosky, C.J., et al., *Ligands for the receptor tyrosine kinases hek and elk: isolation of cDNAs encoding a family of proteins.* Oncogene, 1995. **10**(2): p. 299-306.

20. Shao, H., et al., *Characterization of B61, the ligand for the Eck receptor protein-tyrosine kinase.* J Biol Chem, 1995. **270**(10): p. 5636-41.
21. Beckmann, M.P., et al., *Molecular characterization of a family of ligands for eph-related tyrosine kinase receptors.* EMBO J, 1994. **13**(16): p. 3757-62.
22. Pasquale, E.B., *Eph receptor signalling casts a wide net on cell behaviour.* Nat Rev Mol Cell Biol, 2005. **6**(6): p. 462-75.
23. Committee, E.N., *Unified nomenclature for Eph family receptors and their ligands, the ephrins. Eph Nomenclature Committee.* Cell, 1997. **90**(3): p. 403-4.
24. Noberini, R., E. Rubio de la Torre, and E.B. Pasquale, *Profiling Eph receptor expression in cells and tissues: a targeted mass spectrometry approach.* Cell Adh Migr, 2012. **6**(2): p. 102-12.
25. Himanen, J.P., et al., *Repelling class discrimination: ephrin-A5 binds to and activates EphB2 receptor signaling.* Nat Neurosci, 2004. **7**(5): p. 501-9.
26. Pasquale, E.B., *Eph-ephrin promiscuity is now crystal clear.* Nat Neurosci, 2004. **7**(5): p. 417-8.
27. Tuzi, N.L. and W.J. Gullick, *eph, the largest known family of putative growth factor receptors.* Br J Cancer, 1994. **69**(3): p. 417-21.
28. Drescher, U., *Eph family functions from an evolutionary perspective.* Curr Opin Genet Dev, 2002. **12**(4): p. 397-402.
29. Suga, H., et al., *Extensive gene duplication in the early evolution of animals before the parazoan-eumetazoan split demonstrated by G proteins and protein tyrosine kinases from sponge and hydra.* J Mol Evol, 1999. **48**(6): p. 646-53.
30. Mellott, D.O. and R.D. Burke, *The molecular phylogeny of eph receptors and ephrin ligands.* BMC Cell Biol, 2008. **9**: p. 27.
31. Flanagan, J.G. and P. Vanderhaeghen, *The ephrins and Eph receptors in neural development.* Annu Rev Neurosci, 1998. **21**: p. 309-45.
32. Kania, A. and R. Klein, *Mechanisms of ephrin-Eph signalling in development, physiology and disease.* Nat Rev Mol Cell Biol, 2016. **17**(4): p. 240-56.
33. Cowan, C.A. and M. Henkemeyer, *The SH2/SH3 adaptor Grb4 transduces B-ephrin reverse signals.* Nature, 2001. **413**(6852): p. 174-9.
34. Holland, S.J., et al., *Bidirectional signalling through the EPH-family receptor Nuk and its transmembrane ligands.* Nature, 1996. **383**(6602): p. 722-5.
35. Xu, N.J. and M. Henkemeyer, *Ephrin-B3 reverse signaling through Grb4 and cytoskeletal regulators mediates axon pruning.* Nat Neurosci, 2009. **12**(3): p. 268-76.
36. Bruckner, K., E.B. Pasquale, and R. Klein, *Tyrosine phosphorylation of transmembrane ligands for Eph receptors.* Science, 1997. **275**(5306): p. 1640-3.
37. Palmer, A., et al., *EphrinB phosphorylation and reverse signaling: regulation by Src kinases and PTP-BL phosphatase.* Mol Cell, 2002. **9**(4): p. 725-37.
38. Lee, H.S., et al., *EphrinB1 controls cell-cell junctions through the Par polarity complex.* Nat Cell Biol, 2008. **10**(8): p. 979-86.
39. Daar, I.O., *Non-SH2/PDZ reverse signaling by ephrins.* Semin Cell Dev Biol, 2012. **23**(1): p. 65-74.
40. Davy, A. and S.M. Robbins, *Ephrin-A5 modulates cell adhesion and morphology in an integrin-dependent manner.* EMBO J, 2000. **19**(20): p. 5396-405.

41. Davy, A., et al., *Compartmentalized signaling by GPI-anchored ephrin-A5 requires the Fyn tyrosine kinase to regulate cellular adhesion.* Genes Dev, 1999. **13**(23): p. 3125-35.
42. Li, J.J., et al., *EphrinA5 acts as a tumor suppressor in glioma by negative regulation of epidermal growth factor receptor.* Oncogene, 2009. **28**(15): p. 1759-68.
43. Holen, H.L., et al., *Signaling through ephrin-A ligand leads to activation of Src-family kinases, Akt phosphorylation, and inhibition of antigen receptor-induced apoptosis.* J Leukoc Biol, 2008. **84**(4): p. 1183-91.
44. Wimmer-Kleikamp, S.H., et al., *Recruitment of Eph receptors into signaling clusters does not require ephrin contact.* J Cell Biol, 2004. **164**(5): p. 661-6.
45. Himanen, J.P., et al., *Crystal structure of an Eph receptor-ephrin complex.* Nature, 2001. **414**(6866): p. 933-8.
46. Ojosnegros, S., et al., *Eph-ephrin signaling modulated by polymerization and condensation of receptors.* Proc Natl Acad Sci U S A, 2017. **114**(50): p. 13188-13193.
47. Himanen, J.P., et al., *Architecture of Eph receptor clusters.* Proc Natl Acad Sci U S A, 2010. **107**(24): p. 10860-5.
48. Egea, J., et al., *Regulation of EphA 4 kinase activity is required for a subset of axon guidance decisions suggesting a key role for receptor clustering in Eph function.* Neuron, 2005. **47**(4): p. 515-28.
49. Seiradake, E., et al., *An extracellular steric seeding mechanism for Eph-ephrin signaling platform assembly.* Nat Struct Mol Biol, 2010. **17**(4): p. 398-402.
50. Egea, J. and R. Klein, *Bidirectional Eph-ephrin signaling during axon guidance.* Trends Cell Biol, 2007. **17**(5): p. 230-8.
51. Carvalho, R.F., et al., *Silencing of EphA3 through a cis interaction with ephrinA5.* Nat Neurosci, 2006. **9**(3): p. 322-30.
52. Yin, Y., et al., *EphA receptor tyrosine kinases interact with co-expressed ephrin-A ligands in cis.* Neurosci Res, 2004. **48**(3): p. 285-96.
53. Feldheim, D.A., et al., *Loss-of-function analysis of EphA receptors in retinotectal mapping.* J Neurosci, 2004. **24**(10): p. 2542-50.
54. Falivelli, G., et al., *Attenuation of eph receptor kinase activation in cancer cells by coexpressed ephrin ligands.* PLoS One, 2013. **8**(11): p. e81445.
55. Sahin, M., et al., *Eph-dependent tyrosine phosphorylation of ephexin1 modulates growth cone collapse.* Neuron, 2005. **46**(2): p. 191-204.
56. Walker, M.R. and T.S. Stappenbeck, *Deciphering the 'black box' of the intestinal stem cell niche: taking direction from other systems.* Curr Opin Gastroenterol, 2008. **24**(2): p. 115-20.
57. Hsu, Y.C. and E. Fuchs, *A family business: stem cell progeny join the niche to regulate homeostasis.* Nat Rev Mol Cell Biol, 2012. **13**(2): p. 103-14.
58. Lane, S.W., D.A. Williams, and F.M. Watt, *Modulating the stem cell niche for tissue regeneration.* Nat Biotechnol, 2014. **32**(8): p. 795-803.
59. Goichberg, P., et al., *The ephrin A1-EphA2 system promotes cardiac stem cell migration after infarction.* Circ Res, 2011. **108**(9): p. 1071-83.
60. Kaplan, N., et al., *EphA2/Ephrin-A1 Mediate Corneal Epithelial Cell Compartmentalization via ADAM10 Regulation of EGFR Signaling.* Invest Ophthalmol Vis Sci, 2018. **59**(1): p. 393-406.

61. Pasquale, E.B., *Eph-ephrin bidirectional signaling in physiology and disease.* Cell, 2008. **133**(1): p. 38-52.
62. Vaught, D., D.M. Brantley-Sieders, and J. Chen, *Eph receptors in breast cancer: roles in tumor promotion and tumor suppression.* Breast Cancer Res, 2008. **10**(6): p. 217.
63. Jones, T.L., et al., *Identification of XLerk, an Eph family ligand regulated during mesoderm induction and neurogenesis in Xenopus laevis.* Oncogene, 1997. **14**(18): p. 2159-66.
64. Hwang, Y.S., et al., *The Smurf ubiquitin ligases regulate tissue separation via antagonistic interactions with ephrinB1.* Genes Dev, 2013. **27**(5): p. 491-503.
65. Bong, Y.S., et al., *ephrinB1 signals from the cell surface to the nucleus by recruitment of STAT3.* Proc Natl Acad Sci U S A, 2007. **104**(44): p. 17305-10.
66. Carpenter, R.L. and H.W. Lo, *STAT3 Target Genes Relevant to Human Cancers.* Cancers (Basel), 2014. **6**(2): p. 897-925.
67. Yamashita, S., et al., *Stat3 Controls Cell Movements during Zebrafish Gastrulation.* Dev Cell, 2002. **2**(3): p. 363-75.
68. Fagotto, F., R. Winklbauer, and N. Rohani, *Ephrin-Eph signaling in embryonic tissue separation.* Cell Adh Migr, 2014. **8**(4): p. 308-26.
69. Rohani, N., et al., *Variable combinations of specific ephrin ligand/Eph receptor pairs control embryonic tissue separation.* PLoS Biol, 2014. **12**(9): p. e1001955.
70. Rohani, N., et al., *EphrinB/EphB signaling controls embryonic germ layer separation by contact-induced cell detachment.* PLoS Biol, 2011. **9**(3): p. e1000597.
71. Garraway, L.A. and W.R. Sellers, *Lineage dependency and lineage-survival oncogenes in human cancer.* Nat Rev Cancer, 2006. **6**(8): p. 593-602.
72. Zantek, N.D., et al., *E-cadherin regulates the function of the EphA2 receptor tyrosine kinase.* Cell Growth Differ, 1999. **10**(9): p. 629-38.
73. Miura, K., et al., *EphA2 engages Git1 to suppress Arf6 activity modulating epithelial cell-cell contacts.* Mol Biol Cell, 2009. **20**(7): p. 1949-59.
74. Cortina, C., et al., *EphB-ephrin-B interactions suppress colorectal cancer progression by compartmentalizing tumor cells.* Nat Genet, 2007. **39**(11): p. 1376-83.
75. Kao, T.J. and A. Kania, *Ephrin-mediated cis-attenuation of Eph receptor signaling is essential for spinal motor axon guidance.* Neuron, 2011. **71**(1): p. 76-91.
76. Dudanova, I. and R. Klein, *The axon's balancing act: cis- and trans-interactions between Ephs and ephrins.* Neuron, 2011. **71**(1): p. 1-3.
77. Zelinski, D.P., et al., *EphA2 overexpression causes tumorigenesis of mammary epithelial cells.* Cancer Res, 2001. **61**(5): p. 2301-6.
78. Noren, N.K., et al., *The EphB4 receptor suppresses breast cancer cell tumorigenicity through an Abl-Crk pathway.* Nat Cell Biol, 2006. **8**(8): p. 815-25.
79. Kumar, S.R., et al., *Preferential induction of EphB4 over EphB2 and its implication in colorectal cancer progression.* Cancer Res, 2009. **69**(9): p. 3736-45.
80. Miao, H., et al., *EphA2 mediates ligand-dependent inhibition and ligand-independent promotion of cell migration and invasion via a reciprocal regulatory loop with Akt.* Cancer Cell, 2009. **16**(1): p. 9-20.

81. Noblitt, L.W., et al., *Decreased tumorigenic potential of EphA2-overexpressing breast cancer cells following treatment with adenoviral vectors that express EphrinA1.* Cancer Gene Ther, 2004. **11**(11): p. 757-66.
82. Noren, N.K. and E.B. Pasquale, *Paradoxes of the EphB4 receptor in cancer.* Cancer Res, 2007. **67**(9): p. 3994-7.
83. Pitulescu, M.E. and R.H. Adams, *Eph/ephrin molecules--a hub for signaling and endocytosis.* Genes Dev, 2010. **24**(22): p. 2480-92.
84. Himanen, J.P. and D.B. Nikolov, *Eph signaling: a structural view.* Trends Neurosci, 2003. **26**(1): p. 46-51.
85. Murai, K.K. and E.B. Pasquale, *'Eph'ective signaling: forward, reverse and crosstalk.* J Cell Sci, 2003. **116**(Pt 14): p. 2823-32.
86. Toth, J., et al., *Crystal structure of an ephrin ectodomain.* Dev Cell, 2001. **1**(1): p. 83-92.
87. Himanen, J.P., *Ectodomain structures of Eph receptors.* Semin Cell Dev Biol, 2012. **23**(1): p. 35-42.
88. Labrador, J.P., R. Brambilla, and R. Klein, *The N-terminal globular domain of Eph receptors is sufficient for ligand binding and receptor signaling.* EMBO J, 1997. **16**(13): p. 3889-97.
89. Smith, F.M., et al., *Dissecting the EphA3/Ephrin-A5 interactions using a novel functional mutagenesis screen.* J Biol Chem, 2004. **279**(10): p. 9522-31.
90. Chavent, M., et al., *Structures of the EphA2 Receptor at the Membrane: Role of Lipid Interactions.* Structure, 2016. **24**(2): p. 337-47.
91. Bocharov, E.V., et al., *Conformational transitions and interactions underlying the function of membrane embedded receptor protein kinases.* Biochim Biophys Acta, 2017. **1859**(9 Pt A): p. 1417-1429.
92. Sharonov, G.V., et al., *Point mutations in dimerization motifs of the transmembrane domain stabilize active or inactive state of the EphA2 receptor tyrosine kinase.* J Biol Chem, 2014. **289**(21): p. 14955-64.
93. Bocharov, E.V., et al., *Left-handed dimer of EphA2 transmembrane domain: Helix packing diversity among receptor tyrosine kinases.* Biophys J, 2010. **98**(5): p. 881-9.
94. Muhle-Goll, C., et al., *Hydrophobic matching controls the tilt and stability of the dimeric platelet-derived growth factor receptor (PDGFR) beta transmembrane segment.* J Biol Chem, 2012. **287**(31): p. 26178-86.
95. Janes, P.W., et al., *Cytoplasmic relaxation of active Eph controls ephrin shedding by ADAM10.* PLoS Biol, 2009. **7**(10): p. e1000215.
96. Lisabeth, E.M., G. Falivelli, and E.B. Pasquale, *Eph receptor signaling and ephrins.* Cold Spring Harb Perspect Biol, 2013. **5**(9).
97. Fang, W.B., et al., *Identification and functional analysis of phosphorylated tyrosine residues within EphA2 receptor tyrosine kinase.* J Biol Chem, 2008. **283**(23): p. 16017-26.
98. Binns, K.L., et al., *Phosphorylation of tyrosine residues in the kinase domain and juxtamembrane region regulates the biological and catalytic activities of Eph receptors.* Mol Cell Biol, 2000. **20**(13): p. 4791-805.
99. Schultz, J., et al., *SAM as a protein interaction domain involved in developmental regulation.* Protein Sci, 1997. **6**(1): p. 249-53.

100. Stapleton, D., et al., *The crystal structure of an Eph receptor SAM domain reveals a mechanism for modular dimerization.* Nat Struct Biol, 1999. **6**(1): p. 44-9.
101. Torres, R., et al., *PDZ proteins bind, cluster, and synaptically colocalize with Eph receptors and their ephrin ligands.* Neuron, 1998. **21**(6): p. 1453-63.
102. Boyd, A.W., P.F. Bartlett, and M. Lackmann, *Therapeutic targeting of EPH receptors and their ligands.* Nat Rev Drug Discov, 2014. **13**(1): p. 39-62.
103. Diaz-Rohrer, B.B., et al., *Membrane raft association is a determinant of plasma membrane localization.* Proc Natl Acad Sci U S A, 2014. **111**(23): p. 8500-5.
104. Coulthard, M.G., et al., *Characterization of the Epha1 receptor tyrosine kinase: expression in epithelial tissues.* Growth Factors, 2001. **18**(4): p. 303-17.
105. Watt, F.M., *Mammalian skin cell biology: at the interface between laboratory and clinic.* Science, 2014. **346**(6212): p. 937-40.
106. Gonzales, K.A.U. and E. Fuchs, *Skin and Its Regenerative Powers: An Alliance between Stem Cells and Their Niche.* Dev Cell, 2017. **43**(4): p. 387-401.
107. Rivera-Gonzalez, G., B. Shook, and V. Horsley, *Adipocytes in skin health and disease.* Cold Spring Harb Perspect Med, 2014. **4**(3).
108. Festa, E., et al., *Adipocyte lineage cells contribute to the skin stem cell niche to drive hair cycling.* Cell, 2011. **146**(5): p. 761-71.
109. Poulson, N.D. and T. Lechler, *Asymmetric cell divisions in the epidermis.* Int Rev Cell Mol Biol, 2012. **295**: p. 199-232.
110. Byrne, C., M. Tainsky, and E. Fuchs, *Programming gene expression in developing epidermis.* Development, 1994. **120**(9): p. 2369-83.
111. Lechler, T. and E. Fuchs, *Asymmetric cell divisions promote stratification and differentiation of mammalian skin.* Nature, 2005. **437**(7056): p. 275-80.
112. Koster, M.I. and D.R. Roop, *Mechanisms regulating epithelial stratification.* Annu Rev Cell Dev Biol, 2007. **23**: p. 93-113.
113. Flenniken, A.M., et al., *Distinct and overlapping expression patterns of ligands for Eph-related receptor tyrosine kinases during mouse embryogenesis.* Dev Biol, 1996. **179**(2): p. 382-401.
114. Gale, N.W., et al., *Eph receptors and ligands comprise two major specificity subclasses and are reciprocally compartmentalized during embryogenesis.* Neuron, 1996. **17**(1): p. 9-19.
115. Rubsam, M., et al., *Adherens Junctions and Desmosomes Coordinate Mechanics and Signaling to Orchestrate Tissue Morphogenesis and Function: An Evolutionary Perspective.* Cold Spring Harb Perspect Biol, 2017.
116. Watt, F.M., *Role of integrins in regulating epidermal adhesion, growth and differentiation.* EMBO J, 2002. **21**(15): p. 3919-26.
117. Jones, P.H. and F.M. Watt, *Separation of human epidermal stem cells from transit amplifying cells on the basis of differences in integrin function and expression.* Cell, 1993. **73**(4): p. 713-24.
118. Muller, E.J., et al., *Outside-in signaling through integrins and cadherins: a central mechanism to control epidermal growth and differentiation?* J Invest Dermatol, 2008. **128**(3): p. 501-16.

119. Jones, J., et al., *Integrin expression in normal, hyperplastic, dysplastic, and malignant oral epithelium.* J Pathol, 1993. **169**(2): p. 235-43.
120. Downer, C.S., F.M. Watt, and P.M. Speight, *Loss of alpha 6 and beta 4 integrin subunits coincides with loss of basement membrane components in oral squamous cell carcinomas.* J Pathol, 1993. **171**(3): p. 183-90.
121. Kobielak, A. and E. Fuchs, *Alpha-catenin: at the junction of intercellular adhesion and actin dynamics.* Nat Rev Mol Cell Biol, 2004. **5**(8): p. 614-25.
122. Vaezi, A., et al., *Actin cable dynamics and Rho/Rock orchestrate a polarized cytoskeletal architecture in the early steps of assembling a stratified epithelium.* Dev Cell, 2002. **3**(3): p. 367-81.
123. Tinkle, C.L., et al., *Conditional targeting of E-cadherin in skin: insights into hyperproliferative and degenerative responses.* Proc Natl Acad Sci U S A, 2004. **101**(2): p. 552-7.
124. Vasioukhin, V., et al., *Hyperproliferation and defects in epithelial polarity upon conditional ablation of alpha-catenin in skin.* Cell, 2001. **104**(4): p. 605-17.
125. Fuchs, E. and H. Green, *The expression of keratin genes in epidermis and cultured epidermal cells.* Cell, 1978. **15**(3): p. 887-97.
126. Moll, R., et al., *The catalog of human cytokeratins: patterns of expression in normal epithelia, tumors and cultured cells.* Cell, 1982. **31**(1): p. 11-24.
127. Kottke, M.D., E. Delva, and A.P. Kowalczyk, *The desmosome: cell science lessons from human diseases.* J Cell Sci, 2006. **119**(Pt 5): p. 797-806.
128. Eichner, R., P. Bonitz, and T.T. Sun, *Classification of epidermal keratins according to their immunoreactivity, isoelectric point, and mode of expression.* J Cell Biol, 1984. **98**(4): p. 1388-96.
129. Parrish, E.P., et al., *Mouse antisera specific for desmosomal adhesion molecules of suprabasal skin cells, meninges, and meningioma.* Proc Natl Acad Sci U S A, 1986. **83**(8): p. 2657-61.
130. Getsios, S., et al., *Desmoglein 1-dependent suppression of EGFR signaling promotes epidermal differentiation and morphogenesis.* J Cell Biol, 2009. **185**(7): p. 1243-58.
131. Yoshida, K., et al., *Functional tight junction barrier localizes in the second layer of the stratum granulosum of human epidermis.* J Dermatol Sci, 2013. **71**(2): p. 89-99.
132. De Benedetto, A., A. Kubo, and L.A. Beck, *Skin barrier disruption: a requirement for allergen sensitization?* J Invest Dermatol, 2012. **132**(3 Pt 2): p. 949-63.
133. Morita, K. and Y. Miyachi, *Tight junctions in the skin.* J Dermatol Sci, 2003. **31**(2): p. 81-9.
134. Yokouchi, M., et al., *Epidermal cell turnover across tight junctions based on Kelvin's tetrakaidecahedron cell shape.* Elife, 2016. **5**.
135. Fanning, A.S., et al., *The tight junction protein ZO-1 establishes a link between the transmembrane protein occludin and the actin cytoskeleton.* J Biol Chem, 1998. **273**(45): p. 29745-53.
136. Itoh, M., et al., *Direct binding of three tight junction-associated MAGUKs, ZO-1, ZO-2, and ZO-3, with the COOH termini of claudins.* J Cell Biol, 1999. **147**(6): p. 1351-63.
137. Rodgers, L.S., et al., *Epithelial barrier assembly requires coordinated activity of multiple domains of the tight junction protein ZO-1.* J Cell Sci, 2013. **126**(Pt 7): p. 1565-75.

138. Furuse, M., et al., *Claudin-based tight junctions are crucial for the mammalian epidermal barrier: a lesson from claudin-1-deficient mice.* J Cell Biol, 2002. **156**(6): p. 1099-111.
139. De Smet, F., A. Christopoulos, and P. Carmeliet, *Allosteric targeting of receptor tyrosine kinases.* Nat Biotechnol, 2014. **32**(11): p. 1113-20.
140. Lu, Q., et al., *Ephrin-B reverse signaling is mediated by a novel PDZ-RGS protein and selectively inhibits G protein-coupled chemoattraction.* Cell, 2001. **105**(1): p. 69-79.
141. Arvanitis, D. and A. Davy, *Eph/ephrin signaling: networks.* Genes Dev, 2008. **22**(4): p. 416-29.
142. Lee, H. and A.M. Bennett, *Receptor protein tyrosine phosphatase-receptor tyrosine kinase substrate screen identifies EphA2 as a target for LAR in cell migration.* Mol Cell Biol, 2013. **33**(7): p. 1430-41.
143. Shintani, T., et al., *Eph receptors are negatively controlled by protein tyrosine phosphatase receptor type O.* Nat Neurosci, 2006. **9**(6): p. 761-9.
144. Schneider, M.R. and E. Wolf, *The epidermal growth factor receptor ligands at a glance.* J Cell Physiol, 2009. **218**(3): p. 460-6.
145. Muller, A.K., M. Meyer, and S. Werner, *The roles of receptor tyrosine kinases and their ligands in the wound repair process.* Semin Cell Dev Biol, 2012. **23**(9): p. 963-70.
146. Nyati, M.K., et al., *Integration of EGFR inhibitors with radiochemotherapy.* Nat Rev Cancer, 2006. **6**(11): p. 876-85.
147. Tokumaru, S., et al., *Ectodomain shedding of epidermal growth factor receptor ligands is required for keratinocyte migration in cutaneous wound healing.* J Cell Biol, 2000. **151**(2): p. 209-20.
148. Shirakata, Y., et al., *Heparin-binding EGF-like growth factor accelerates keratinocyte migration and skin wound healing.* J Cell Sci, 2005. **118**(Pt 11): p. 2363-70.
149. Wilhelmsen, K., et al., *Serine phosphorylation of the integrin beta4 subunit is necessary for epidermal growth factor receptor induced hemidesmosome disruption.* Mol Biol Cell, 2007. **18**(9): p. 3512-22.
150. Beenken, A. and M. Mohammadi, *The FGF family: biology, pathophysiology and therapy.* Nat Rev Drug Discov, 2009. **8**(3): p. 235-53.
151. Steiling, H. and S. Werner, *Fibroblast growth factors: key players in epithelial morphogenesis, repair and cytoprotection.* Curr Opin Biotechnol, 2003. **14**(5): p. 533-7.
152. Werner, S., et al., *The function of KGF in morphogenesis of epithelium and reepithelialization of wounds.* Science, 1994. **266**(5186): p. 819-22.
153. Yokote, H., et al., *Trans-activation of EphA4 and FGF receptors mediated by direct interactions between their cytoplasmic domains.* Proc Natl Acad Sci U S A, 2005. **102**(52): p. 18866-71.
154. Jones, T.L., et al., *Loss of cell adhesion in Xenopus laevis embryos mediated by the cytoplasmic domain of XLerk, an erythropoietin-producing hepatocellular ligand.* Proc Natl Acad Sci U S A, 1998. **95**(2): p. 576-81.
155. Chong, L.D., et al., *Fibroblast growth factor receptor-mediated rescue of x-ephrin B1-induced cell dissociation in Xenopus embryos.* Mol Cell Biol, 2000. **20**(2): p. 724-34.

156. Gusenbauer, S., P. Vlaicu, and A. Ullrich, *HGF induces novel EGFR functions involved in resistance formation to tyrosine kinase inhibitors.* Oncogene, 2013. **32**(33): p. 3846-56.
157. Neill, T., et al., *EphA2 is a functional receptor for the growth factor progranulin.* J Cell Biol, 2016. **215**(5): p. 687-703.
158. Chitramuthu, B. and A. Bateman, *Progranulin and the receptor tyrosine kinase EphA2, partners in crime?* J Cell Biol, 2016. **215**(5): p. 603-605.
159. Perez White, B.E., et al., *EphA2 proteomics in human keratinocytes reveals a novel association with afadin and epidermal tight junctions.* J Cell Sci, 2017. **130**(1): p. 111-118.
160. Hennings, H., et al., *Calcium regulation of growth and differentiation of mouse epidermal cells in culture.* Cell, 1980. **19**(1): p. 245-54.
161. O'Keefe, E.J., R.A. Briggaman, and B. Herman, *Calcium-induced assembly of adherens junctions in keratinocytes.* J Cell Biol, 1987. **105**(2): p. 807-17.
162. Morrow, A. and T. Lechler, *Studying cell biology in the skin.* Mol Biol Cell, 2015. **26**(23): p. 4183-6.
163. Meyers, C. and L.A. Laimins, *In vitro systems for the study and propagation of human papillomaviruses.* Curr Top Microbiol Immunol, 1994. **186**: p. 199-215.
164. Simpson, C.L., S. Kojima, and S. Getsios, *RNA interference in keratinocytes and an organotypic model of human epidermis.* Methods Mol Biol, 2010. **585**: p. 127-46.
165. Arnette, C., et al., *In Vitro Model of the Epidermis: Connecting Protein Function to 3D Structure.* Methods Enzymol, 2016. **569**: p. 287-308.
166. Justus, C.R., et al., *In vitro cell migration and invasion assays.* J Vis Exp, 2014(88).
167. Safferling, K., et al., *Wound healing revised: a novel reepithelialization mechanism revealed by in vitro and in silico models.* J Cell Biol, 2013. **203**(4): p. 691-709.
168. Guo, H., et al., *Disruption of EphA2 receptor tyrosine kinase leads to increased susceptibility to carcinogenesis in mouse skin.* Cancer Res, 2006. **66**(14): p. 7050-8.
169. Cayuso, J., Q. Xu, and D.G. Wilkinson, *Mechanisms of boundary formation by Eph receptor and ephrin signaling.* Dev Biol, 2015. **401**(1): p. 122-31.
170. Tanaka, M., R. Kamata, and R. Sakai, *EphA2 phosphorylates the cytoplasmic tail of Claudin-4 and mediates paracellular permeability.* J Biol Chem, 2005. **280**(51): p. 42375-82.
171. Larson, J., et al., *Endothelial EphA receptor stimulation increases lung vascular permeability.* Am J Physiol Lung Cell Mol Physiol, 2008. **295**(3): p. L431-9.
172. Zhou, N., et al., *Inactivation of EphA2 promotes tight junction formation and impairs angiogenesis in brain endothelial cells.* Microvasc Res, 2011. **82**(2): p. 113-21.
173. Aragona, M., et al., *Defining stem cell dynamics and migration during wound healing in mouse skin epidermis.* Nat Commun, 2017. **8**: p. 14684.
174. Guo, S. and L.A. Dipietro, *Factors affecting wound healing.* J Dent Res, 2010. **89**(3): p. 219-29.
175. Xu, K. and F.S. Yu, *Impaired epithelial wound healing and EGFR signaling pathways in the corneas of diabetic rats.* Invest Ophthalmol Vis Sci, 2011. **52**(6): p. 3301-8.
176. Macrae, M., et al., *A conditional feedback loop regulates Ras activity through EphA2.* Cancer Cell, 2005. **8**(2): p. 111-8.

177. Chudnovsky, Y., P.A. Khavari, and A.E. Adams, *Melanoma genetics and the development of rational therapeutics.* J Clin Invest, 2005. **115**(4): p. 813-24.
178. Udayakumar, D., et al., *EphA2 is a critical oncogene in melanoma.* Oncogene, 2011. **30**(50): p. 4921-9.
179. Eskandarpour, M., et al., *Oncogenic NRAS has multiple effects on the malignant phenotype of human melanoma cells cultured in vitro.* Int J Cancer, 2009. **124**(1): p. 16-26.
180. Margaryan, N.V., et al., *EphA2 as a promoter of melanoma tumorigenicity.* Cancer Biol Ther, 2009. **8**(3): p. 279-88.
181. Parri, M., et al., *EphA2 reexpression prompts invasion of melanoma cells shifting from mesenchymal to amoeboid-like motility style.* Cancer Res, 2009. **69**(5): p. 2072-81.
182. Grant, B.D. and J.G. Donaldson, *Pathways and mechanisms of endocytic recycling.* Nat Rev Mol Cell Biol, 2009. **10**(9): p. 597-608.
183. Le Roy, C. and J.L. Wrana, *Clathrin- and non-clathrin-mediated endocytic regulation of cell signalling.* Nat Rev Mol Cell Biol, 2005. **6**(2): p. 112-26.
184. Scita, G. and P.P. Di Fiore, *The endocytic matrix.* Nature, 2010. **463**(7280): p. 464-73.
185. Gruenberg, J. and H. Stenmark, *The biogenesis of multivesicular endosomes.* Nat Rev Mol Cell Biol, 2004. **5**(4): p. 317-23.
186. Settembre, C., et al., *Signals from the lysosome: a control centre for cellular clearance and energy metabolism.* Nat Rev Mol Cell Biol, 2013. **14**(5): p. 283-96.
187. Kaur, J. and J. Debnath, *Autophagy at the crossroads of catabolism and anabolism.* Nat Rev Mol Cell Biol, 2015. **16**(8): p. 461-72.
188. Sabet, O., et al., *Ubiquitination switches EphA2 vesicular traffic from a continuous safeguard to a finite signalling mode.* Nat Commun, 2015. **6**: p. 8047.
189. Zhuang, G., et al., *Regulation of EphA2 receptor endocytosis by SHIP2 lipid phosphatase via phosphatidylinositol 3-Kinase-dependent Rac1 activation.* J Biol Chem, 2007. **282**(4): p. 2683-94.
190. Walker-Daniels, J., D.J. Riese, 2nd, and M.S. Kinch, *c-Cbl-dependent EphA2 protein degradation is induced by ligand binding.* Mol Cancer Res, 2002. **1**(1): p. 79-87.
191. Boissier, P., J. Chen, and U. Huynh-Do, *EphA2 signaling following endocytosis: role of Tiam1.* Traffic, 2013. **14**(12): p. 1255-71.
192. Owen, D.M., et al., *Sub-resolution lipid domains exist in the plasma membrane and regulate protein diffusion and distribution.* Nat Commun, 2012. **3**: p. 1256.
193. Allen, J.A., R.A. Halverson-Tamboli, and M.M. Rasenick, *Lipid raft microdomains and neurotransmitter signalling.* Nat Rev Neurosci, 2007. **8**(2): p. 128-40.
194. Simons, K. and E. Ikonen, *Functional rafts in cell membranes.* Nature, 1997. **387**(6633): p. 569-72.
195. Saslowsky, D.E., et al., *Placental alkaline phosphatase is efficiently targeted to rafts in supported lipid bilayers.* J Biol Chem, 2002. **277**(30): p. 26966-70.
196. Garcia-Saez, A.J., S. Chiantia, and P. Schwille, *Effect of line tension on the lateral organization of lipid membranes.* J Biol Chem, 2007. **282**(46): p. 33537-44.
197. Sprong, H., P. van der Sluijs, and G. van Meer, *How proteins move lipids and lipids move proteins.* Nat Rev Mol Cell Biol, 2001. **2**(7): p. 504-13.

198. Lin, Q. and E. London, *Altering hydrophobic sequence lengths shows that hydrophobic mismatch controls affinity for ordered lipid domains (rafts) in the multitransmembrane strand protein perfringolysin O.* J Biol Chem, 2013. **288**(2): p. 1340-52.
199. Lorent, J.H., et al., *Structural determinants and functional consequences of protein affinity for membrane rafts.* Nat Commun, 2017. **8**(1): p. 1219.
200. Levental, I., M. Grzybek, and K. Simons, *Greasing their way: lipid modifications determine protein association with membrane rafts.* Biochemistry, 2010. **49**(30): p. 6305-16.
201. Fukata, Y. and M. Fukata, *Protein palmitoylation in neuronal development and synaptic plasticity.* Nat Rev Neurosci, 2010. **11**(3): p. 161-75.
202. Rocks, O., et al., *An acylation cycle regulates localization and activity of palmitoylated Ras isoforms.* Science, 2005. **307**(5716): p. 1746-52.
203. Shah, A., et al., *RaftProt: mammalian lipid raft proteome database.* Nucleic Acids Res, 2015. **43**(Database issue): p. D335-8.
204. McGuinn, K.P. and M.G. Mahoney, *Lipid rafts and detergent-resistant membranes in epithelial keratinocytes.* Methods Mol Biol, 2014. **1195**: p. 133-44.
205. Jans, R., et al., *Cholesterol depletion upregulates involucrin expression in epidermal keratinocytes through activation of p38.* J Invest Dermatol, 2004. **123**(3): p. 564-73.
206. Lambert, S., et al., *Internalization of EGF receptor following lipid rafts disruption in keratinocytes is delayed and dependent on p38 MAPK activation.* J Cell Physiol, 2008. **217**(3): p. 834-45.
207. Mathay, C., et al., *Heparin-binding EGF-like growth factor is induced by disruption of lipid rafts and oxidative stress in keratinocytes and participates in the epidermal response to cutaneous wounds.* J Invest Dermatol, 2008. **128**(3): p. 717-27.
208. Giltaire, S., S. Lambert, and Y. Poumay, *HB-EGF synthesis and release induced by cholesterol depletion of human epidermal keratinocytes is controlled by extracellular ATP and involves both p38 and ERK1/2 signaling pathways.* J Cell Physiol, 2011. **226**(6): p. 1651-9.
209. Lambert, S., et al., *Ligand-independent activation of the EGFR by lipid raft disruption.* J Invest Dermatol, 2006. **126**(5): p. 954-62.
210. Calay, D., et al., *Inhibition of Akt signaling by exclusion from lipid rafts in normal and transformed epidermal keratinocytes.* J Invest Dermatol, 2010. **130**(4): p. 1136-45.
211. Gniadecki, R. and B. Bang, *Flotillas of lipid rafts in transit amplifying cell-like keratinocytes.* J Invest Dermatol, 2003. **121**(3): p. 522-8.
212. Couet, J., et al., *Identification of peptide and protein ligands for the caveolin-scaffolding domain. Implications for the interaction of caveolin with caveolae-associated proteins.* J Biol Chem, 1997. **272**(10): p. 6525-33.
213. Delos Santos, R.C., C. Garay, and C.N. Antonescu, *Charming neighborhoods on the cell surface: plasma membrane microdomains regulate receptor tyrosine kinase signaling.* Cell Signal, 2015. **27**(10): p. 1963-76.
214. Abulrob, A., et al., *Interactions of EGFR and caveolin-1 in human glioblastoma cells: evidence that tyrosine phosphorylation regulates EGFR association with caveolae.* Oncogene, 2004. **23**(41): p. 6967-79.

215. Puri, C., et al., *Relationships between EGFR signaling-competent and endocytosis-competent membrane microdomains.* Mol Biol Cell, 2005. **16**(6): p. 2704-18.
216. Williams, T.M., et al., *Caveolin-1 gene disruption promotes mammary tumorigenesis and dramatically enhances lung metastasis in vivo. Role of Cav-1 in cell invasiveness and matrix metalloproteinase (MMP-2/9) secretion.* J Biol Chem, 2004. **279**(49): p. 51630-46.
217. Pike, L.J. and L. Casey, *Cholesterol levels modulate EGF receptor-mediated signaling by altering receptor function and trafficking.* Biochemistry, 2002. **41**(32): p. 10315-22.
218. Amaddii, M., et al., *Flotillin-1/reggie-2 protein plays dual role in activation of receptor-tyrosine kinase/mitogen-activated protein kinase signaling.* J Biol Chem, 2012. **287**(10): p. 7265-78.
219. Couet, J., M. Sargiacomo, and M.P. Lisanti, *Interaction of a receptor tyrosine kinase, EGF-R, with caveolins. Caveolin binding negatively regulates tyrosine and serine/threonine kinase activities.* J Biol Chem, 1997. **272**(48): p. 30429-38.
220. Vihanto, M.M., et al., *Caveolin-1 is required for signaling and membrane targeting of EphB1 receptor tyrosine kinase.* J Cell Sci, 2006. **119**(Pt 11): p. 2299-309.
221. Gauthier, L.R. and S.M. Robbins, *Ephrin signaling: One raft to rule them all? One raft to sort them? One raft to spread their call and in signaling bind them?* Life Sci, 2003. **74**(2-3): p. 207-16.
222. Campbell, T.N., et al., *Distinct membrane compartmentalization and signaling of ephrin-A5 and ephrin-B1.* Biochem Biophys Res Commun, 2008. **375**(3): p. 362-6.
223. Bruckner, K., et al., *EphrinB ligands recruit GRIP family PDZ adaptor proteins into raft membrane microdomains.* Neuron, 1999. **22**(3): p. 511-24.
224. Jiang, G., et al., *In human leukemia cells ephrin-B-induced invasive activity is supported by Lck and is associated with reassembling of lipid raft signaling complexes.* Mol Cancer Res, 2008. **6**(2): p. 291-305.
225. Meyer, S., et al., *Lubrol-RAFTs in melanoma cells: a molecular platform for tumor-promoting ephrin-B2-integrin-beta1 interaction.* J Invest Dermatol, 2007. **127**(7): p. 1615-21.
226. Hay, R.J., et al., *The Global Burden of Skin Disease in 2010: An Analysis of the Prevalence and Impact of Skin Conditions.* J Invest Dermatol, 2013.
227. Hay, R.J., et al., *The global burden of skin disease in 2010: an analysis of the prevalence and impact of skin conditions.* J Invest Dermatol, 2014. **134**(6): p. 1527-1534.
228. Swindell, W.R., et al., *Proteogenomic analysis of psoriasis reveals discordant and concordant changes in mRNA and protein abundance.* Genome Med, 2015. **7**(1): p. 86.
229. Kim, D., et al., *TopHat2: accurate alignment of transcriptomes in the presence of insertions, deletions and gene fusions.* Genome Biol, 2013. **14**(4): p. R36.
230. Trapnell, C., et al., *Differential gene and transcript expression analysis of RNA-seq experiments with TopHat and Cufflinks.* Nat Protoc, 2012. **7**(3): p. 562-78.
231. Edgar, R., M. Domrachev, and A.E. Lash, *Gene Expression Omnibus: NCBI gene expression and hybridization array data repository.* Nucleic Acids Res, 2002. **30**(1): p. 207-10.
232. Gregory R. Warnes, B.B., Lodewijk Bonebakker, Robert Gentleman, Wolfgang Huber, Andy Liaw, Thomas Lumley, Martin Maechler, Arni Magnusson, Steffen Moeller, Marc

Schwartz, Bill Venables, *gplots: Various R Programming Tools for Plotting Data*, in *R package* 2015.
233. Schindelin, J., et al., *Fiji: an open-source platform for biological-image analysis.* Nat Methods, 2012. **9**(7): p. 676-82.
234. Denning, M.F., et al., *Caspase activation and disruption of mitochondrial membrane potential during UV radiation-induced apoptosis of human keratinocytes requires activation of protein kinase C.* Cell Death Differ, 2002. **9**(1): p. 40-52.
235. Wykosky, J., D.M. Gibo, and W. Debinski, *A novel, potent, and specific ephrinA1-based cytotoxin against EphA2 receptor expressing tumor cells.* Mol Cancer Ther, 2007. **6**(12 Pt 1): p. 3208-18.
236. Getsios, S., et al., *Coordinated expression of desmoglein 1 and desmocollin 1 regulates intercellular adhesion.* Differentiation, 2004. **72**(8): p. 419-33.
237. Miao, H., et al., *EphA2 promotes infiltrative invasion of glioma stem cells in vivo through cross-talk with Akt and regulates stem cell properties.* Oncogene, 2015. **34**(5): p. 558-67.
238. Song, K.S., et al., *Co-purification and direct interaction of Ras with caveolin, an integral membrane protein of caveolae microdomains. Detergent-free purification of caveolae microdomains.* J Biol Chem, 1996. **271**(16): p. 9690-7.
239. Averaimo, S., et al., *A plasma membrane microdomain compartmentalizes ephrin-generated cAMP signals to prune developing retinal axon arbors.* Nat Commun, 2016. **7**: p. 12896.
240. Roberts, B.J., et al., *Palmitoylation of plakophilin is required for desmosome assembly.* J Cell Sci, 2014. **127**(Pt 17): p. 3782-93.
241. Roberts, B.J., et al., *Palmitoylation of Desmoglein 2 Is a Regulator of Assembly Dynamics and Protein Turnover.* J Biol Chem, 2016. **291**(48): p. 24857-24865.
242. Percher, A., et al., *Mass-tag labeling reveals site-specific and endogenous levels of protein S-fatty acylation.* Proc Natl Acad Sci U S A, 2016. **113**(16): p. 4302-7.
243. Chen, J., et al., *The C-terminal unique region of desmoglein 2 inhibits its internalization via tail-tail interactions.* J Cell Biol, 2012. **199**(4): p. 699-711.
244. Yu, J., et al., *MicroRNA-205 promotes keratinocyte migration via the lipid phosphatase SHIP2.* FASEB J, 2010. **24**(10): p. 3950-9.
245. Gygi, S.P., et al., *Correlation between protein and mRNA abundance in yeast.* Mol Cell Biol, 1999. **19**(3): p. 1720-30.
246. Barquilla, A. and E.B. Pasquale, *Eph receptors and ephrins: therapeutic opportunities.* Annu Rev Pharmacol Toxicol, 2015. **55**: p. 465-87.
247. Singh, D.R., et al., *EphA2 Receptor Unliganded Dimers Suppress EphA2 Pro-tumorigenic Signaling.* J Biol Chem, 2015. **290**(45): p. 27271-9.
248. Stahley, S.N., et al., *Desmosome assembly and disassembly are membrane raft-dependent.* PLoS One, 2014. **9**(1): p. e87809.
249. Overmiller, A.M., et al., *c-Src/Cav1-dependent activation of the EGFR by Dsg2.* Oncotarget, 2016. **7**(25): p. 37536-37555.
250. Mollinedo, F. and C. Gajate, *Lipid rafts as major platforms for signaling regulation in cancer.* Adv Biol Regul, 2015. **57**: p. 130-46.
251. Yao, Y., et al., *The differential protein and lipid compositions of noncaveolar lipid microdomains and caveolae.* Cell Res, 2009. **19**(4): p. 497-506.

252. Wan, J., et al., *Palmitoylated proteins: purification and identification.* Nat Protoc, 2007. **2**(7): p. 1573-84.
253. Yin, T., et al., *Plakoglobin suppresses keratinocyte motility through both cell-cell adhesion-dependent and -independent mechanisms.* Proc Natl Acad Sci U S A, 2005. **102**(15): p. 5420-5.
254. Bocharov, E.V., et al., *Conformational transitions and interactions underlying the function of membrane embedded receptor protein kinases.* Biochim Biophys Acta, 2017.
255. Rajendran, L. and K. Simons, *Lipid rafts and membrane dynamics.* J Cell Sci, 2005. **118**(Pt 6): p. 1099-102.
256. Beauchamp, A., et al., *EphrinA1 is released in three forms from cancer cells by matrix metalloproteases.* Mol Cell Biol, 2012. **32**(16): p. 3253-64.
257. Janes, P.W., et al., *Adam meets Eph: an ADAM substrate recognition module acts as a molecular switch for ephrin cleavage in trans.* Cell, 2005. **123**(2): p. 291-304.
258. Wykosky, J., et al., *Soluble monomeric EphrinA1 is released from tumor cells and is a functional ligand for the EphA2 receptor.* Oncogene, 2008. **27**(58): p. 7260-73.
259. Miao, H. and B. Wang, *EphA receptor signaling--complexity and emerging themes.* Semin Cell Dev Biol, 2012. **23**(1): p. 16-25.
260. Poliakov, A., M. Cotrina, and D.G. Wilkinson, *Diverse roles of eph receptors and ephrins in the regulation of cell migration and tissue assembly.* Dev Cell, 2004. **7**(4): p. 465-80.
261. Ventrella, R., N. Kaplan, and S. Getsios, *Asymmetry at cell-cell interfaces direct cell sorting, boundary formation, and tissue morphogenesis.* Exp Cell Res, 2017.
262. Murai, T., *Lipid Raft-Mediated Regulation of Hyaluronan-CD44 Interactions in Inflammation and Cancer.* Front Immunol, 2015. **6**: p. 420.
263. Oliferenko, S., et al., *Analysis of CD44-containing lipid rafts: Recruitment of annexin II and stabilization by the actin cytoskeleton.* J Cell Biol, 1999. **146**(4): p. 843-54.
264. Salaita, K., et al., *Restriction of receptor movement alters cellular response: physical force sensing by EphA2.* Science, 2010. **327**(5971): p. 1380-5.
265. Park, E.C., et al., *The involvement of Eph-Ephrin signaling in tissue separation and convergence during Xenopus gastrulation movements.* Dev Biol, 2011. **350**(2): p. 441-50.
266. Sahin, U., et al., *Distinct roles for ADAM10 and ADAM17 in ectodomain shedding of six EGFR ligands.* J Cell Biol, 2004. **164**(5): p. 769-79.
267. Mancia, F. and L. Shapiro, *ADAM and Eph: how Ephrin-signaling cells become detached.* Cell, 2005. **123**(2): p. 185-7.
268. Coon, B.G., et al., *Intramembrane binding of VE-cadherin to VEGFR2 and VEGFR3 assembles the endothelial mechanosensory complex.* J Cell Biol, 2015. **208**(7): p. 975-86.
269. Atapattu, L., et al., *Antibodies binding the ADAM10 substrate recognition domain inhibit Eph function.* J Cell Sci, 2012. **125**(Pt 24): p. 6084-93.
270. Yuan, Z., et al., *Predicting the solvent accessibility of transmembrane residues from protein sequence.* J Proteome Res, 2006. **5**(5): p. 1063-70.
271. Shi, X., et al., *A role of the SAM domain in EphA2 receptor activation.* Sci Rep, 2017. **7**: p. 45084.
272. Singh, D.R., et al., *The SAM domain inhibits EphA2 interactions in the plasma membrane.* Biochim Biophys Acta, 2017. **1864**(1): p. 31-38.

273. Wendland, B., *Epsins: adaptors in endocytosis?* Nat Rev Mol Cell Biol, 2002. **3**(12): p. 971-7.
274. Sigismund, S., et al., *Clathrin-independent endocytosis of ubiquitinated cargos.* Proc Natl Acad Sci U S A, 2005. **102**(8): p. 2760-5.
275. Chen, H. and P. De Camilli, *The association of epsin with ubiquitinated cargo along the endocytic pathway is negatively regulated by its interaction with clathrin.* Proc Natl Acad Sci U S A, 2005. **102**(8): p. 2766-71.
276. Aguilar, R.C. and B. Wendland, *Endocytosis of membrane receptors: two pathways are better than one.* Proc Natl Acad Sci U S A, 2005. **102**(8): p. 2679-80.
277. Enrich, C., et al., *Role of cholesterol in SNARE-mediated trafficking on intracellular membranes.* J Cell Sci, 2015. **128**(6): p. 1071-81.
278. Salaun, C., G.W. Gould, and L.H. Chamberlain, *The SNARE proteins SNAP-25 and SNAP-23 display different affinities for lipid rafts in PC12 cells. Regulation by distinct cysteine-rich domains.* J Biol Chem, 2005. **280**(2): p. 1236-40.
279. Predescu, S.A., et al., *Cholesterol-dependent syntaxin-4 and SNAP-23 clustering regulates caveolar fusion with the endothelial plasma membrane.* J Biol Chem, 2005. **280**(44): p. 37130-8.
280. Williams, K.C., R.E. McNeilly, and M.G. Coppolino, *SNAP23, Syntaxin4, and vesicle-associated membrane protein 7 (VAMP7) mediate trafficking of membrane type 1-matrix metalloproteinase (MT1-MMP) during invadopodium formation and tumor cell invasion.* Mol Biol Cell, 2014. **25**(13): p. 2061-70.
281. Cai, B., et al., *Pre-sorting endosomal transport of the GPI-anchored protein, CD59, is regulated by EHD1.* Traffic, 2011. **12**(1): p. 102-20.
282. Ioannou, M.S. and P.S. McPherson, *Regulation of Cancer Cell Behavior by the Small GTPase Rab13.* J Biol Chem, 2016. **291**(19): p. 9929-37.
283. Kelly, E.E., C.P. Horgan, and M.W. McCaffrey, *Rab11 proteins in health and disease.* Biochem Soc Trans, 2012. **40**(6): p. 1360-7.
284. Cummins, P.M., *Occludin: one protein, many forms.* Mol Cell Biol, 2012. **32**(2): p. 242-50.
285. Noren, N.K. and E.B. Pasquale, *Eph receptor-ephrin bidirectional signals that target Ras and Rho proteins.* Cell Signal, 2004. **16**(6): p. 655-66.
286. Zihni, C. and S.J. Terry, *RhoGTPase signalling at epithelial tight junctions: Bridging the GAP between polarity and cancer.* Int J Biochem Cell Biol, 2015. **64**: p. 120-5.
287. Soyka, M.B., et al., *Defective epithelial barrier in chronic rhinosinusitis: the regulation of tight junctions by IFN-gamma and IL-4.* J Allergy Clin Immunol, 2012. **130**(5): p. 1087-1096 e10.
288. Schulzke, J.D., et al., *Epithelial tight junctions in intestinal inflammation.* Ann N Y Acad Sci, 2009. **1165**: p. 294-300.
289. Xiao, C., et al., *Defective epithelial barrier function in asthma.* J Allergy Clin Immunol, 2011. **128**(3): p. 549-56 e1-12.
290. Koolpe, M., M. Dail, and E.B. Pasquale, *An ephrin mimetic peptide that selectively targets the EphA2 receptor.* J Biol Chem, 2002. **277**(49): p. 46974-9.
291. Mitra, S., et al., *Structure-activity relationship analysis of peptides targeting the EphA2 receptor.* Biochemistry, 2010. **49**(31): p. 6687-95.

292. Gao, X., et al., *PI3K/Akt signaling requires spatial compartmentalization in plasma membrane microdomains.* Proc Natl Acad Sci U S A, 2011. **108**(35): p. 14509-14.
293. Li, Y.C., et al., *Elevated levels of cholesterol-rich lipid rafts in cancer cells are correlated with apoptosis sensitivity induced by cholesterol-depleting agents.* Am J Pathol, 2006. **168**(4): p. 1107-18; quiz 1404-5.

CURRICULUM VITA

EDUCATION

Northwestern University Feinberg School of Medicine, Chicago, IL
Driskill Graduate Program
PhD Cell Biology and Dermatology

University of Illinois at Urbana Champaign, IL
Major: Bioengineering
Minor: Business
GPA: 3.85/4.00
BS Degree, May 2012

AWARDS AND HONORS

1. Albert M. Kligman Travel Fellowship, Society for Investigative Dermatology Conference, 2017
2. Genetic Medicine Travel Fellowship Award, Robert H. Lurie Comprehensive Cancer Center of Northwestern University, Spring 2017
3. Driskill Graduate Program (DGP) Travel Award, Northwestern University, Spring 2017
4. The Graduate School (TGS) Travel Award, Northwestern University, Spring 2017
5. Cancer Smashers' Fellowship Award, Basic Sciences Research Division of the Robert H. Lurie Comprehensive Cancer Center of Northwestern University, June 2016
6. Katten Muchin Rosenman Travel Scholarship, Robert H. Lurie Comprehensive Cancer Center of Northwestern University, Spring 2014
7. Society for Investigative Dermatology Student Research Travel Award, 2014
8. University of Illinois at Urbana Champaign Engineering Highest Honors, May 2012
9. University of Illinois at Urbana Champaign James Scholar, Fall 2008-present
10. University of Illinois at Urbana Champaign Dean's List, Fall 2008-present

SCIENTIFIC FUNDING

1. Cellular and Molecular Basis of Disease Training Grant. March 1, 2014-April 30, 2017

PUBLICATIONS

1. **Ventrella R.,** Kaplan N., Hoover P., Perez White B.E., Lavker R.M., Getsios S. EphA2 transmembrane domain is uniquely required for keratinocyte migration by regulating ephrin-A1 levels. *JID.* [Accepted].
2. Kaplan N., Peng H., Pal-Ghosh S., **Ventrella R.,** Arvanitis C., Rappoport J.Z., Mitchell B.J., Stepp M., Lavker R.M., Getsios S. Ephrin-A1/EphA2 mediated corneal epithelial cell compartment organization is dependent on ADAM10 regulation of EGFR signaling. *IOVS.* 2018 Jan 1. *(Recommended by Faculty of 1000).*

3. **Ventrella R.,** Kaplan N., Getsios S. Asymmetry at cell-cell interfaces direct cell sorting, boundary formation, and tissue morphogenesis. *Exp Cell Res.* 2017 Mar 18. Review.
4. Perez White B.E., **Ventrella R.,** Kaplan N., Cable C.J., Thomas P.M., Getsios S. EphA2 proteomics in human keratinocytes reveals a novel association with afadin and epidermal tight junctions. *Journal of Cell Science.* 2016 Nov 4.
5. Hamill K.J., Hiroyasu S., Colburn Z.T., **Ventrella, R.V.,** Hopkinson S.B., Skalli O., Jones J.C. Alpha actinin-1 regulates cell-matrix adhesion organization in keratinocytes: consequences for skin cell motility. *J Invest Dermatol.* 2015 Apr; 135(4):1043-52.
6. Madak-Erdogan Z., **Ventrella R.,** Petry L., Katzenellenbogen B.S. Novel roles for ERK5 and cofilin as critical mediators linking ERα-driven transcription, actin reorganization and invasiveness in breast cancer. *Mol Cancer Res.* 2014 May; 12(5):714-27.
7. Kyuri K., Madak-Erdogan Z., **Ventrella R.,** Katzenellenbogen B.S. A MicroRNA196a2* and TP63 Circuit Regulated by Estrogen Receptor-α and ERK2 that Controls Breast Cancer Proliferation and Invasiveness Properties. *Horm Canc.* 2013; 4(2): 78-91.

PLATFORM PRESENTATIONS

1. **R. Ventrella,** N. Kaplan, P. Hoover, B. E. Perez White, R. M. Lavker, S. Getsios. "EphA2 transmembrane domain governs receptor membrane distribution and differentiation-associated signaling in keratinocytes". 2017 Gordon Research Seminar on Epithelial Differentiation and Keratinization. May 6-12, 2017. Tuscany, Italy.
2. **R. Ventrella,** N. Kaplan, P. Hoover, B. E. Perez White, R. M. Lavker, S. Getsios. "EphA2 transmembrane domain governs receptor membrane distribution and differentiation-associated signaling in keratinocytes". The Society for Investigative Dermatology's 76th Annual Meeting, April 26-29, 2017. Portland, Oregon.
3. **R. Ventrella**, B. E. Perez White, K. Xia, N. Kaplan, H. Peng, R. M. Lavker, S. Getsios. "Building a better tight junction barrier by targeting epidermal Eph receptors". The Society for Investigative Dermatology's 73rd Annual Meeting, May 7-10, 2013. Albuquerque, New Mexico.

UNIVERSITY PRESENTATIONS

1. "The EphA2 transmembrane domain is uniquely required for keratinocyte migration by regulating ephrin-A1 levels". Dermatology Research Faculty Meeting. December 20, 2017.
2. "The transmembrane domain of EphA2 regulates differentiation signaling in keratinocytes." Northwestern University. Epithelial Biology Meeting. February 10, 2017.
3. "EphA1/EphA2 Crosstalk Promotes Epidermal Differentiation." Northwestern University. Epithelial Biology Meeting. March 25, 2016.
4. "Eph/ephrin signaling regulates epidermal barrier formation and function." Northwestern University. Epithelial Biology Meeting. December 4, 2014.
5. "EphrinA1 Regulation of Epidermal Barrier Characteristics." Northwestern University Department of Dermatology, Work in Progress Seminar Series. January 22, 2014.

POSTER PRESENTATIONS

1. **R. Ventrella,** N. Kaplan, P. Hoover, B. E. Perez White, R. M. Lavker, S. Getsios. "EphA2 transmembrane domain governs receptor membrane distribution and differentiation-associated signaling in keratinocytes". 2017 Gordon Research Seminar on Epithelial Differentiation and Keratinization. May 6-12, 2017. Tuscany, Italy.
2. **R. Ventrella,** N. Kaplan, P. Hoover, B. E. Perez White, R. M. Lavker, S. Getsios. "EphA2 transmembrane domain governs receptor membrane distribution and differentiation-associated signaling in keratinocytes". The Society for Investigative Dermatology's 76th Annual Meeting, April 26-29, 2017. Portland, Oregon.
3. **Ventrella R.,** Perez White B.E., Wahl J.K., Getsios S. "Regulation of Eph receptor tyrosine kinase communication and trafficking during epidermal differentiation." Robert H. Lurie Comprehensive Cancer Center of Northwestern University 27th Annual Scientific Poster Session. Chicago, Illinois. June 23, 2016.
4. **Ventrella R.,** Hoover P., Swindell W.R., Gudjonsson J.E., Getsios S. "Transcriptome analysis of cell-cell adhesion and communication complexes during human keratinocyte differentiation in 2-D and 3-D culture models." Northwestern University, Cellular and Molecular Basis of Disease Training Grant Symposium on Aging and Regeneration. Chicago, Illinois. March 24, 2016.
5. Kaplan N., Peng H., Ventrella R., Arvanitis C., Lavker R.M., Getsios S. "EphA2/ephrinA1 signaling helps to set the limbal-corneal epithelial boundary as revealed by a novel cell confrontational co-culture model." The Association for Research in Vision and Opthamology (ARVO) Annual Meeting 2015, May 3-7. Denver, Colorado.
6. **Ventrella R.,** Hoover P., Swindell W.R., Gudjonsson J.E., Getsios S. "Transcriptome analysis of cell-cell adhesion and communication complexes during human keratinocyte differentiation in 2-D and 3-D culture models." Northwestern University Skin Disease Research Center, Research Retreat. Chicago, Illinois. July 28, 2015.
7. Kaplan N., Perez White B.E., Zheng J., Hoover P., **Ventrella R.,** Swindell W.R., Gudjonsson J.E., Wang B., Getsios S. "Ephrin-A ligand loss enhances keratinocyte migration via ligand-independent EphA2 action." Chicago Symposium on Cell Signaling $(CS)^2$. Chicago, Illinois. May 21. 2015.
8. **Ventrella R.,** Perez White B.E., Xia K., Kaplan N., Peng H., Lavker R.M, Getsios S. "Building a Better Epidermal Barrier by Targeting EphA Receptors." Robert H. Lurie Comprehensive Cancer Center of Northwestern University 25th Annual Scientific Poster Session. Chicago, Illinois. July 11, 2014.
9. **Ventrella R.,** Perez White B.E., Xia K., Kaplan N., Peng H., Lavker R.M, Getsios S. "Building a Better Epidermal Barrier by Targeting EphA Receptors." Northwestern University Skin Disease Research Center, Research Retreat. Chicago, Illinois. Jun 17, 2014.
10. **Ventrella R.,** Perez White B.E., Xia K., Kaplan N., Peng H., Lavker R.M, Getsios S. "Building a Better Epidermal Barrier by Targeting EphA Receptors." The Society for Investigative Dermatology's 73rd Annual Meeting, May 7-10. Albuquerque, New Mexico.

11. **Ventrella R.,** Perez White B.E., Xia K., Kaplan N., Peng H., Lavker R.M, Getsios S. "Building a Better Epidermal Barrier by Targeting EphA Receptors." Feinberg School of Medicine Research Day. Chicago, Illinois. April 3, 2014.

TEACHING AND MENTORING EXPERIENCE

Northwestern University, Searle Center for Advancing Learning and Teaching
Center for Integration of Research, Teaching and Learning (CIRTL)
CIRTL Associate, *June 2017*

1. Northwestern University Biochemistry Study Group Facilitator. **Biochemistry, DGP 401.** Fall 2017.
2. CIRTL at Northwestern University, Topics in STEMinism CIRTLCast Series Discussion Facilitator. Fall 2017.
3. Northwestern University Teaching Assistant. **Biochemistry, BIOL SCI 308.** Spring 2017. Instructor: Dr. Erin Lambers.
4. Continuing Umbrella of Research Experience (CURE) Summer Program for Undergraduate Students. Robert H. Lurie Comprehensive Cancer Center of Northwestern University. **Student mentor,** Summer 2016.
5. Student Assisted Mentoring Program (StAMP), Student peer mentoring program **Student mentor,** Fall 2015-present
6. Northwestern University Teaching Assistant. **Molecular Mechanisms of Carcinogenesis, IGP 480.** Winter 2015. Course Coordinator: Dr. Kathy Green.

PROFESSIONAL EXPERIENCE

June 2013-present
Affiliation: Northwestern University, Department of Dermatology
Advisor: Dr. Spiro Getsios
Position: PhD Student
Project: Eph/ephrin Signaling in Epidermal Differentiation

February 2010-August 2012
Affiliation: University of Illinois Urbana-Champaign, Department of Molecular and Integrative Physiology
Advisor: Dr. Benita Katzenellenbogen
Position: Undergraduate research assistant
Project: Integration of Nuclear and Extranuclear Initiated Actions of Estrogens and Estrogen Receptors

May 2009-August 2009
Affiliation: FONA International
Advisor: Dr. Bob Sobel and Dr. Atul Khare
Position: Summer Research Assistant

Project: Nanosolubilization of Flavor using Vitamin E Tocopheryl Polyethylene Glycol 1000 Succinate (Vitamin E TPGS)

COURSEWORK

Summer 2017: Mentored Discussions of Teaching (MDT). The Center for the Integration of Research Teaching and Learning (CIRTL).
Spring 2017: An Introduction to Evidence-Based STEM Undergraduate Teaching. The Center for the Integration of Research Teaching and Learning (CIRTL). Completed with distinction.
Fall 2015: Programming for Statistical Analysis
Winter 2015: Intermediate Epidemiology
Fall 2014: Intermediate Biostatistics
Summer 2014: Writing for Peer Reviewing for Publication, Artificial Epidemics and Changes in Human Culture
Winter 2014: Molecular Mechanisms of Carcinogenesis
Fall 2013: Health Economics and Healthcare Financing
Summer 2013: Introduction to Translational Research
Spring 2013: Tumor Cell Biology, Control and Prevention of Communicable Diseases
Winter 2013: Cell Biology, Introduction to Epidemiology
Fall 2012: Biochemistry, Molecular Biology, Introduction to Biostatistics

EXTRACURRICULAR ACTIVITIES

Northwestern University Cell and Molecular Biology (CMB) Search Committee, Graduate Student Representative, Fall 2017-present

Cellular and Molecular Basis of Disease Training Grant Symposium Planning Committee
Symposium on Aging and Regeneration, Chicago, IL. March 24, 2016.

Northwestern University
Epithelial Cell Biology Seminar Series, R. H. Lurie Cancer Center, 2013-present
Dermatology Research Faculty Meeting Seminar Series, Dept. of Dermatology, 2013-present